THE EFFECT OF ORGANIC TERRAIN AND SURFACE MODIFICATION ON ACTIVE LAYER DEVELOPMENT

THE EFFECT of ORGANIC TERRAIN and SURFACE MODIFICATION ON ACTIVE
LAYER DEVELOPMENT

SEAN KEVIN CAREY

A Thesis
Submitted to the School of Graduate Studies
in Partial Fulfillment of the Requirements
for the Degree of Masters of Science
McMaster University, Hamilton, Ontario

i

MASTER OF SCIENCE (1996)   MCMASTER UNIVERSITY

(Geography)   Hamilton, Ontario

TITLE: THE EFFECT of ORGANIC TERRAIN and SURFACE MODIFICATION ON ACTIVE LAYER DEVELOPMENT

AUTHOR: Sean Kevin Carey, B.Sc. (University of Guelph)

SUPERVISOR: Dr. Ming-ko Woo

NUMBER OF PAGES: xii, 114

ABSTRACT

During the summer of 1995, ground energy balance was calculated for six organic soils at different stages of development and nine mineral soils subject to forced modification near Resolute, N.W.T. Ground temperature, frost and water tables, and soil moisture were monitored at each site on 9 m^2 plots, allowing inter-comparisons in an attempt to assess how active layer development was related to changes in soil structure, hydrology and boundary conditions.

In organic soils, both the degree of humification and the position of the water table were the principal controls on active layer thaw. Developing organic soils with water tables near the surface had deeper thaw and warmer soil profiles than decomposing organics. The presence of ground ice also limits thaw depth because of large latent heat requirements for ice melt. In organic soils, both conduction and convection of heat are important processes. A feedback mechanism may exist whereby wetland organics are maintained by keeping the active layer shallow through a reduction in heat transfer when dry.

The responses of mineral soils to changing boundary conditions were inconclusive. Modifications to surface albedo, rainfall, snowfall and soil structure all affected soil parameters. Decreased albedo and increased snowcover had the greatest influence on active layer thaw when compared with unmodified conditions of the previous year. Placing a gravel pad over surfaces modified thaw depths in both mineral and organic soils.

The results of this study show the importance of hydrologic conditions, properties of surface organic layer, soil heterogeneity and ground ice on active layer thermodynamics. In all soils, heat flowing into the permafrost was the greatest component of the ground energy expenditure, followed by heat consumed in phase change and lastly by sensible heat used in warming the active layer. Current numerical models of active layer development are simplified, and this study shows that complexities not accounted for in models may hinder their ability to predict active layer responses to changing environments.

ACKNOWLEDGMENTS

TABLE OF CONTENTS

TABLE OF FIGURES

TABLE OF TABLES

CHAPTER ONE

Introduction

General Circulation Models (GCMs) of the earth's climate indicate that a doubling

of atmospheric CO_2 will increase global temperatures, with the greatest warming

occurring in the high latitudes (Ramanathan 1988). Specific models suggest that Arctic air

temperatures may warm 3°C to 6°C (Schlesinger & Mitchell 1987). Associated with this

warming is the possibility that climatically wetter conditions will prevail, with greater

summer rainfall and winter snow accumulation (Maxwell 1992). Climatic change has

numerous ramifications in hydrology; and in permafrost regions, hydrologic responses are

amplified due to the seasonal behaviour of energy and moisture fluxes (Kane *et al.* 1992).

These predicted changes represent the potential for large scale permafrost degradation as

thousands of square kilometers have ground temperatures within a few degrees of 0°C

(Smith 1990). Roots (1989) discusses more broadly the impacts of climate change on high

latitude regions with specific reference to Canadian issues.

In permafrost regions, both heat and water balances are fundamentally linked and

must be considered in conjunction when discussing possible environmental changes. Arctic

hydrologic processes have a distinct seasonality and latent heat fluxes are dominant in

many components of the hydrologic cycle: evaporation, transpiration, snowmelt,

condensation, soil freezing and thawing and sublimation (Hinzman & Kane 1992).

Although some hydrologic processes occur in the winter months, the majority of activity

takes place over the short summer beginning with snowpack ablation. In regions of continuous permafrost, hydrology is simplified as processes are essentially confined to a layer of seasonally thawed ground, termed the active layer. Woo (1986) and Van Everdingen (1987) present comprehensive treatments of hydrologic processes in permafrost environments.

In assessing the potential impact of climate change, researchers have often compared areas subject to different present-day climatic conditions to draw analogies (e.g. Woo 1990). Specific examples include the boundary between continuous and discontinuous permafrost moving northwards, changing fluvial regimes and thickening active layers. Most predictions, however, do not consider transitional phases of warming when, for example, ice-rich permafrost degradation may supersaturate soils creating thermokarst lakes. The change in permafrost hydrologic and thermal regimes cannot be considered jumps between equilibrium states, but a gradual transition as permafrost responds to disequilibrium conditions approaching one of stability (Woo *et al.* 1992).

A thickening active layer, due to warmer conditions forecast for the Arctic and sub-arctic, may lead to increased soil storage capacity which leads to dropping or removing of the perched water table characteristic of permafrost (Kane *et al.* 1992). This in turn may lead to a decline in the distribution of wetlands which cover large areas of permafrost regions. A reduction in wetlands will be accompanied by changes in the development and decomposition of peat and organic soil layers.

terrain and surface modification on active layer development through energy fluxes and hydrologic considerations.

By studying organic soils in different stages of growth and decay, it will be possible to predict the evolution of active layer development with reference to changes in local hydrologic conditions. The processes of heat transfer and the partitioning of energy within organic soils will also be assessed.

Forced modification of soils will show the short-term response of soil parameters, ground thaw and energy fluxes to changing surface boundary conditions. This will provide a greater level of understanding of present-day active layer heat balances, the processes involved and their potential for change.

1.2   Outline

Chapter 2 will outline the theory of ground energy balances and discuss the possible effects of changing environments with respect to this theory. Chapter 3 describes the study area and the methods used to analyze the data. Chapter 4 presents the field measurements and Chapter 5 the energy dynamics of the plots. Discussion of the results appear in Chapter 6, followed by conclusions and possible avenues for future research in Chapter 7.

CHAPTER TWO

Theory

This chapter will present the theory behind soil energy balances in the permafrost environment, water and heat movement within the active layer and the effects of changes to subsurface microclimates on active layer development.

2.1   Surface Energy Balance

The energy balance is an effective and proven method of accounting for fluxes of heat in boundary layer studies:

$$Q^* = Q_H + Q_E + Q_G \qquad (2.1)$$

where Q^* is the net all wave radiation at the surface, Q_H is the sensible heat flux, Q_E is the latent evaporative heat flux and Q_G is the ground heat flux term. Q^* can also be expressed as a function of short and long wave radiation,

$$Q^* = (1-a)K\downarrow + L\downarrow - L\uparrow \qquad (2.2)$$

where L is the long wave radiation, K is the short wave radiation and a is the albedo $(K\uparrow/K\downarrow)$. The arrows indicate the direction of flux. Lunardini (1981) presents a comprehensive treatment of heat transfer in cold climates.

In addition to the radiative energy which provides heat flux to the ground, convective heat flux through the infiltration of meltwater or rainwater is an additional heat source so that

$$Q_G = k \frac{dT}{dz}\Big|_{surface} + c_w \Delta T \frac{dF}{dt} \qquad (2.3)$$

where dT/dz is the temperature gradient in the vertical direction, k is the thermal conductivity of the soil, c_w is the volumetric heat capacity of water, ΔT is the temperature difference between the infiltrated water and the soil and dF/dt is the rate of infiltration.

This study will not explicitly examine fluxes of heat within the atmosphere, but will focus on the role of ground energy fluxes.

2.2   Subsurface Energy Balance

The subsurface climate is governed not only by the atmosphere and surface conditions, but by physical and thermal properties of the ground. In permafrost regions, heat flux into the active layer (Q_G) is consumed in warming the substrate and melting ground ice (Q_F),

$$Q_G = \int_0^{z_0} c_z \frac{\partial T}{\partial t} dz + Q_F \qquad (2.4)$$

where c_z is the bulk heat capacity, t is time, T is the ground temperature, z is depth and z_0 is the depth of zero temperature amplitude (Woo 1986). Instrumentation in this study does not allow for the measurement of temperatures beneath the active layer, thus, the active layer and the permafrost must be treated as separate layers. The one dimensional energy balance of the active layer can be considered

$$Q_G = Q_o + Q_s + Q_F \qquad (2.5)$$

where Q_O is the flux of energy into or from the permafrost, Q_S is the heat used in warming and cooling the active layer and Q_F is the latent heat related to the freezing or melting of ground ice.

Water in all its forms affects thermal properties and is the soil component which is most responsive to temperature changes (Farouki 1981). In permafrost soils, there is always some moisture movement caused by both thermal and moisture potential gradients. In turn, moisture distribution and redistribution affect soil temperatures. Heat and mass transfer have been recognized as the fundamental physical processes occurring in the active layer (Nakano & Brown 1971).

In developing equations for heat and mass transfer, for moisture flux,

$$\frac{\partial}{\partial z}\left(k'\frac{\partial H}{\partial z}\right) = \frac{\partial \theta w}{\partial t} + \frac{\rho i}{\rho w}\frac{\partial \theta i}{\partial t} \qquad (2.6)$$

and for heat flux,

$$\frac{\partial}{\partial z}\left(k\frac{\partial T}{\partial z}\right) = \rho c\frac{\partial T}{\partial t} - \lambda \rho i\frac{\partial \theta i}{\partial t} \qquad (2.7)$$

where k' is the hydraulic conductivity, H is the hydraulic head, θw and θi are fractional moisture and ice contents in the soil, ρ, ρw and ρi are densities of the soil, water and ice respectively, k is the thermal conductivity, c is the heat capacity, λ is latent heat of fusion, T is temperature, t is time and z is depth (Woo 1986). In theory, equations 2.2 and 2.3 can be coupled through the fractional ice content term; an approach commonly used in active

layer modeling. Difficulties in modeling active layer development arise as soil properties vary in the three coordinate directions. Furthermore, determination of soil hydraulic and thermal parameters is difficult as they change with time and with respect to each other. When modeling the active layer, equations 2.6 and 2.7 must be solved through finite difference or finite element techniques, as no exact solution exists (Lunardini 1981).

The flux of heat downward into the permafrost is,

$$Q_O = k \frac{dT}{dz}\Big|_{base} \qquad (2.8)$$

where dT/dz is the temperature gradient at the base of the active layer. The energy passing downward into the permafrost warms the soil to the depth of zero annual amplitude where an equilibrium exists with the geothermal heat flux.

Energy used to sensibly warm the soil column within the active layer is determined by,

$$Q_S = c \frac{dT}{dt} z \qquad (2.9)$$

where c is the heat capacity of the soil matrix and dT/dt is the daily variation in temperature over the depth of the active layer z.

The final term in the active layer energy balance is the amount of energy expended in melting the ice within the pores is,

$$Q_F = \rho \lambda f_{ice} \frac{dh}{dt} \qquad (2.10)$$

where f_{ice} is the fractional ice content, dh/dt the rate of ground thaw, ρ the density of ice and λ is the latent heat of fusion. The value of k is a function of compositional, volumetric and other structural factors discussed in section 2.2.1.

2.2.1 Soil Thermal Properties

Thermal conductivity, k, is a function of several factors including mineralogy, geometry of the pore space and the volumetric proportion of minerals, water (in all phases), organics and air. The determination of thermal conductivity is a difficult process in which several empirical approaches can be used. In this study, bulk thermal conductivity for a soil layer is estimated by (Farouki 1981)

$$k = k_m^{\Phi_m} \times k_w^{\Phi_w} \times k_i^{\Phi_i} \times k_o^{\Phi_o} \times k_a^{\Phi_a} \qquad (2.11)$$

where Φ_m, Φ_w, Φ_i, Φ_o, Φ_a, which sum to unity, are the volumetric fractions of mineral grains, water, ice, organics and air respectively. The subscripted k values are the individual thermal conductivities of the soil components: mineral, water, ice, organic and air. The thermal conductivity of constituents in W/(m °C) are estimated from (Hallet & Rasmussen 1993)

$$k_m = 3.6649 - 0.010893T + 2.9914 \times 10^{-5} T^2 - 3.1401 \times 10^{-8} T^3$$

$$k_w = -0.5818 + 6.357 \times 10^{-3} T_{abs} - 7.9663 \times 10^{-6} T_{abs}^2$$

$$k_i = -0.21286 + 670 / T_{abs} \qquad (2.12)$$

$$k_o = 0.25$$

$$k_a = 0.025$$

where k of the various constituents are often weakly temperature dependent. The thermal conductivity of organic material is related to the level of humification (Boelter 1969), yet for this study k_o is taken as 0.25 W/(m °C) for all organics.

The heat capacity of the soil, c, defined as the energy required to raise a specified volume of soil 1 °C is estimated from the equation (Farouki 1981)

$$c = c_m \Phi_m + c_w \Phi_w + c_i \Phi_i + c_o \Phi_o + c_a \Phi_a \qquad (2.13)$$

where the subscripted c values are the heat capacities of the soil constituents listed above. The values of specific heat capacities are shown in table 2.1 (de Vries 1963, Farouki 1981).

Table 2.1   Heat Capacity of Materials for calculation

Soil Component	Heat Capacity MJ/(m^3 °C)
mineral	1.926
water	4.180
ice	1.900
organic	2.508
air	0.00125

The behaviour of both k and c in permafrost soils is variable. The changes which occur within the pore spaces give thermal conductivity and heat capacity a distinct seasonality as ice is replaced by water, which in turn may be replaced with air.

Thermal conductivity and heat capacity can be expressed as a ratio,

$$\alpha = \frac{k}{c} \qquad (2.14)$$

where α is the thermal diffusivity, a term which indicates how temperature rises as heat diffuses through a substance.

The theory described by Fourier's law of conduction, and its assumptions, provide a method for describing subsurface climates. In reality, many of these assumptions are not valid due to the inability in obtaining adequate parameters in heterogeneous soils (Williams 1982). Most soils are stratified and changes in lithology, moisture content and physical properties exist among layers, causing thermal properties to vary in both time and space. Furthermore, differences between thermal properties of frozen and thawed soils along with changes in the soil moisture status that can either liberate or consume heat are both factors not considered in theory.

2.3   Effects of Environmental Change on the Active Layer

The possibility of environmental change in the Arctic has been outlined in chapter 1. How these changes, both natural and anthropogenic, affect the development of the active layer must be related to the theory of active layer heat flux outlined above.

Future changes to the natural environment can occur in response to changing climates. Both the magnitude and timing of winter snowfall and summer rain may be affected, modifying hydrologic regimes. Furthermore, changes in the amount of solar radiation reaching the surface, and the albedo of the surface, will alter the magnitude of ground heat flux.

The total depth and distribution of snow in time affects ground temperatures. Snow acts as an insulator, preventing ground heat loss as Q_G becomes negative in the

winter (Nicholson 1976, Rouse 1984). Increasing snow depth can result in substantial rises in mean annual ground temperatures, with some effect on summer thaw depth (Goodrich 1982). The seasonal distribution of snowcover is critical; snowfall in the autumn cools the active layer by melting after it initially falls on the warm ground surface, reversing the temperature gradient and drawing energy towards the surface (Hinzman *et al.* 1991). Spring snowmelt rate, although having little influence on annual soil temperatures (Goodrich 1982), delays heating of the ground surface by keeping snow-ground interface temperatures at 0°C. This reduces the total input of Q_G for the summer season, resulting in decreased thaw depths as more energy is expended as latent heat early in the summer to melt snow.

Changing snowfall and rainfall may affect moisture content of the active layer. Changes in soil moisture will potentially affect all components of the surface and subsurface energy balance. Rises in soil moisture will alter the partitioning of Q^*, increasing Q_E as more energy is consumed in evaporation. Greater evaporation in turn may act to cool surface temperatures, decreasing thermal gradients and reducing Q_G. Increased soil moisture raises thermal conductivity and heat capacity of the soil, affecting both Q_G and Q_S. Decreased soil moisture, particularly before the freeze-back period, will reduce the ground ice content and hence affect the Q_F and Q_S partitioning of Q_G.

Changes in surface albedo as a result of human disturbance are primarily associated with the disruption of vegetated surfaces, or changes in the moisture status of soils (Nelson & Outcalt 1982). Albedo change will affect Q* through equation 2.2 and

therefore, will indirectly modify Q_G in equation 2.1. In the absence of a change in soil moisture, the increase in Q_G will result in greater thaw depths and warmer ground surfaces.

2.3.1 Organic Material

In general, organic soils have higher specific heats, lower thermal conductivities and lower thermal diffusivities than well drained mineral soils (Moore 1987). The rate of thermal conduction in organic material is a function of humification (Boelter 1969). Undecomposed organic soils have a higher porosity, which decreases k. Pore space decreases as decomposition increases, raising thermal conductivity.

Unfrozen peat soils which are not completely saturated have low thermal conductivities due to large air contents in the organic matrix, providing excellent insulation for the underlying frozen material. Peat which is saturated does not have the same insulative ability, as water conducts heat more effectively. During summer, saturated organic soils may become dry at the surface, retarding heat transfer into the active layer as k is reduced. This reduction in thermal conductivity does not allow warm surface temperatures to penetrate beneath the organic layer. During the early autumn when precipitation increases, organic layers usually become saturated before freezing. As the saturated organics freeze, k approaches k_i, allowing great heat loss to the atmosphere in the winter. Furthermore, in the spring, significant amounts of latent heat are required to melt large volumes of ground ice. The large differences in thermal conductivity of organics

between thawed and frozen states allows permafrost to be maintained even in regions where the mean annual temperatures are slightly above 0°C (Williams & Smith 1989).

Water table position is a controlling factor in the development of the thawed zone in organic soils. If the surface remains saturated, heat can be effectively transferred downward into the soil. If the organic surface becomes dry, the processes described above limit thaw penetration, creating a shallow active layer.

2.3.2 Human Activities

Previous research on the effect of human activities has examined the response of site specific disturbances from changes in soil characteristics, vegetation cover, albedo or less distinct influences such as drainage dislocation (e.g. French 1980, Nelson & Outcalt 1982, Lawson 1986).

Compaction of tundra soils, which alters thermal and hydraulic properties, is the most common disturbance. Compaction increases thermal conductivity as there is more solid matter per unit volume, less air space and pore water per unit volume and better heat transfer across grain contacts (Farouki 1981). Increased thermal conductivity increases Q_G, thickening the active layer; a result commonly found in disturbed permafrost environments.

An entire branch of literature exists surrounding construction in permafrost environments. Engineers have long sought to insulate heated buildings from the permafrost using a variety of techniques attempting to minimize Q_G (Harris 1986). Placing a gravel pad over existing mineral soils is one technique used, as gravel is a thaw stable

aggregate. By placing gravel atop mineral soils, the stratigraphy of the soil column is changed. Thermal conductivity, heat capacity and albedo will change, affecting Q_G and the other components of ground heat flux. Furthermore, gravel as a substance has large pore spaces which do not create suction potentials; an important factor in mineral permafrost soils responsible for frost heave and ice segregation. The decreased specific yield of gravel soils will inhibit Q_E as water drains to the mineral layer beneath. The decline in Q_E, assuming no change in Q^*, will increase sensible heating of both the air and soil.

2.4   Feedbacks

Within an idealized system, both positive and negative feedback processes between different components of the energy balance occur. Changes in the ground surface affect the partitioning of energy within the atmospheric boundary layer. For example, if Q^* rises from decreased albedo, caused by increases in soil moisture, Q_E will increase as more soil water is available for evaporation. As soil water evaporates, Q_E will decline, and so will albedo, reducing Q^*. Soil moisture is an important component of both surface-atmosphere and subsurface energy balances as it controls energy partitioning and soil thermal properties. In soils with water tables at or near the surface, evaporation will be high, and sensible heating of the atmosphere and soil may be reduced. Soils with limited moisture will have greater proportions of energy directed to Q_H and Q_G. The experimental design of this study, however, does not allow for the determination of feedbacks as the atmospheric energy balance was calculated at only two sites. Furthermore, the scale of the

plots may allow for boundary layer effects and the forced disturbances do not truly represent equilibrium ground energy balances.

CHAPTER THREE

Study Area and Methods

3.0   Study Area

Field work was carried out approximately 5 km northeast of Resolute, Cornwallis Island, NWT (74°43'N,94°59'W) within the McMaster River Basin, where hydrologic studies have continued over the past 20 years (Figure 3.1). Physiographically, the area lies within the Innuition Region, which is characterized by a rugged northern topography with a more rolling topography to the south. The coastal areas, where this study was undertaken, are topographically less hilly with elevations below 200 m above sea level (Bostock 1970).

Geologically, the area is underlain by limestone and dolomite of the Allen Bay and Reed Bay formations (Thorsteinsson 1959). Surficial materials are predominantly composed of gravel and sandy loam covered by patchy tundra vegetation. Cruickshank (1971) subdivided these materials into 1. lithosols composed primarily of shattered limestone and gravel 2. polar desert soils made up of limestone and dolomite gravels in a sand silt matrix and 3. bog (or fen) soils which are characteristically sandy loam covered by peat, black lichen, mosses and vascular plants.

The distribution of soils within the McMaster River Basin is related to both geologic, topographic and hydrologic considerations. While polar desert soils predominate, bog soils are found where local water supply, such as lateral seepage, maintains the water table sufficiently close to the surface (Woo & Xia 1995).
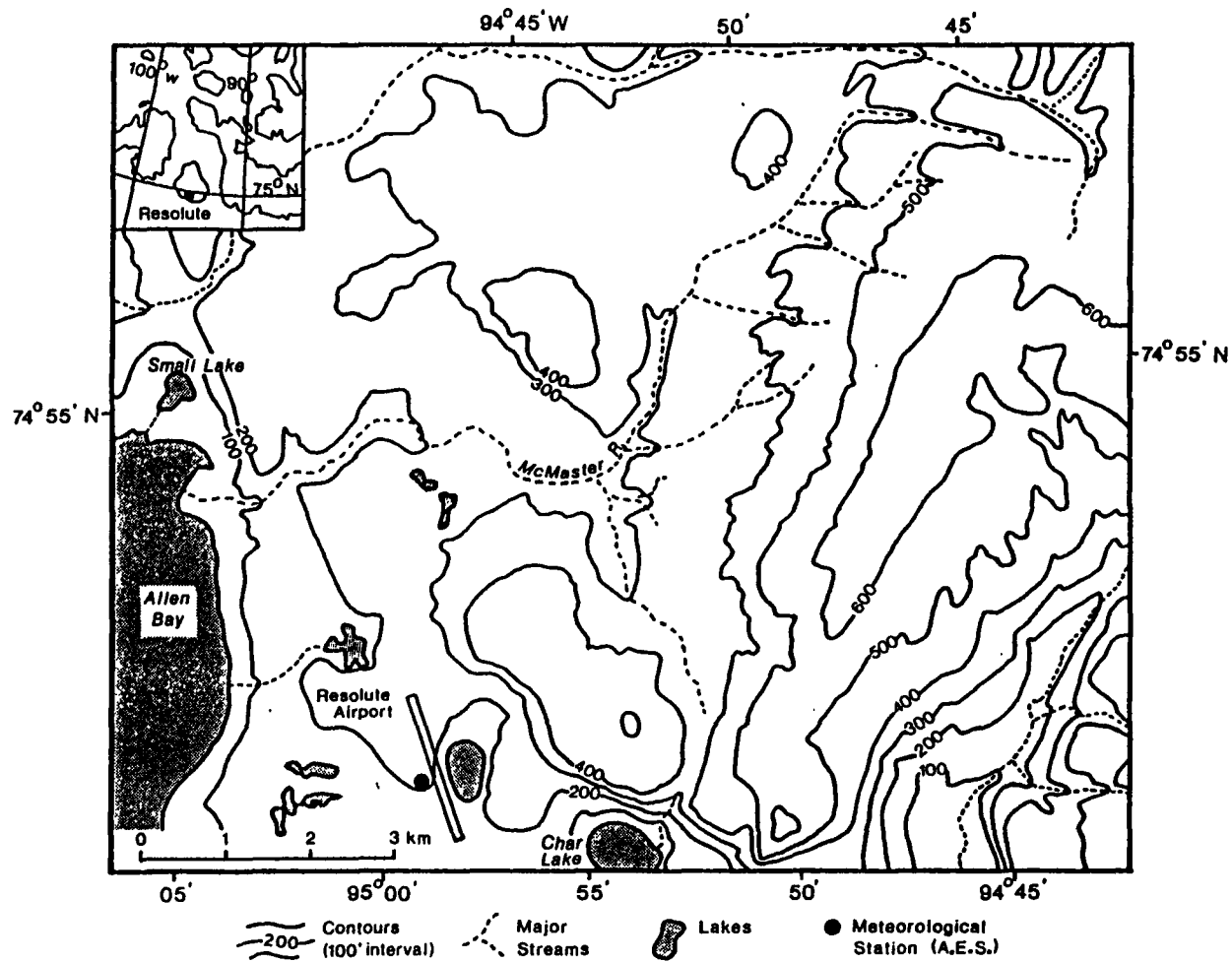
Figure 3.1 General location of the study area near Resolute, Cornwallis Island, Northwest Territories (from Steer 1983).

18

3.0.1 Climate

Maxwell (1980) places the study area climatically in the northwestern zone of the Canadian Arctic. Polar night lasts from November 4 to February 5 and 24 hour daylight from April 30 to August 15. This extreme asymmetry in the radiation regime contributes to the low annual temperature, which is -13.5°C at the Resolute Airport. Summer temperatures are generally below 10°C with winter temperatures reaching -35°C.

Mean annual precipitation is very low for this region, with the Resolute weather station recording an average of 130 mm; 80 per cent of which falls as snow. This value is considered an underestimate as redistribution of snow by wind to topographically low regions and undercatches by gauges provide for significant error (Woo *et al.* 1983).

3.0.2 Permafrost

Permafrost is defined as ground which remains below 0°C for more than two consecutive years, regardless of other properties such as moisture content and lithology (Washburn 1979). The thickness of permafrost in the Arctic varies, a function of past and present climates and the geothermal heat flux. At Resolute, permafrost thickness is estimated at 390 m (Meisner 1955), which may decline if the climate becomes significantly warmer in the future.

The zone lying above the permafrost subject to annual freeze and thaw is termed the active layer. In regions of continuous permafrost, hydrologic activities are essentially confined to this region. Typical active layer thickness near Resolute is 50 cm with significant variation primarily due to slope, aspect, drainage characteristics, vegetation and

Figure 3.2   Air Photo of Study area. 1. is the general location of the *Fen*, *Isolated* and *Desiccated* sites, 2. is the location of the *Wetland, Palsa* and *GravOrg* sites and 3. is the location of the polar desert soils. The approximate distance between sites 1 and 3 is 1 km.
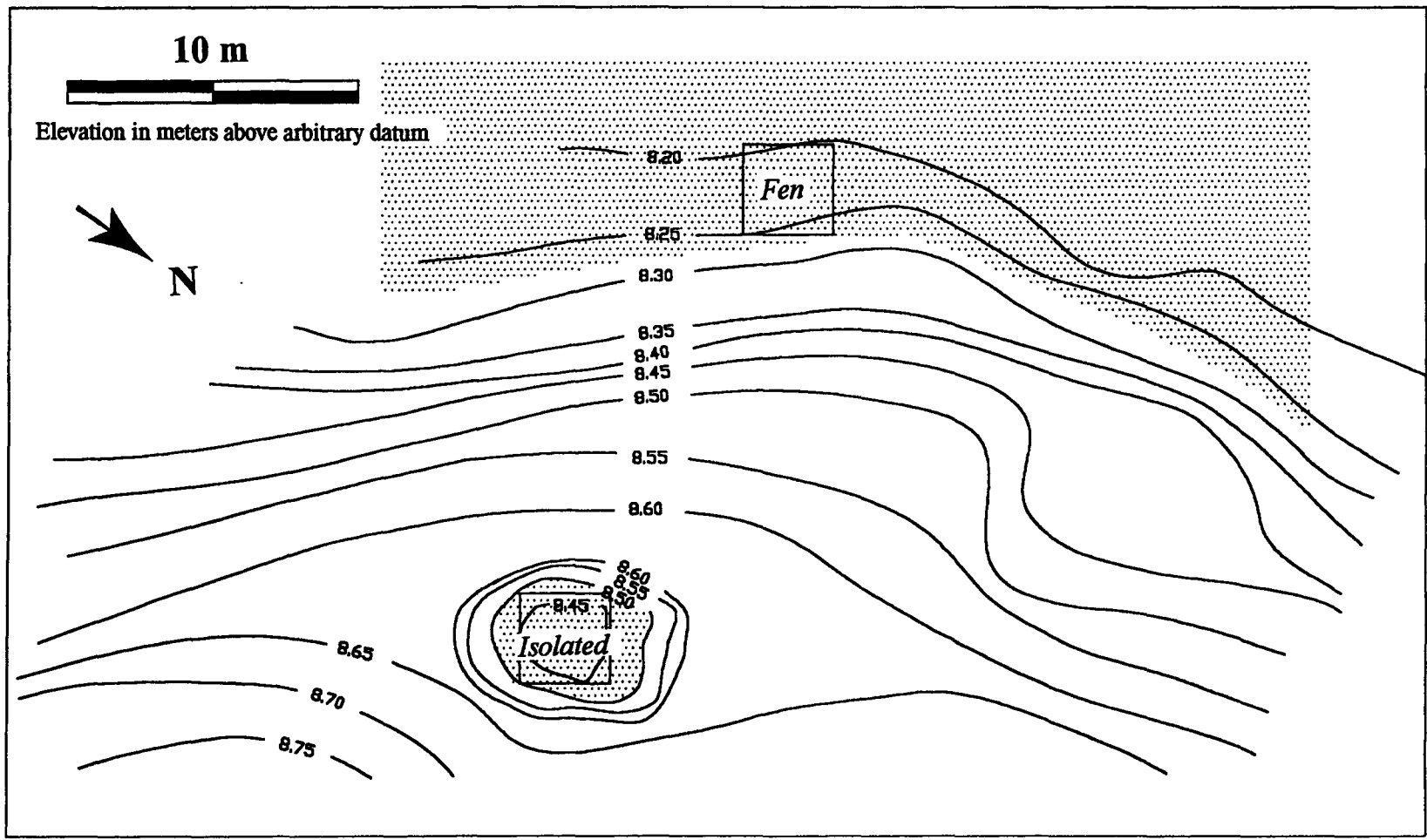
Figure 3.3 Map of the *Fen* and *Isolated* sites. The shaded area represents zones where the soil is saturated.
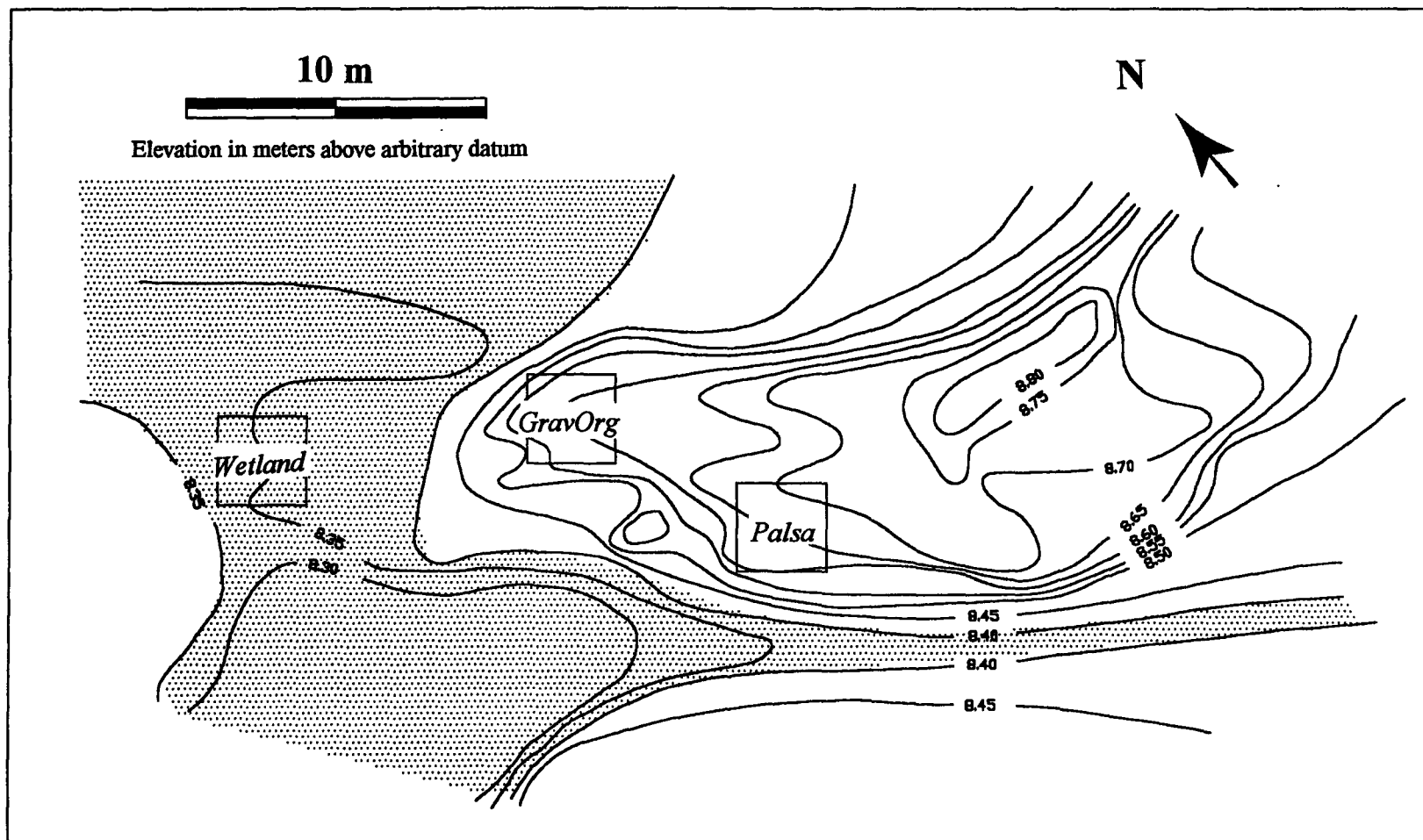
Figure 3.4 Map of the *Wetland, Palsa* and *Isolated* sites. The shaded area represents zones where the soil is saturated.

Some decomposition had occurred near the base of the organics, and is inferred to have undergone more development than at the *Fen* site.

The final plot containing developing organic material (*Isolated*), was located in a small depression bounded by polar desert soils (Figure 3.3). The only sources of water were snowmelt and rainfall as minimal lateral inflow occurred. A 5 cm moss/sedge mat overlaid a highly anoxic silty clay. The organic soil, although having some sedge growth at the surface, was heavily humified at depth. Decomposition occurs because late in the summer, evaporation exceeds the precipitation inputs necessary to maintain a water table near the surface.

At the *Palsa* site, the organic soil has ceased to develop. Although located only 10m from the *Wetland* site (Figure 3.4), it was raised from the surrounding organic terrain by an ice-core (Figure 3.5). This heaved mound prevented lateral supply of water from the late lying snowbank. The organic layer consisted of the same material as the *Wetland* site, with a 7 cm moss/sedge mat overlying a silty clay substrate. The organics had undergone moderate humification (Figure 3.5). The thickness of the organic layer on the ice core was irregular, and there were occasional pockets of void separating the organic material from the mineral soil.

The organic soil representing an advanced level of humification was termed the *Desiccated* site (Figure 3.6). It consisted of long dead, highly decomposed organics which extended to depths greater than the active layer (Figure 3.7). Water sources were snowmelt and rainfall, neither of which was sufficient to saturate the soil. The surface had

Figure 3.5   Ice core at the *Palsa* site.

10 m

Elevation in meters above arbitrary datum

N

8.80
8.85
8.90
8.95
9.00
9.05
9.10
9.15
9.20
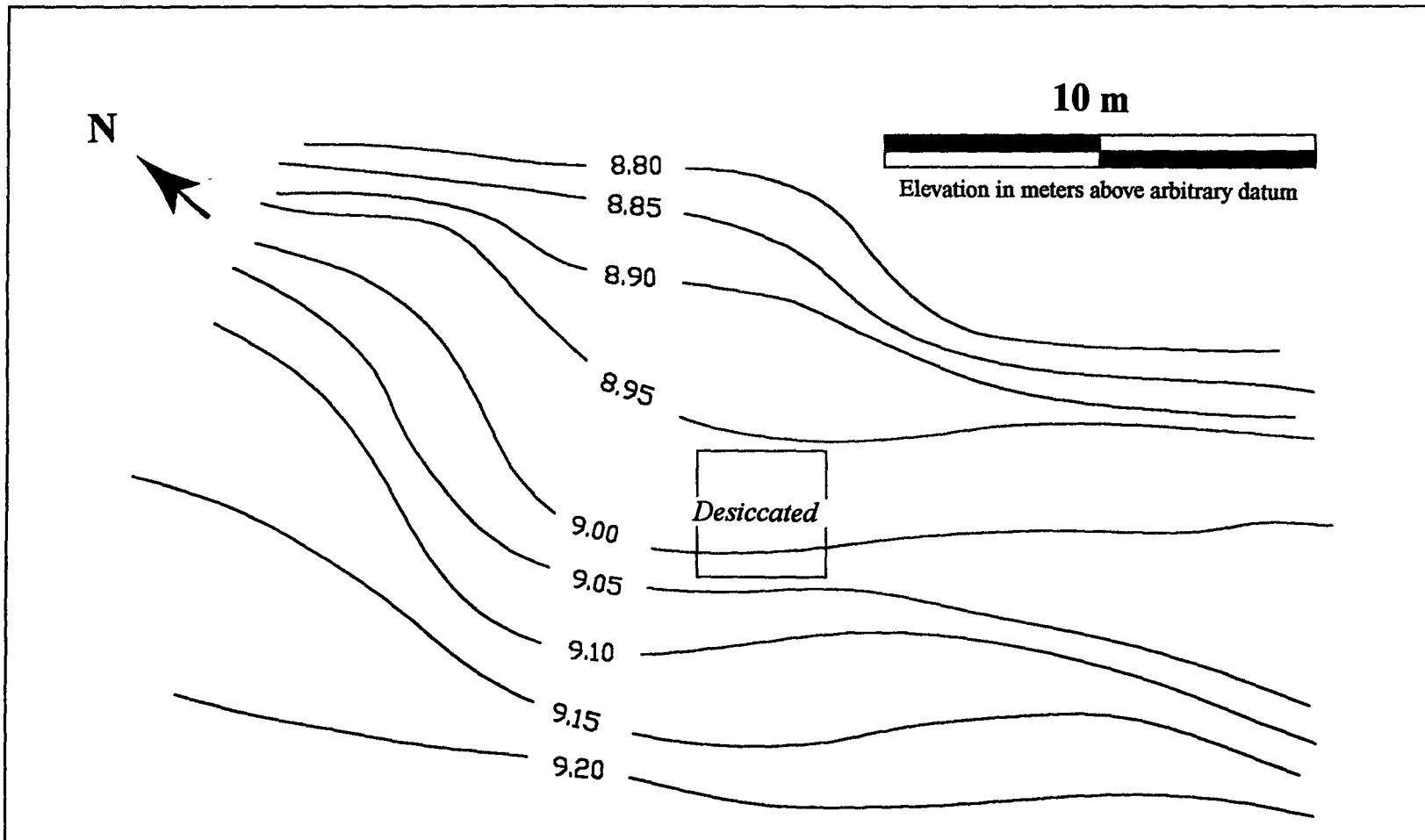
Desiccated

Figure 3.6   Map of the *Desiccated* site.

Figure 3 7   Humified organic soils at the *Desiccated* plot.

a desiccated appearance with some lichen growth. This plot has been isolated from its former later water source, once a late lying snowbank whose drainage pattern had shifted for at least centuries. Prior to this, the organics grew under favorable conditions to accumulate thick layers of peat.

The final organic soil, *GravOrg*, falls under the second set of experiments. In 1994 a 10 cm gravel pad was placed atop an organic mat to determine the effect thaw-stable aggregates and stratigraphic modification on ground thaw. The plot was adjacent to the *Palsa* site (Figure 3.4) with similar organic material and an ice rich core.

3.1.2 Polar Desert Soils

Polar desert soils were the primary substrate used to assess the short term response of the active layer to forced environmental change. The study area was located on an area of level terrain to minimize slope effects between a fen and a track created by repeated usage of all terrain vehicles (ATV) (Figure 3.8). The experiments were conducted on nine $9m^2$ plots which were assumed large enough to show variations among the treatments, yet separated by a sufficient boundary to minimize the masking of the effects of the modifications.

Modifications were divided into two groups: environmental change and human disturbance. Changes to rainfall, surface albedo and snowcover were assessed under the framework of a changing environment while surface compaction and placing a gravel pad over the surface were considered human disturbances.
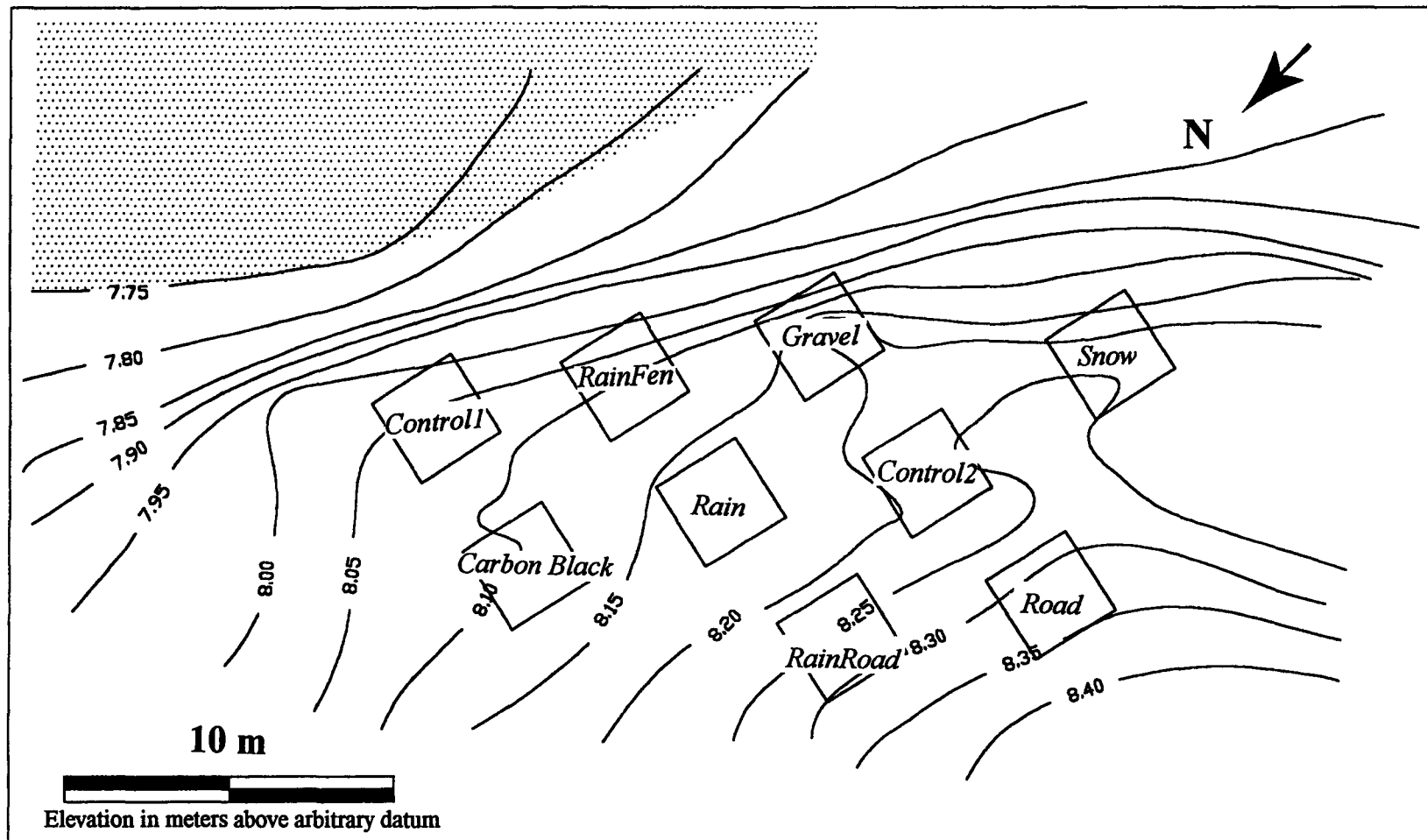
Figure 3.8 Map of the polar desert study area. The shaded area represents zones where the soil is saturated.

Warmer and wetter conditions are predicted for the Arctic by GCMs under an increase of greenhouse gasses in the atmosphere. A rainfall simulator was used to assess the effect of increased rainfall on three plots: *RainRoad*, located on a compacted ATV road, *Rain* near the center of the study site and *RainFen* adjacent to the fen (Figure 3.8). The distribution of the three plots helped to isolate the effects of the rainfall from those of the road and the fen. Determining the influence of increased rainfall on soil moisture is critical as water plays a key role in affecting the soil thermal properties and transferring heat within the active layer. Both hydrologic and thermal regimes will respond to increased rainfall, potentially affecting the water table position, evaporation, ground ice and heat transfer processes.

The relationship between soil moisture and albedo is well established (Nelson & Outcalt 1982). A reduction in albedo enhances Q_G through equation 2.2 and 2.1. To isolate the effects of increasing Q_G by lowering the albedo, carbon black was spread over an experimental plot (*CarbonBlack*) immediately after snowmelt. Increased Q_G may also be a surrogate for warmer atmospheric temperatures which increase the proportion of the ground heat flux in the surface energy balance (equation 2.1).

The total depth and duration of the snow cover affect the thermal regime of the active layer. The greater the depth of snow, the greater the insulation as snow is an effective mechanism for preventing ground heat loss in winter (Nicholson 1976, Goodrich 1982, Rouse 1984). The *Snow* plot was used to assess the effects of an increased snowpack on active layer development. In this study a snow fence was constructed in the

fall of 1994 to increase winter snow accumulation, but it failed to work as the prevailing winter winds blew from the southeast as opposed to the climatically normal, northwest. In the spring, snow had to be removed from the zone of excess snow to cover the experimental plot to approximately double the winter snowfall. This is analogous to having a heavy snowfall just prior to melt.

The most common form of disturbance from human activity is compaction, altering soil thermal and hydraulic properties. In general, modification of soil properties causes the active layer to thicken by increasing soil thermal conductivity. More solid matter per unit volume, less air space and pore water per unit volume and better transfer across grain contacts are three causes outlined by Farouki (1981) to explain increased k as bulk density increases. An ATV road (Figure 3.9) which has been used for approximately ten years provided the necessary disturbance for examining the role of surface compaction on ground thaw. Two plots were established on the road; *RainRoad* previously discussed and *Road*, not subjected to simulated rainfall.

While construction practices compact soils, buildings modify the thermal regime of the soils they overly. Engineers have long sought to insulate heated buildings from permafrost using a variety of techniques (Harris 1986). Gravel is often used as a thaw-stable aggregate, preventing heave and providing nominal insulation. The final modified plot (*Gravel*) had a 10 cm gravel pad overlying polar desert soil. In effect, this treatment changed the stratigraphy of the soil profile.

Figure 3.9 All-terrain vehicle path on the polar desert soils.

Two control plots (*Control1*, *Control2*) served as benchmarks to which the other experiments were compared. *Control1* was located nearer to the fen than *Control2*, in the approximate center of the polar desert study area (Figure 3.8). This positioning helped determine the influence of the fen on active layer temperatures, moisture and thaw depths.

3.2   Field Methods

Two fully instrumented micro-meteorological towers operated throughout the study period; one located adjacent to the *Wetland* site and the other in a region near the polar desert soils. Temperature and relative humidity were recorded using a Campbell 207 probe housed in a Gill radiation shield 1.5 m above the surface and by three levels of wet and dry copper/Constantan thermocouples each in a housing with radiation shielding and ventilated by a 12 volt fan. Wicking from a water bottle was supplied to one of the thermocouples in each housing. The housings were separated by 0.5 m, the lowest being at 1 m. Net radiation was measured using Middleton net radiometers situated 1.5 m above the ground. Upward and downward short-wave radiation was measured with Eppley pyranometers mounted on a tripod. The location of the pyranometers was moved to measure the albedo of various surface. All instruments were connected to a Campbell CR-10 data-logger, sampling every 15 minutes and recording hourly averages.

A detailed snow survey was carried out on June 1 (JD 152), dividing each plot into nine 1 m^2 cells and taking depth measurements at each node. Snow density measurements were taken at 14 locations adjacent to the plots using and Eastern Snow Conference snow

sampler to establish snow water equivalence above each site without disturbing the snowcover.

During snowmelt, measurements of ground temperature began. Soil temperature was measured at the center of each plot using copper/Constantan thermocouples, installed the previous summer and wired to a Campbell CR-10 data-logging system. Sampling time was 15 minutes with an output averaged over one hour. The depths of the thermocouple junctions were variable. In organic soils, depths were at 2, 10 and 25 cm along with a junction at the organic/mineral interface (Table 4.4). All of the polar desert plots had temperatures measured at 2, 10 and 50 cm. Furthermore, *Control1* and *Control2* had additional junctions at 5, 10 and 25 cm.

Frost table was measured every second day at each plot by pounding a steel bar into the soil until frozen ground was reached. Water table was also recorded bi-daily in perforated PVC wells of various diameters using an electronic beeping device which closed a circuit upon contact with water. A stocking was used to cover the wells ensuring the passage of water into the wells while restricting sediment input.

Natural rainfall was measured using a Texas Electronics tipping-bucket rain gauge. The rainfall simulator consisted of a reservoir to which water was added through a tube and several hundred small nozzles were located at the bottom of the reservoir to simulate precipitation (Figure 3.10). The rainfall simulator was calibrated so each artificial event had a duration of approximately 1 hour, depositing 1 cm of water on the plot. The
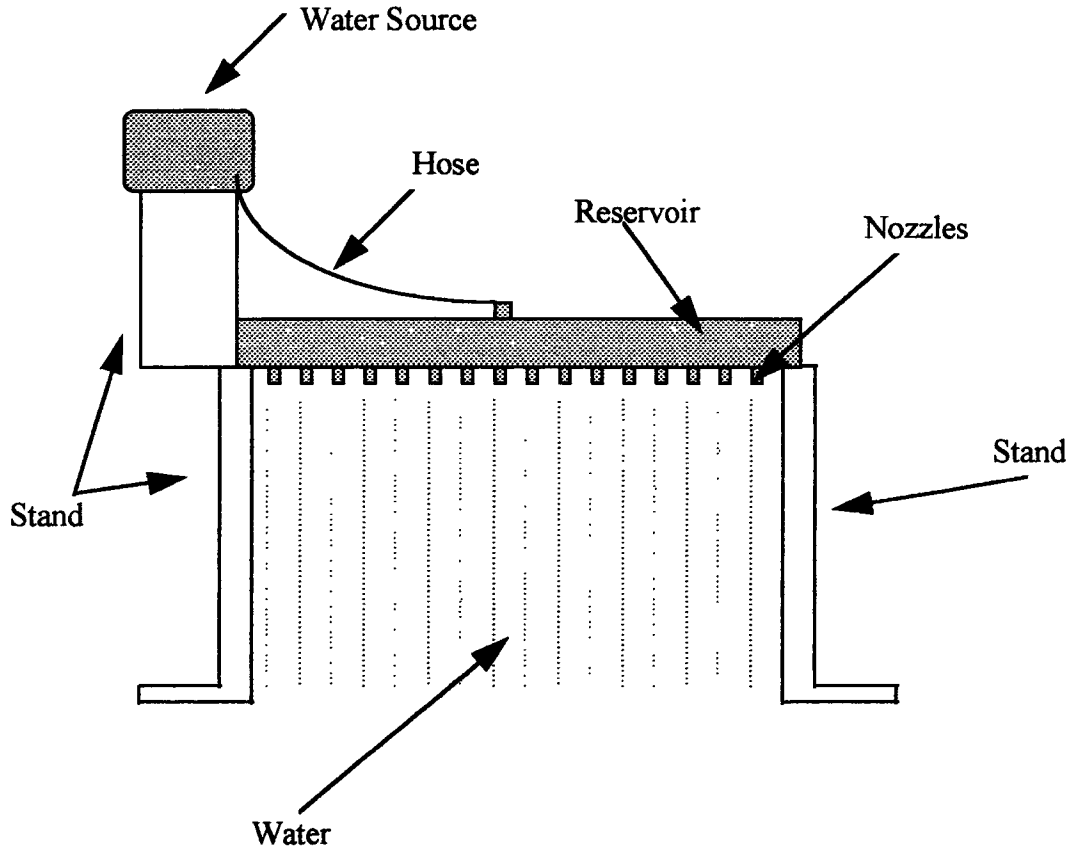
Figure 3.10 Schematic diagram of rainfall simulator. The dimensions of the reservoir are 1.5 m x 1 m. The intensity of the rainfall is 10 mm per hour.

intensity was not constant as a stable head was not maintained in the water source. The rainfall simulator was centered over the plots as it had a dimension of only 1.5 m by 1 m. Artificial rainfall began immediately after the soil became sufficiently dry to support the rainfall simulator, and was repeated approximately every second day depending on soil moisture and natural rainfall events. Water for the simulator was obtained in an adjacent fen prior to the simulations.

3.2.1 Soil Parameters

Several calculations of porosity, bulk density and organic content were completed for the soil layers of each plot. Porosity, n, is defined as the volume of voids relative to the total volume of the soil sample,

$$n = 1 - \frac{\rho_b}{\rho_s} \qquad (3.1)$$

where ρ_b is the bulk mass density and ρ_s is the particle mass density. The bulk mass density is the oven dried mass of a sample divided by its field volume which was determined by the water displacement technique. Particle mass density for the polar desert soils was estimated at 2650 kg/m^3.

Obtaining the density of organic soils is more difficult,

$$\rho_d = \frac{M_d}{V_d} = \frac{\rho_w W_d}{(W_d - W_s)} \qquad (3.2)$$

where ρ_d is the density of dry organic material, ρ_w the density of water, M_d the dry mass in air, V_d the volume of the dry organic substance, W_d and W_s are the dry weight in air and

the weight submerged in water. Precise determination of bulk density was possible by cutting organic soils to a known dimension and drying them in an oven at 105 °C for 24 hours at McMaster University. Particle mass density of organic soils was calculated by displacing known weights of dry organics in water.

For both organic and mineral soils, water content on a volumetric basis (ϕ_v) is,

$$\phi_v = \frac{(M_w - M_d)}{\rho_w V} \tag{3.3}$$

where V is the field volume of the sample. Surface soil water content was determined on a minimum bi-daily basis for the polar desert plots and the organic soils subject to short term changes, (*Palsa, Desiccated, GravOrg*) by grab samples.

Organic content for the mineral soils was determined from combustion tests. Ice content of the soil was estimated from melted soil samples broken out of the frozen soil at the beginning of the study period. Ice content of the polar desert soils was assumed to be constant with depth.

3.3   Energy Balance Calculations

Various components of the ground energy balance (equation 2.5) were determined from averages of daily soil temperatures and from parameters based on the volumetric composition of the soil (equation 2.11, 2.13). Q_G (equation 2.3) was calculated as

$$Q_G = k \frac{T_{z1} - T_{z2}}{(z_2 - z_1)} \tag{3.4}$$

where T_{z1} is temperature measured at the 2 cm thermocouple, T_{z2} is the 10 cm temperature in the polar desert soil and the interface temperature in the organic soils, z_1 and z_2 are the

position of the thermocouples and k is the thermal conductivity (equation 2.11) of the layer. The time step for the calculation was one day. Convected heat from rainfall was considered negligible.

Outgoing heat flux to the permafrost (equation 2.8) was determined by,

$$Q_O = k_f \frac{T_{0^o} - T_b}{(z_b - z_{0^o})} \qquad (3.5)$$

where the T_{0o} is the 0°C temperature, T_b is the temperature at the bottom thermocouple, z_{0o} is the position of the 0°C isotherm as inferred from frost table position, z_b is the depth of the bottom thermocouple and k_f is the thermal conductivity of the frozen layer. As the frost table approached the deepest thermocouple, errors were generated from the imprecision in the position of the 0°C isotherm as determined from frost table probing and the denominator becoming very small, generating spurious values. In these cases, Q_O was calculated as

$$Q_O = k_{(z2-b)} \frac{T_{z2} - T_b}{(z_b - z_2)} \qquad (3.6)$$

where T_{z2} is the 10 cm temperature and $k_{(z2-b)}$ is the thermal conductivity of the layer between 10 cm and the bottom thermocouple. Over the entire season, both methods provided similar values of Q_O independently.

Sensible heating of the active layer (equation 2.9) was calculated as

$$Q_S = \sum Q_{S_l} = \sum c_l \frac{(\overline{T}_{t+1} - \overline{T}_t)_l}{\Delta t} z_l \qquad (3.7)$$

where Q_{sl} is the sensible heating of a layer, Δt is a one day time step, c_l the heat capacity of a layer (equation 2.13) , z_l the layer thickness and T the average daily temperature of a layer with a one day time step. In organic soils, Q_{Sl} was determined for both the organic and mineral substrate while the polar desert soils were divided into 2 to 10 cm and 10 to 50 cm layers. The plots with the gravel pad placed atop the soil (*GravOrg, Gravel*) had Q_S calculated from three layers. The rationale behind dividing the soil into layers was the non-linearity of the temperature profile over the entire depth of the active layer.

Latent heat of fusion (equation 2.10) was determined as

$$Q_F = \lambda \phi_i \frac{\Delta z}{\Delta t} \qquad (3.8)$$

where λ is the latent heat of fusion (333.7 MJ/kg), ϕ_i is the volumetric content of ice and $\Delta z/\Delta t$ is the daily decline in the frost table as determined from probing.

CHAPTER FOUR

Field Measurements

Field observations were made between June 1 (JD 152) and August 6 (JD 218), 1995. This chapter presents values obtained from instrumentation and manual surveys.

4.1 Weather Conditions

The study period (June 9 to August 6) was both warmer and drier than the climatic means for Resolute. Furthermore, the winter snowfall accumulation for 1994-1995 was greater than average (Maxwell 1980). Figure 4.1 shows air temperature for the study period. Temperatures rose above freezing at the beginning of the study, reached maximum values in late June and early July and then declined near the end of the study. The mean daily temperature for this period was 3.7°C.

4.1.1 Snow Cover

A snow survey on June 1, 1995 established the mean depth of snow accumulation and snow water equivalence over each experimental plot. For the polar desert soils, this survey was completed prior to any melt, while several of the organic soils had experienced melt and were virtually snow free. Table 4.1 contains the average snow depths and water equivalence for the plots.
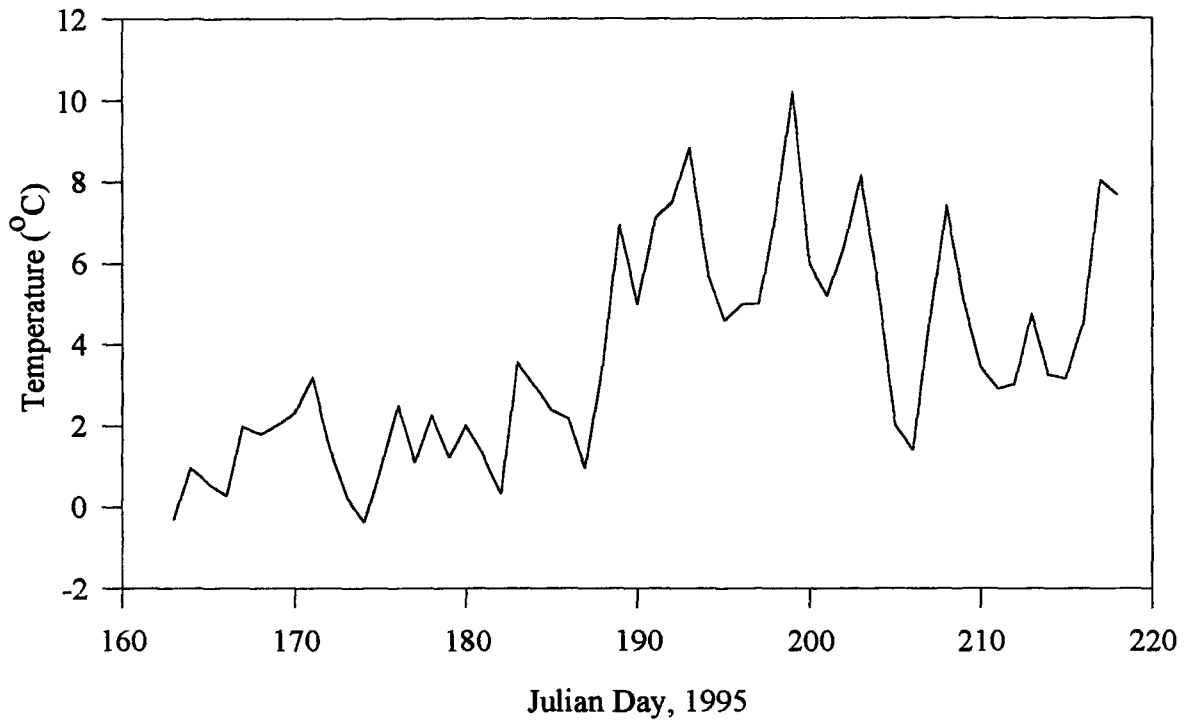
Figure 4.1. Mean daily air temperatures for the wetland site, 1995.
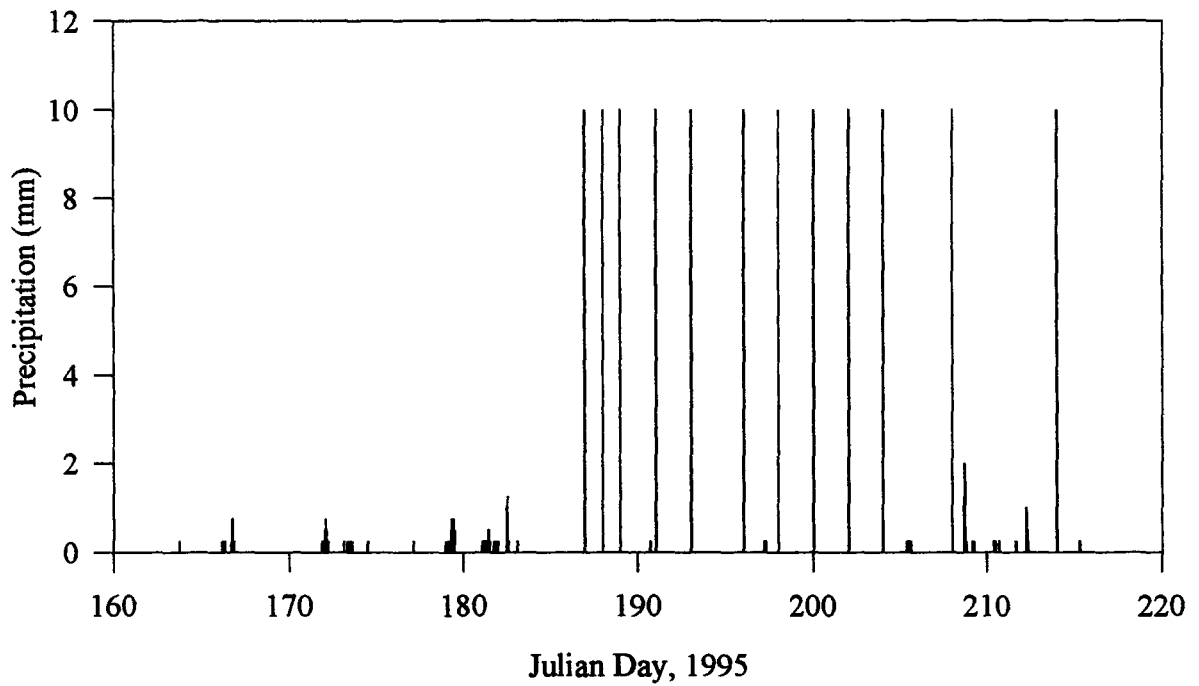
Figure 4.2. Daily precipitation for both natural and simulated rainfall. All artificial rainfall events have a magnitude of 10 mm.

Table 4.1   Snow Survey Results, June 1 1995

Plot	Average Snow Depth (cm)	Water Equivalent (mm)
Control1	48	177
Control2	60	333
Carbon Black	52	192
Snow	111	411
Rain	50	184
RainFen	57	211
RainRoad	55	202
Road	60	221
Gravel	62	229
Fen	40	146
Wetland	24	89
Isolated	30	111
Palsa	1	3
Desiccated	0	0
GravelOrg	9	35

The mean snow depth for the polar desert study area was 55 cm with a standard deviation of 6 cm. Mean snow water equivalence was 204 mm with a standard deviation of 23 mm. The *Snow* plot had approximately twice the snow depth and water equivalence of the surrounding polar desert study area. The snow accumulations over the organic soils were much more variable as they were located far apart. The *Desiccated* site had no snow on the day of the survey. Snow cover disappearance, which marked the beginning of active layer thaw, was completed at all sites by June 20.

4.1.2   Precipitation

Only trace amounts of snowfall fell in the summer as most precipitation fell as rain. Figure 4.2 shows precipitation for 1995 and the simulated rainfall. Only 28 mm of rain fell in 1995, which can be considered a dry year (Steer 1983). The total precipitation on the

plots subject to artificially increased rainfall was approximately 158 mm. Although more

than five times the rainfall experienced in 1995, it is less than twice the value of 90 mm of

rain which fell in 1994. The simulated rainfall may be considered to be representative of an

extremely wet year.

4.2   Organic Soils

Each of the six organic soils examined in this study have different structural

properties. Table 4.2 summarizes the bulk density and porosity of the organic soils and

their underlying mineral soils.

Table 4.2   Organic Soil Physical Properties

Site	*Organic Soil* Bulk Density (kg/m³)	Thickness (cm)	Porosity	*Mineral Soil* Bulk Density (kg/m³)	Porosity
Fen	37	8	0.80	1193	0.55
Wetland	48	8	0.91	1246	0.53
Isolated	93	5	0.60	1219	0.54
Palsa	34	7	0.79	1033	0.61
Desiccated	557	25+	0.41	-	-
GravelOrg	130	4	0.50	1045	0.60
gravel pad	1800	10	0.32		

Combustion tests indicate that approximately 10 per cent by volume of the solid

matter in the mineral soils is organic material. Although there is little variation in mineral

soil properties, the organic soils vary considerably, showing some relation to the degree of

humification. The *Desiccated* site is the most obvious anomaly with a bulk density

approaching those of the mineral soils. The *Isolated* site has the second highest bulk

density because of humification occurring beneath the sedge cover. The differences among

the other sites are small but compaction of the organic layer beneath the gravel pad (*GravOrg*) greatly increases bulk density and reduces porosity.

4.2.1 Organic Soil Temperatures

Soil temperatures throughout the study period are shown in Figure 4.3 (*a-i*). At the beginning of the measurement period, the three plots with developing organic layers were covered with snow and temperatures remained below 0°C throughout the profile. The other three organic plots were snow-free with near surface temperatures above freezing. On June 8 (JD 159), temperatures at 2 cm for the *Palsa* and *GravOrg* plots exceeded 10°C, providing the largest temperature gradients for the entire season as warmer conditions had not yet penetrated to depth.

The temperatures at the 2 cm, organic-mineral soil interface and 10 cm depths responded rapidly to surface temperature fluctuations later in the summer as temperatures rose above 0°C. When temperatures at depth were below freezing, they rose slowly towards 0°C as significant quantities of energy were required to raise temperatures and melt ground ice. Once the temperature at a specified depth rose above 0°C, temperatures responded rapidly to surface heating.

The period over which the temperatures were recorded varied and by June 19 (JD 170), temperatures were taken at all plots. The average soil temperatures for different depths between June 19 (JD 170) and August 6 (JD 218) are shown in table 4.3.
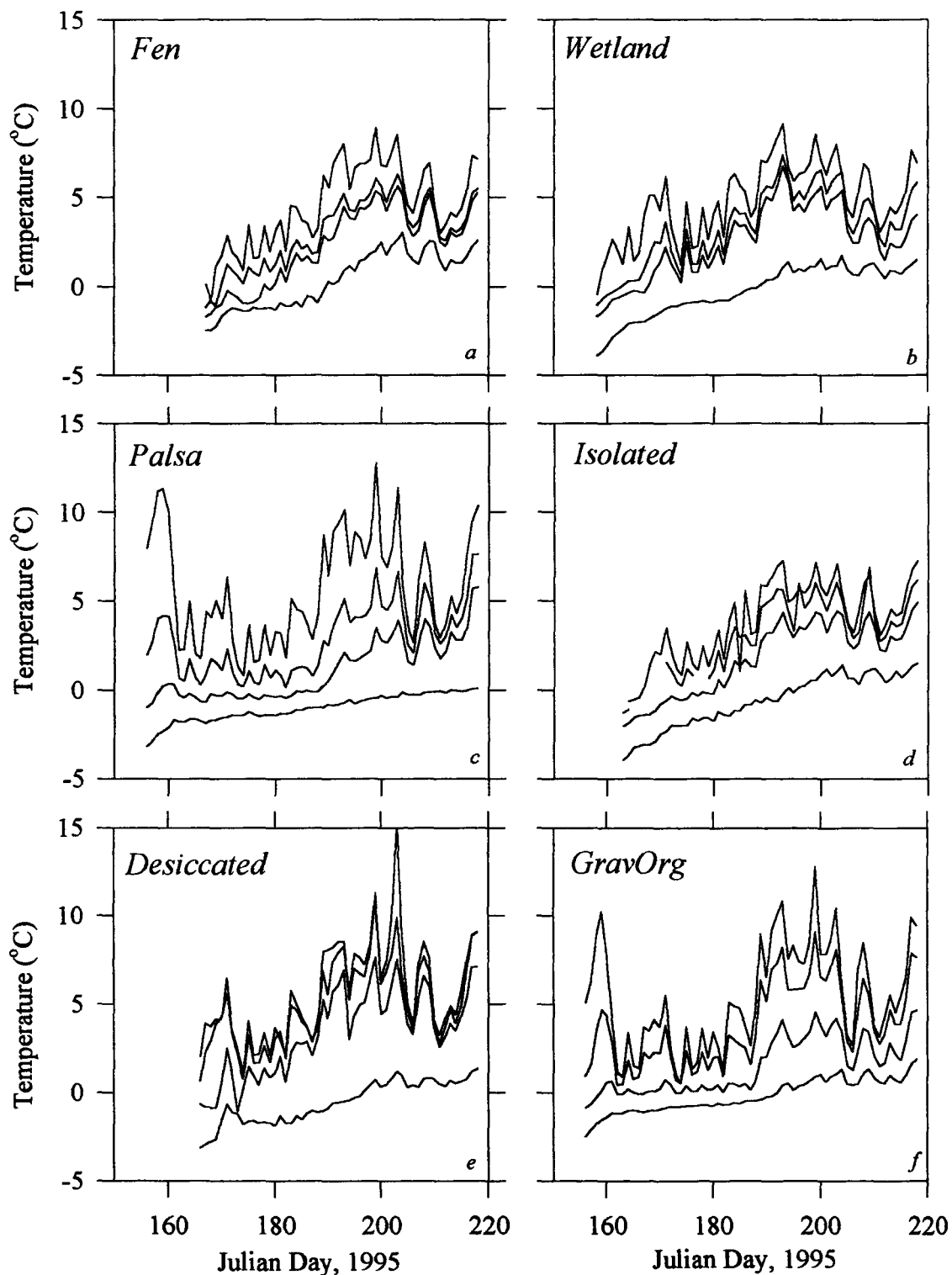
Figure 4.3 (*a-f*) Plots of daily average temperature vs. depth for the organic soils. The lines represent from the warmest to the coolest temperatures, the 2, interface, 10 and 25 cm thermocouples.

Temperature fluctuations are dampened progressively with depth.

Table 4.3   Average Organic Soil Temperatures - Julian Day 170 to 218

Site	2 cm (°C)	Interface (°C)	10 cm (°C)	25 cm (°C)
Fen	4.81	3.26 - 8 cm	2.53	0.55
Wetland	5.38	4.06 - 8 cm	3.23	0.31
Isolated	4.35	3.66 - 5 cm	2.23	-0.26
Palsa	5.69	3.08 - 7 cm	1.47	-0.72
Desiccated	5.86	5.21 - 5 cm	3.70	-0.36
GravOrg	5.66	4.28 - 10 cm	1.93 - **14 cm**	0.14

The highest average surface temperatures were recorded at the plots which did not have lateral inflow. The *Desiccated* surface was the warmest because of it's low surface albedo. The *Palsa* and *GravOrg* sites, which had low water contents at the surface, were also comparatively warm. The *Wetland* plot, which was humified, had high surface temperatures and warm temperatures down to 25 cm.

The temperatures at the interface between the organic and mineral layers (except for the *Desiccated*) followed different patterns. The saturated organic soils were warmer at the organic-mineral interface while the *Palsa* site, with a warm surface, exhibited coolest interface temperatures. This reflects both the insulative ability of the organic layer at the *Palsa* site and more efficient methods of heat transfer in saturated soils. By 10 cm, the temperatures were noticeably different between most plots. The *GravOrg* site had a large drop in temperatures between 10 cm and 14 cm, a layer consisting of compacted organics which did not transfer heat as efficiently as mineral soils. The *Palsa* and *Desiccated* plots were the two sites which had the lowest temperatures at 25 cm. The ability of dry peat to prevent the downward transfer of heat is clearly shown in the *Palsa*

site. The *Desiccated* site also had cold average temperatures at depth and a shallow active layer. The *GravOrg* site, with 10 cm of gravel placed on a soil similar to the *Palsa* site, showed warm surface and 10 cm temperatures reflecting improved heat transfer in gravel. By altering the soil stratigraphy, 25 cm at this plot had the same soil characteristics as the 15 cm level at the *Palsa* site, yet temperatures were slightly lower. While the thawed zone was thicker in the *GravOrg* site, the active layer depth was shallowest within the mineral soil. Soils with high water tables and actively developing organic surfaces had the greatest 25 cm average temperatures, again reflecting the improved ability of saturated soils to transfer heat.

The daily temperature trends were variable between each plot, reflecting the ability of the soils to gain and lose heat. The magnitude of temperature change on a daily basis can be assessed by examining the temperature ranges at each depth. Table 4.4 shows the average daily temperature amplitudes between July 9 and August 6, a period without measurement interruption for all thermocouples.

Table 4.4   Daily Organic Soil Temperature Range - Julian Day 190 to 218

Site	2 cm (°C)	Interface (°C)	10 cm (°C)	25 cm (°C)
Fen	5.41	4.02 - 8 cm	3.63	2.46
Wetland	5.32	3.35 - 8 cm	2.81	1.27
Isolated	4.86	3.78 - 5 cm	3.59	2.33
Palsa	9.11	5.33 - 7 cm	3.67	0.91
Desiccated	8.14	6.49 - 5 cm	5.30	2.18
GravOrg	9.14	5.94 - 10 cm	3.35 - 14 cm	1.53

The site which had the greatest average amplitude at the 2 cm level and daily variation was the *GravOrg* site, followed closely by the *Palsa* and *Desiccated* sites. The greatest near-surface temperature was experienced at the *Desiccated* site on July 22 (JD 203). The daily temperature changes at the saturated sites, *Fen, Wetland* and *Isolated,* were much smaller due to the increased heat capacity of water which buffered the soil column from warming and cooling. Throughout the profile, the *Desiccated* site had the largest temperature changes on a daily basis as ground temperatures responded to surface heating. The *Wetland* site had the smallest variation in temperatures at the surface and throughout the profile with the exception of the 25 cm amplitude at the *Palsa* site. Temperatures at depth did not respond rapidly to surface changes while they were frozen. Once the soils thawed, daily fluctuations in soil temperature were evident.

Table 4.5 shows the average daily temperature gradients between thermocouples which are related to the ability of a soil layer to transfer heat.

Table 4.5   Organic Soil Temperature Gradients

Plot	2 cm to Interface (°C/m)	Interface to 10 cm (°C/m)	10 cm to 25 cm (°C/m)
Fen	25.83	36.50	13.20
Wetland	22.00	41.50	19.47
Isolated	23.00	28.60	16.60
Palsa	52.20	53.67	14.60
Desiccated	21.67	30.20	27.07
GravOrg	17.25 (2-10 cm)	58.75 (10-14 cm)	16.27 (14-25 cm)

The 2cm-interface gradient for the Palsa plot was greater than twice the value for any other organic layer except the 10-14 cm layer of the *GravOrg* plot which corresponds

with the original peat surface below the gravel. The other four plots with surface organics had similar temperature gradients. The *GravOrg* gravel pad had the smallest gradient demonstrating the increased heat transfer ability of gravel material. Between the interface and the 10 cm layer, gradients increased at all plots. This phenomenon is somewhat unclear as the top thermocouple is at the organic/mineral interface and the bottom is in mineral soil and thus the gradients should be similar to those found in the mineral layer beneath. The small spacing between thermocouples and the lack of precision of placement of the organic/mineral thermocouple may be the source of some error. The 10-25 cm slab showed a decline in temperature gradients, except for the *Desiccated* site which consists entirely of organic material at depth.

4.2.2 Organic Soil Frost and Water Tables

The positions of the frost and water tables throughout the study are shown in figure 4.4 (*a-i*). The frost table descended immediately after the ground became snow free, the thawed zone thickened rapidly at the beginning and then deepened at a reduced rate. The deepest active layer development occurred at the *Fen* site, followed by the *Wetland* and *Isolated* sites. The active layer was shallower in the humified and disturbed soils. The *Palsa* site had the shallowest active layer, followed by the *Desiccated* and *GravOrg* sites.

The *Fen* and *Wetland* sites had water tables near the surface for the entire study period with some decline in the *Wetland* level as melt contribution from the snowbank decreased in late July. Water table at the *Fen* site declined until in situ snow melt was complete and then remained constant at the surface for the remainder of the summer. The
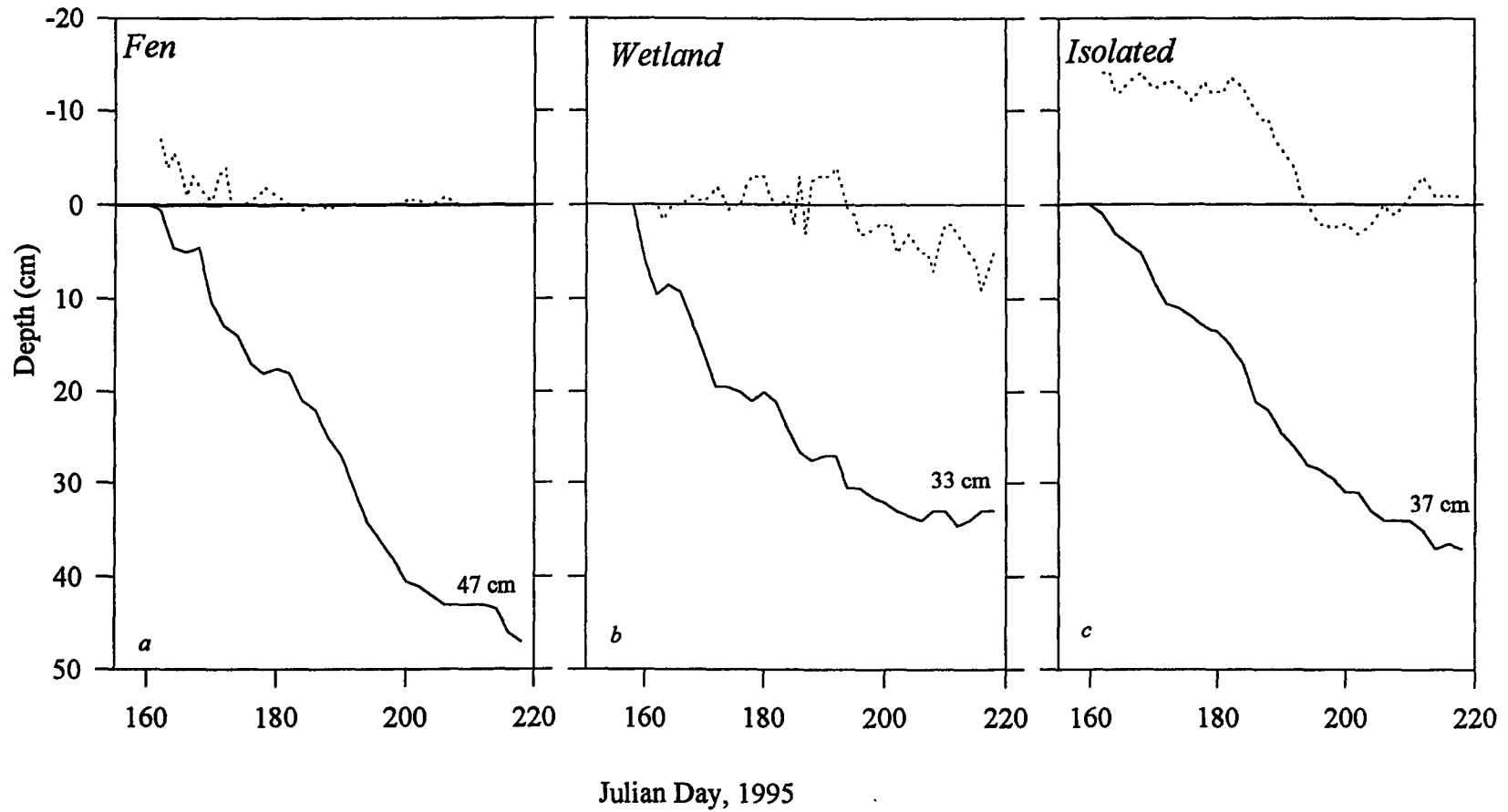
Figure 4.4. (a-f) Frost (full line) and water table (dashed line) positions for the organic soils. Numbers in the lower right corner indicate maximum thaw depth
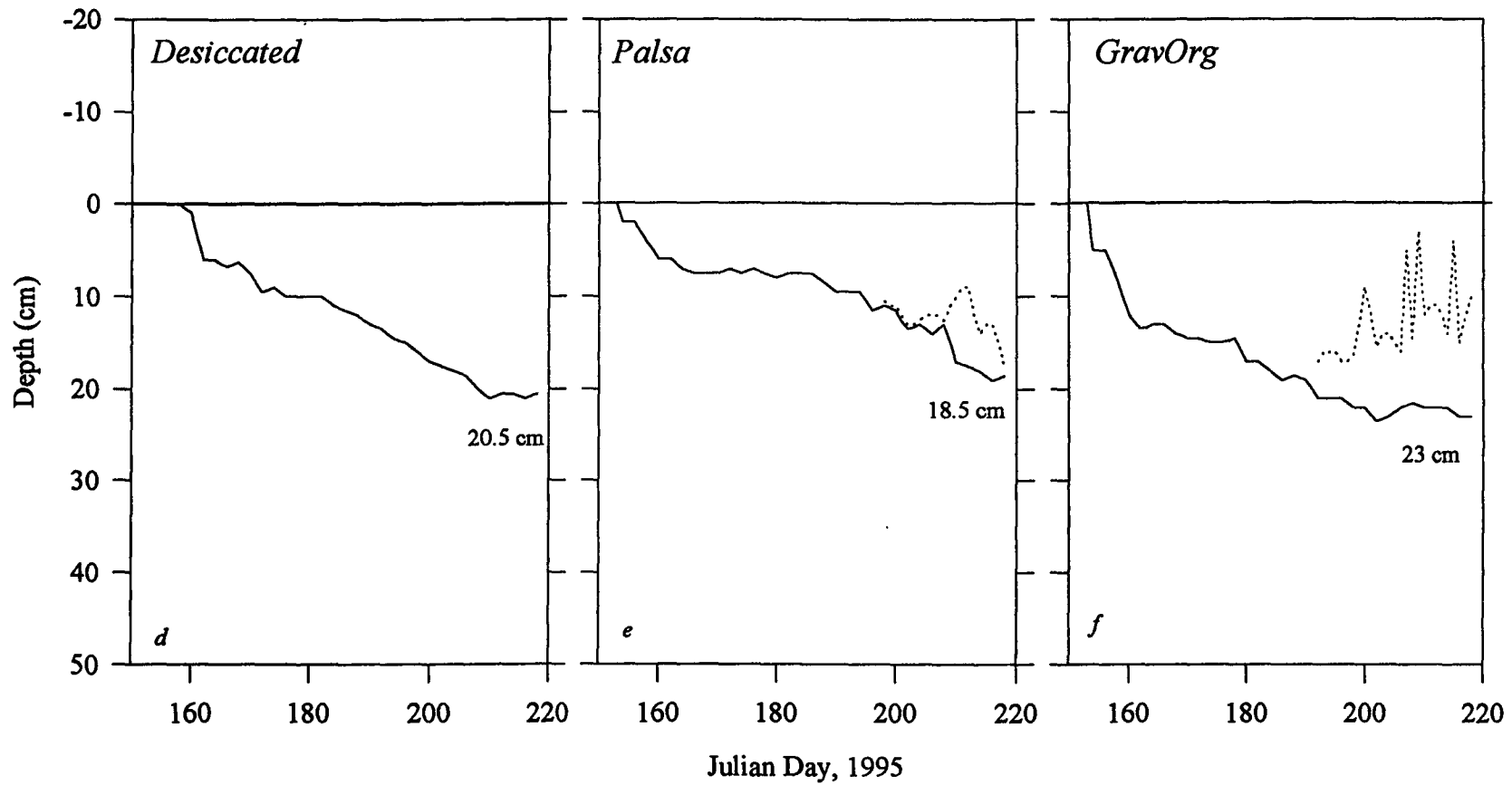
Figure 4.4. (a-f) Frost (full line) and water table (dashed line) positions for the organic soils. Numbers in the lower right corner indicate maximum thaw depth

Isolated site showed three phases in water table behaviour. There, water was ponded up to over 10 cm above the surface at the beginning of the study and was sustained throughout early summer. Evaporation increased after the beginning of July causing a drop in water table until approximately July 16 (JD 197) after which it remained static for ten days. Subsequently, rainfall produced a rise in the water table.

For the three plots without actively developing organics, the *Desiccated* site had no free water surface throughout the study period, while the *Palsa* and *GravOrg* sites developed a saturated zone in late summer. This late-summer phreatic surface was sustained by the melting of ground ice. This ground ice melting also caused a sudden lowering of the frost table at the *Palsa* site.

4.2.3 Organic Soils Ground Ice and Soil Moisture

Soil moisture for the both the *Fen* and *Isolated* sites is unchanged throughout the course of the study as they remained saturated. Surface soil moisture was determined for the *Wetland, Palsa* and *Desiccated* sites (Figure 4.5). At the *Wetland* site, ice dominated the organic layer during the beginning days of the study. This ice was soon replaced by water which occupied 90 per cent by volume of the organic layer. The moisture content fluctuated later in the summer, following the relative position of the water table. The moisture content of the organic layer at the *Palsa* site varied by nearly 30 per cent by volume throughout the summer. At the *Desiccated* site, soil moisture was about 10 per cent by volume at the onset of the study and rose to approximately 20 per cent. The mineral soil water content at a depth of 10 cm beneath the *Palsa* site increased
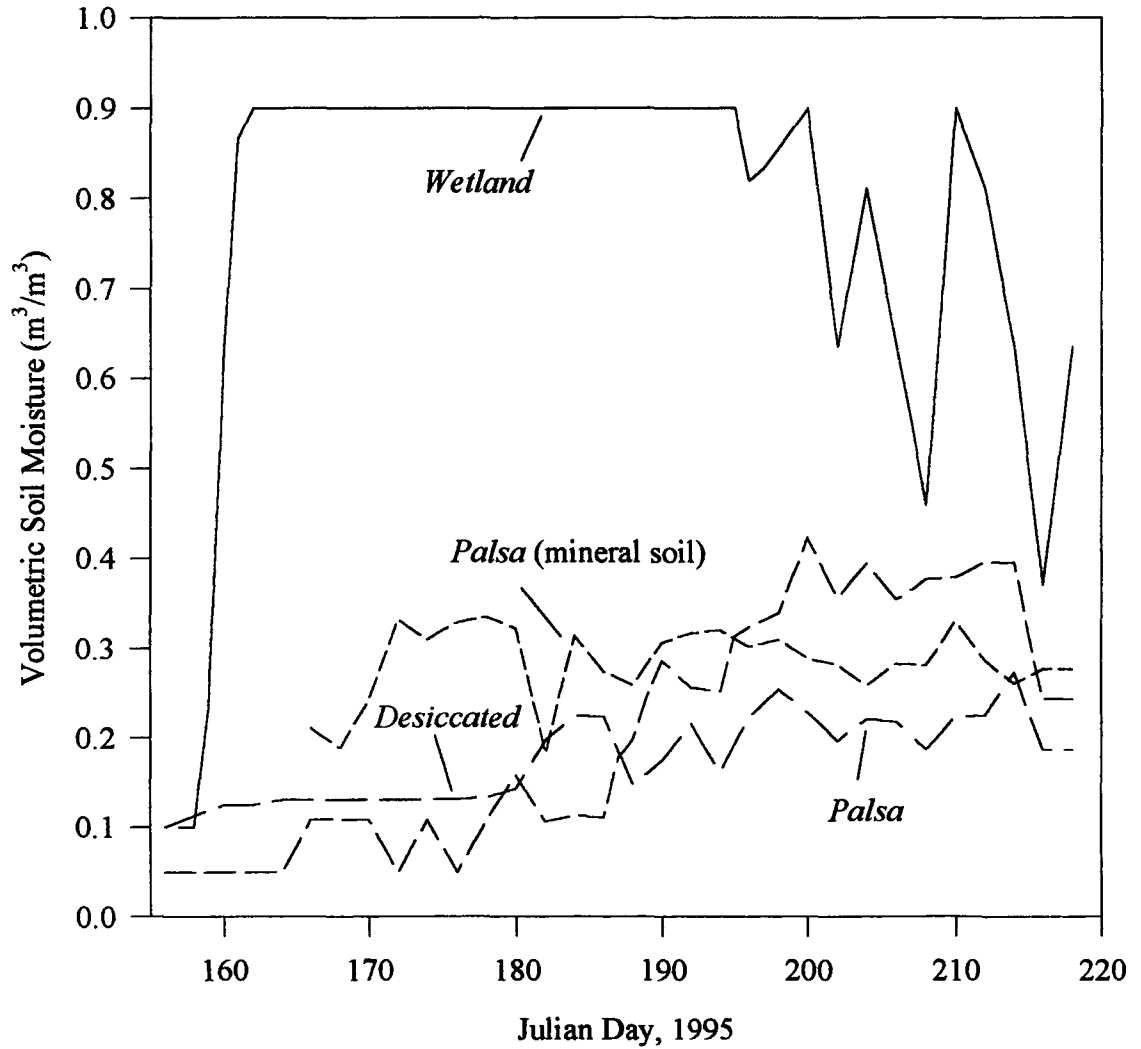
Figure 4.5. Surface soil moisture for selected organic plots. The Palsa (mineral soil) is the moisture content of the mineral substrate beneath the organic layer.

as ground ice melted, rising from values lower than 10 per cent by volume to values over 30 per cent.

4.3   Polar Desert Soils

The mean bulk density and porosity of the of the polar desert soils at each experimental plot, along with parameters at depth obtained adjacent to the study area, are presented in table 4.6.

Table 4.6   Polar Desert Soil Physical Properties

Site	Bulk Density (kg/m^3)	Porosity (%)
Control1	1575	40
Control2	1627	39
Carbon Black	1690	36
Snow	1616	39
Rain	1710	35
RainFen	1557	41
RainRoad	1800	32
Road	1745	34
Gravel (10 cm)	1800	32
10 cm (adjacent area)	1569	41
25 cm (adjacent area)	1676	37
40 cm (adjacent area)	1585	40

The calculation of bulk density takes into consideration that the soils have approximately 2 per cent organics by volume, as determined from combustion tests. For the sites with polar desert material at the surface, the compacted soils have the highest bulk density and the lowest porosity. There is some variability in bulk density among the plots; values nearer the fen are lower than those further away.

Along a typical vertical profile, some textural changes occur at the 25 and 40 cm depths. There is a higher concentration of gravel within the soil column both at the surface and the base of the active layer. At around 25 cm, a more platy silt-clay like horizon is discernible, though not pronounced.

4.3.1 Polar Desert Soil Temperatures

Soil temperatures for six of the nine polar desert plots are shown in Figure 4.6 (*a-i*). When measurements began on June 11 (JD 162), all plots had snow cover and melt had only proceeded for several days. Temperatures were below 0 °C at all depths, reaching -5°C at 50 cm. The plots became snow free between June 18 (JD 169) for the *Gravel* plot to July 4 (JD 185) for the *Snow* plot. Once the ground was exposed, it responded rapidly to surface heating. Temperature amplitudes and daily responses were similar between the experimental plots. Fluctuations in temperature were small when the soil was below freezing, changing dramatically as the temperatures rose above 0°C, as seen from the 10 cm thermocouple at the Snow site around July 4 (JD 185) (Figure 4.7).

Temperatures at 2, 10 and 50 cm fluctuated in the same manner at all plots throughout the study season, with the *Gravel* site being an exception. At the *Gravel* site, the 2 and 10 cm curves had a greater separation, indicating reduced heat transfer within the gravel pad. Furthermore, the separation between the 2 and 10 cm temperature traces on the *Road* plot was less than at the other polar desert soils, indicative of increased heat transfer across compacted grains.
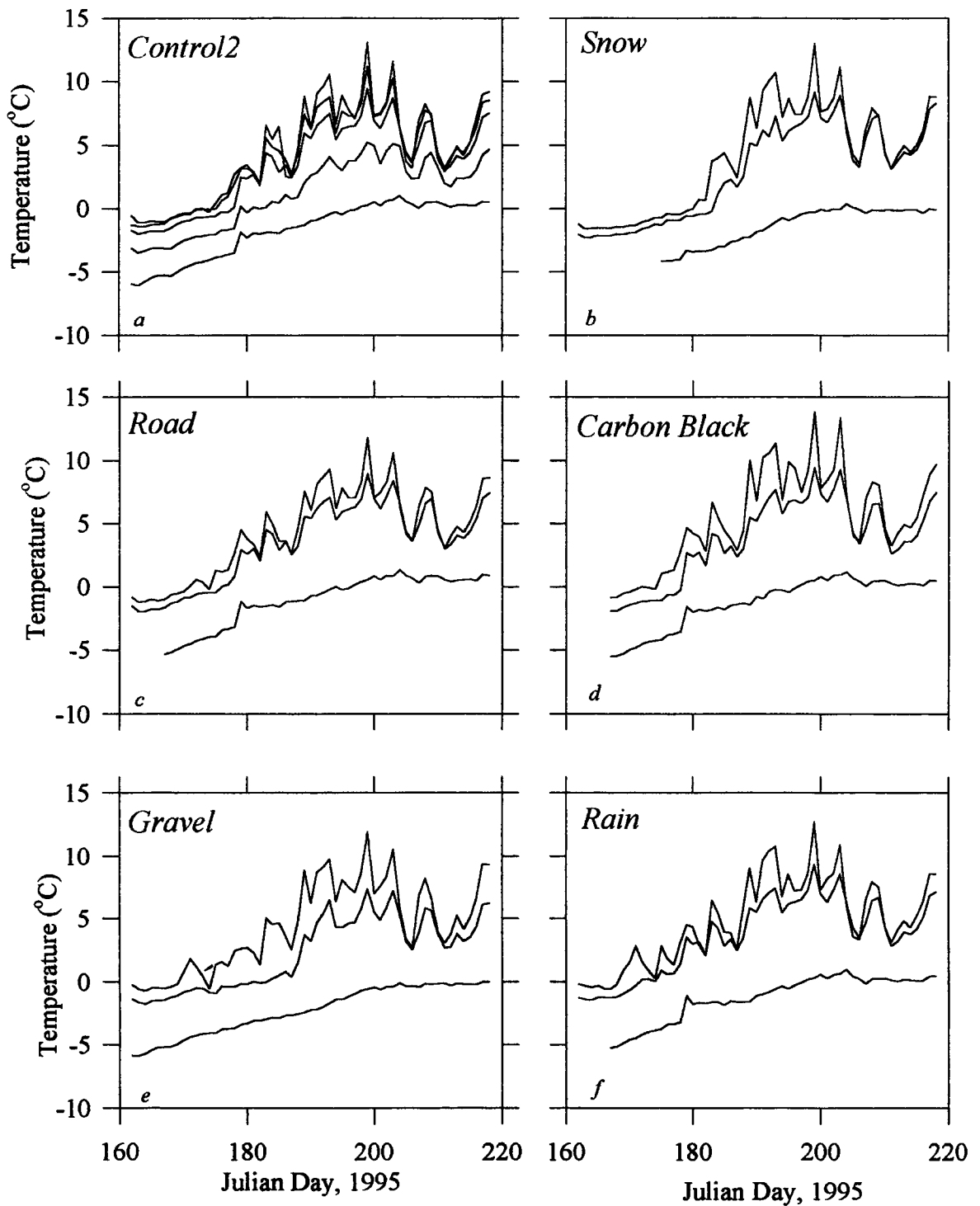
Figure 4.6 (*a-f*). Plots of daily temperature vs. depth for selected polar desert soils.
Thermocouple depths are 2, 10 and 50 cm for all sites except
Control2 with temperature at 2, 5, 10, 25 and 50 cm.
Temperature fluctuations are dampened progressively with depth.
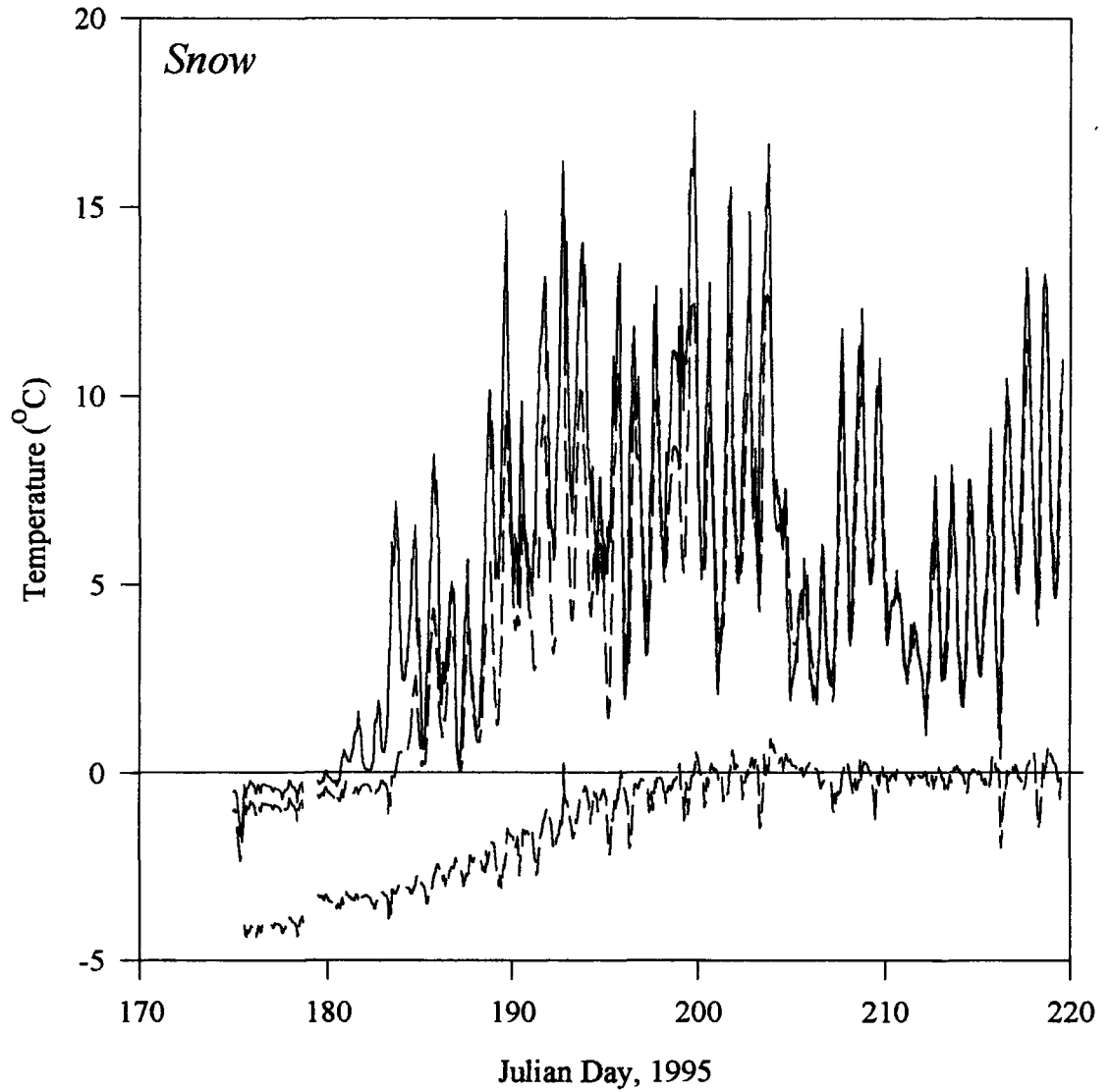
Figure 4.7. Hourly temperatures at the *Snow* plot. Thermocouple depths are 2, 10
and 50 cm.

The average polar desert soil temperatures for the period between June 19 (JD 170) and August 6 (JD 218) are presented in table 4.7.

Table 4.7   Average Polar Desert Soil Temperatures - Julian Day 170 to 218

Site	2 cm (°C)	10 cm (°C)	50 cm (°C)
Control1	5.93	4.48	-0.58
Control2	5.48	4.26	-0.98
Carbon Black	5.89	4.12	-0.99
Snow	4.90	3.72	-1.23
Rain	5.65	4.36	-1.00
RainFen	5.49	4.03	-0.70
RainRoad	5.52	4.35	-0.82
Road	5.23	4.24	-0.73
Gravel	5.06	2.76	-1.85

The *Snow* plot had the coldest surface temperatures due to the late start in ground surface heating. The *Gravel* site had the second coldest temperatures despite being the first plot to become snow-free; potentially a function of the higher albedo of gravel. The other plots did not show clear patterns at the 2 cm level. It would have been expected that the *Carbon Black* plot, which was covered with carbon black on Julian Day 175, to be the warmest due to the low albedo, yet *Control1* was slightly warmer.

The same general trends are apparent at the 10 cm depth. The *Gravel* site was much cooler than the other sites, followed by the *Snow* plot. The *Carbon Black* plot is anomalous in that it experienced the greatest temperature drop over the 8 cm of soil. At the 50 cm level, the coldest temperatures were again the *Gravel* and *Carbon Black* plots. The *Control1* plot was the warmest throughout the profile, yet had a shallow active layer

as seen in section 4.3.2. The second warmest plot at 50 cm was the *RainFen* site, which like the *Control1* plot had limited active layer development. Both of these plots lie adjacent to the nearby fen which may influence active layer thermodynamics. There also was no clear effect of rainfall on mean seasonal surface temperatures. The variability of temperatures at 50 cm among sites was probably due to intrinsic soil variations and measurement error.

4.3.1.1 Short Term Response of Disturbances on Polar Desert Temperatures

Increased rainfall did not have a pronounced effect on mean summer temperatures (table 4.6). This may however be an artifact of time, which acts to dampen short term temperature signals. Figure 4.8 (*a,b*) represents a five day period with three simulated and no natural rainfall events. For the soils located on the ATV road, there appeared to be no short term discernible effect of rainfall on active layer temperatures. There was more variability in 2 cm temperatures between the *Control2* and *Rain* plots. Surface temperatures became warmer on JD 201 at the *Rain* site and after the simulated rainfall on JD 202, the 2 cm temperature fluctuated, dropping after rainfall began and then becoming warmer. These temperature increases may be a function of either increased thermal conductivity of wet soils or a lowering of albedo. On JD 203 when temperatures rose dramatically, the *Rain* site near-surface temperature rose slower, perhaps due to the increased heat capacity of the wet soil. Neither active layer cooling from increased evaporation or sensible warming form convected rain was evident at either the compacted
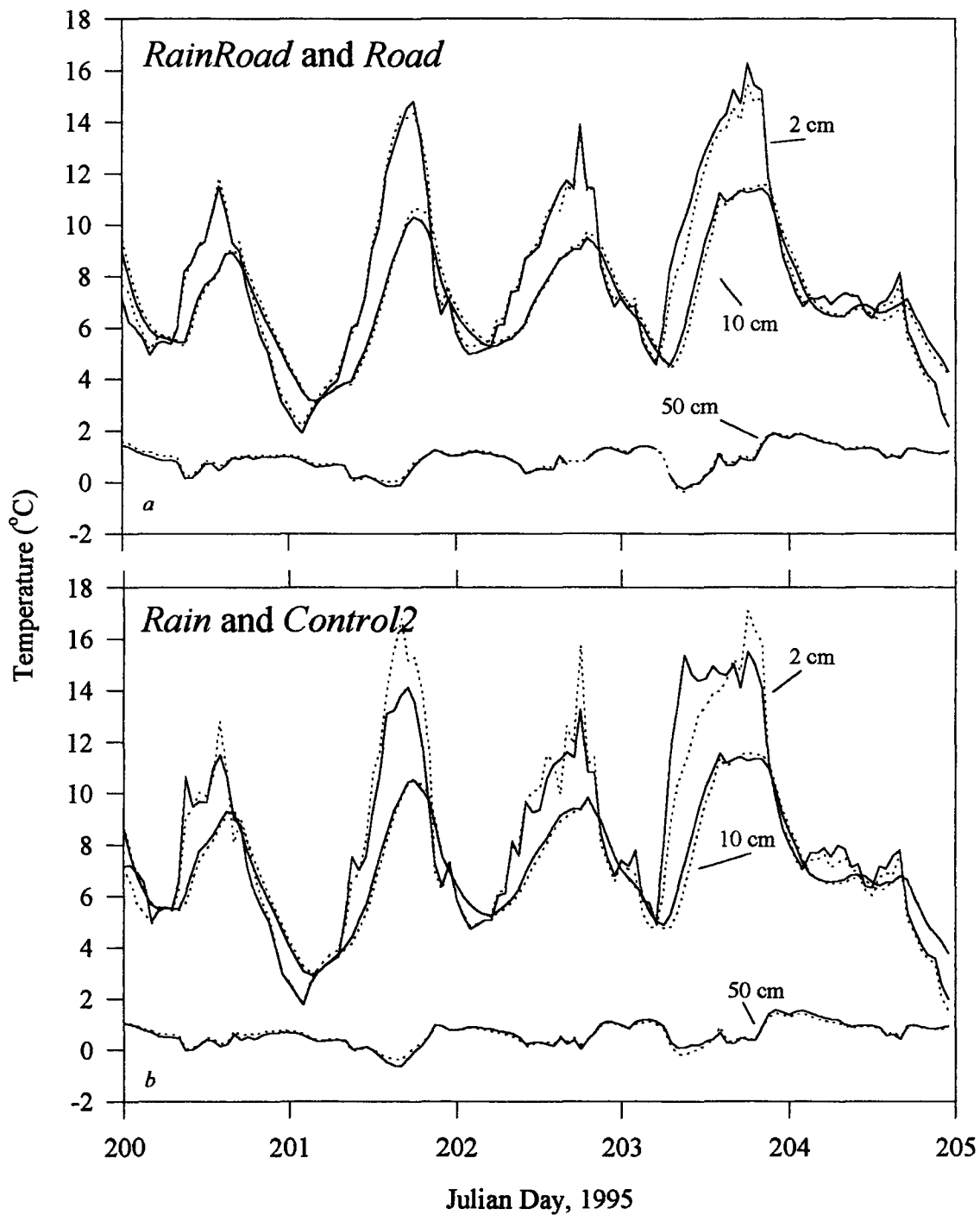
Figure 4.8 (a, b) Hourly temperatures comparing adjacent plots, one subject to rainfall (dashed lines) and one without (full lines).

and non-compacted plots. There also appeared to be very little influence on temperatures at 10 and 50 cm.

Carbon black was added to the *Carbon Black* plot on June 24 (JD 175), lowering the mean albedo from 0.17 to 0.075. No immediate response was evident as all of the plots were becoming snow-free at this time and direct comparison was impossible. Later in the summer, temperatures throughout the profile at the *Carbon Black* plot on an hourly basis were warmer than the nearby *Control2* plot (Figure 4.9). Both the surface and 10 cm temperatures rose to greater values during the middle of the day. The *Carbon Black* surface cooled rapidly and the daily descending limb of the 2 cm temperature curve closely followed the cooling of the *Control2* plot. The 10 cm level temperature cooling phase was lagged at the *Carbon Black* plot, often producing a situation at night when 10 cm temperatures were warmer than 2 cm temperatures, showing a reversal of heat flux. The magnitude of the temperature reversal at the *Control2* plot was much less pronounced. On a seasonal scale, this reversal became obscure and its effect on heat flux can be ignored.

Surface temperatures at the *Gravel* and *Control2* plots between July 19 and 24 (JD 200-205) were similar, the principal deviation occurred during the rapid heating event on JD 203 (Figure 4.10). At the 10 and 50 cm depths, the gravel site had cooler temperatures yet relative response of the curves to surface heating appeared similar.

4.3.2 Polar Desert Frost and Water Tables.

Frost and water table changes are shown in Figure 4.11 (*a-l*). Ground thaw began after the snow melted at each plot. Thawing was delayed by approximately 10 days at the
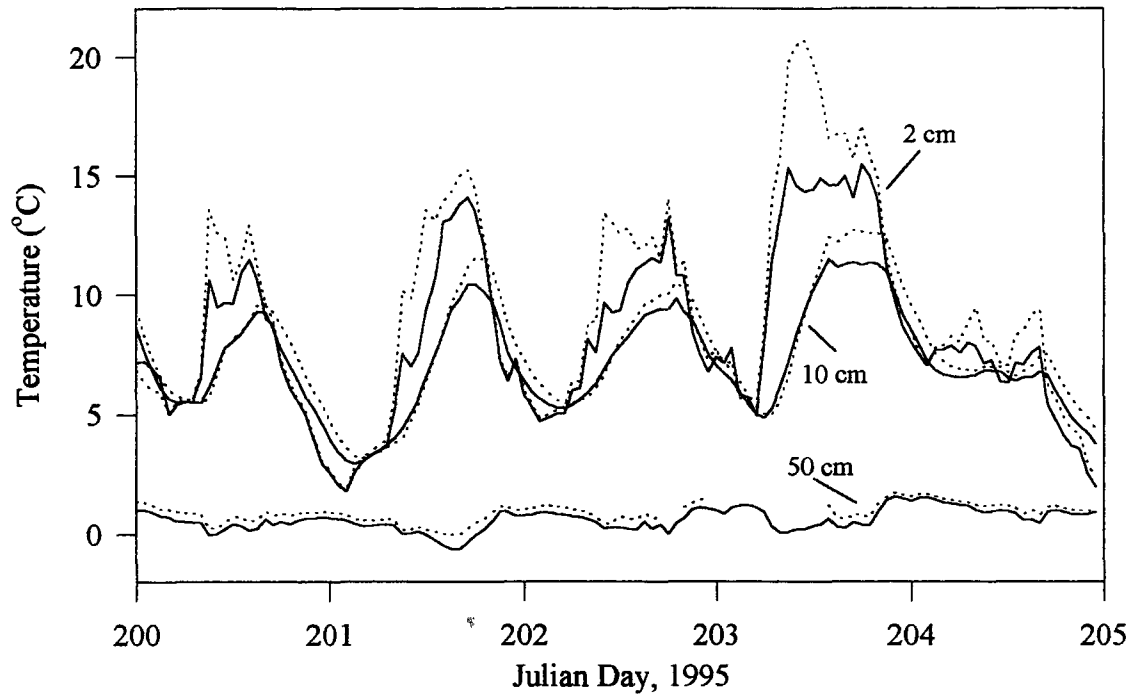
Figure 4.9 Hourly temperatures of *Carbon Black* (dashed lines) and *Control2* (full lines) at depths of 2, 10 and 50 cm.
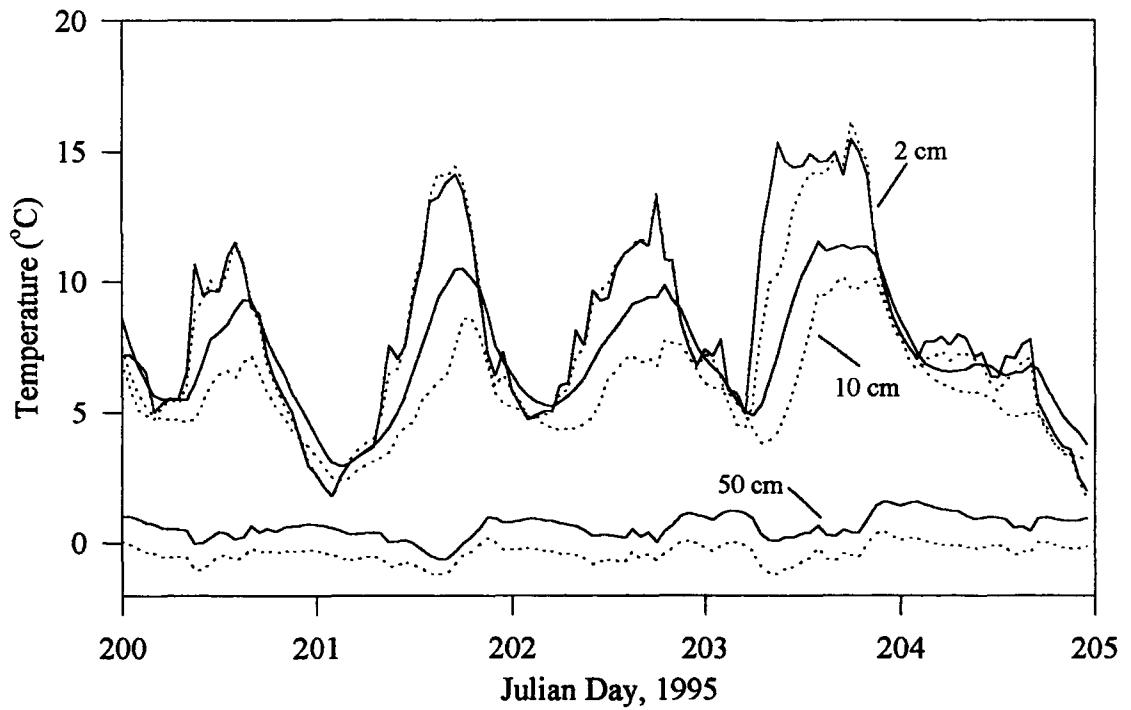
Figure 4.10 Hourly temperatures of *Gravel* (dashed lines) and *Control2* (full lines) at depths of 2, 10 and 50 cm.
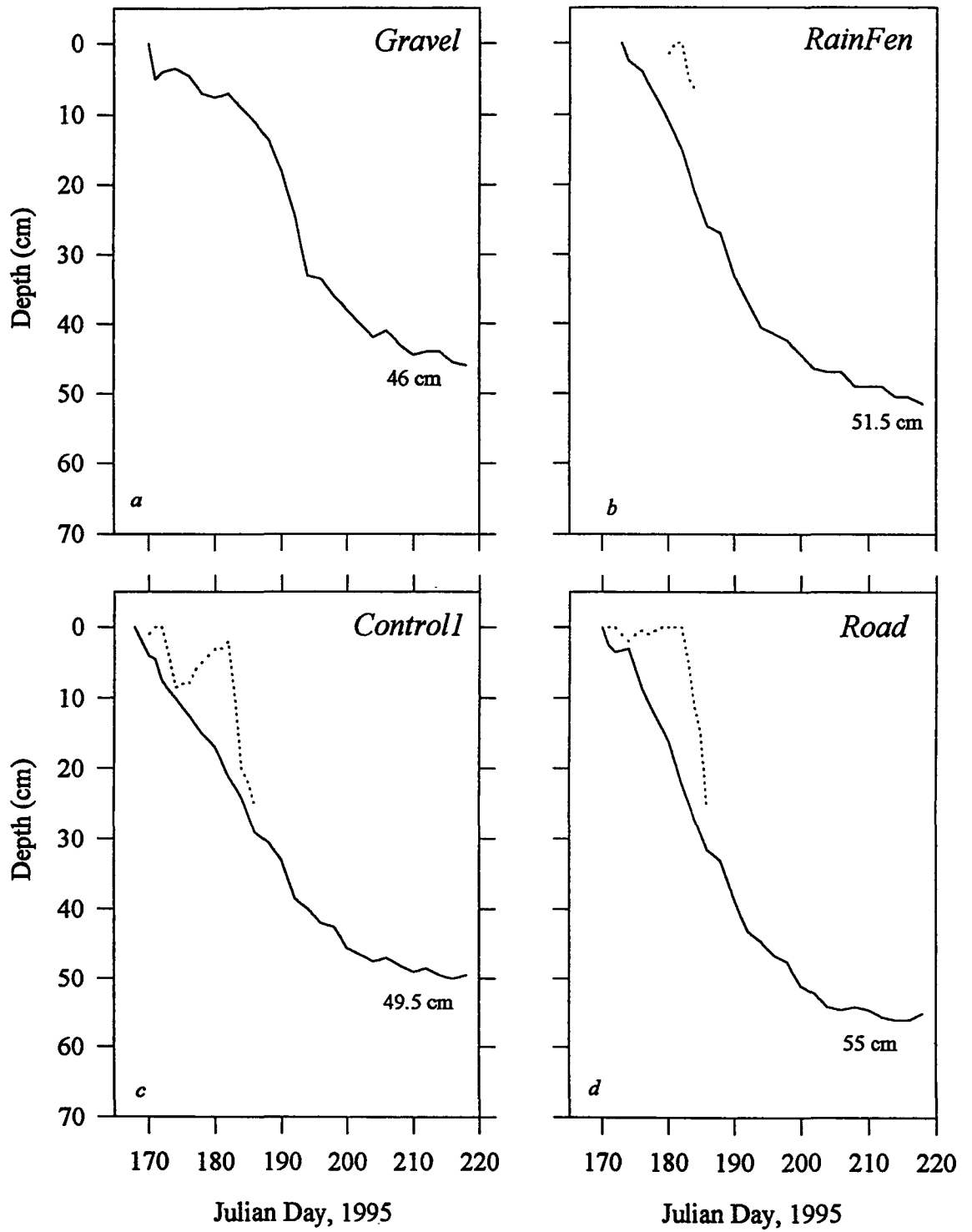
Figure 4.11 (*a-i*)   Frost (full line) and water table position (dashed line) for polar
desert soils.
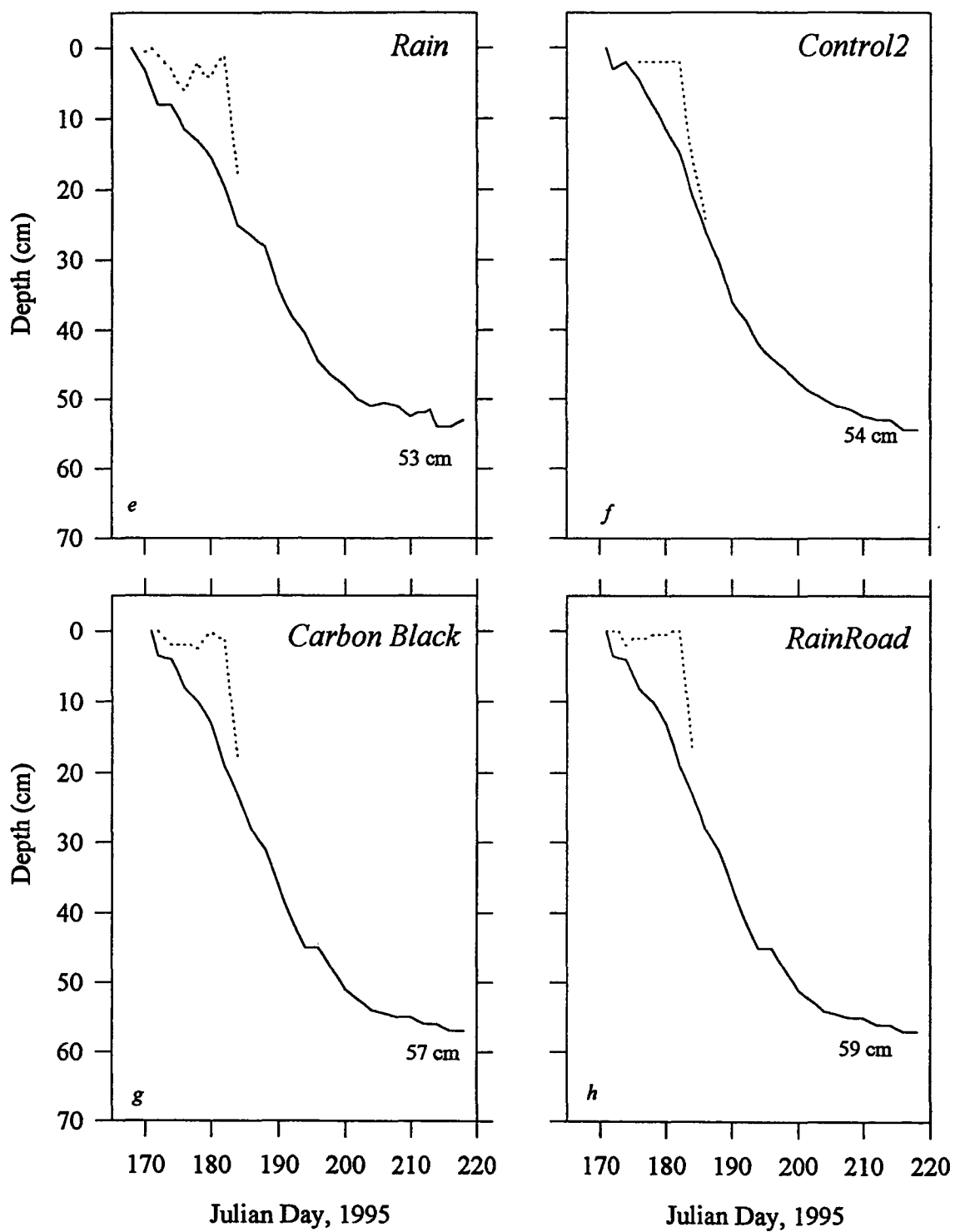
Figure 4.11 (*a-i*) Frost (full line) and water table position (dashed line) for polar desert soils.
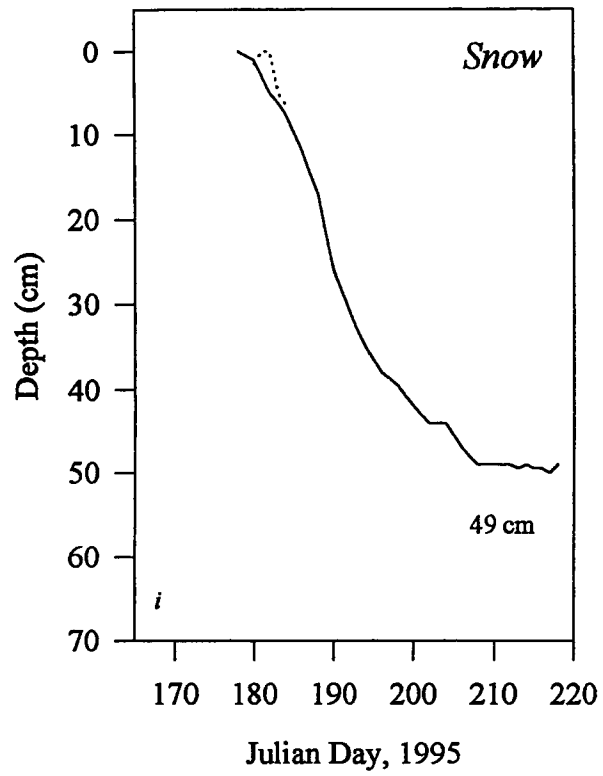
Figure 4.11 (*a-i*)   Frost (full line) and water table position (dashed line) for polar desert soils.

Snow plot. Following snowmelt, the descent of the frost table was rapid for all sites except the *Gravel* which showed two steps, caused by a retardation of thaw when the frost table reached the base of the gravel.

For the other plots, the descent of the frost table proceeded approximately at a rate proportional to the square root of time (Woo 1976). The maximum thaw depth approached the depth of the active layer by the end of the study period. The active layer was the most shallow under the *Gravel* plot, followed by the *Control1* and *RainFen* plots; the three sites closest to the adjacent wetland. The *Conrol2*, *Rainfall* and *Road* plots all had similar active layer depths by the end of the study. The deepest thaw occurred at the *Carbon Black* and *RainRoad* sites, being 57 and 59 cm respectively.

The phreatic surface was present only during the period immediately after snowmelt; the exception being the *Gravel* site where it was never observed. Shallow frost tables prevented downward percolation of abundant meltwater, hence impounding the water near the surface (Marsh & Woo 1993). Once the frost table reached a certain level, the capacity for the soil to hold moisture in tension is realized and the water table "disappeared". Thus, although evaporation and lateral drainage reduce the water held in storage, the disappearance of the water table may also be caused by the adsorption of moisture by the desiccated zone.

4.3.3. Polar Desert Ground Ice and Soil Moisture

The pre-melt ice and water content in the near-surface zone was 75 per cent of porosity as determined from grab samples taken from beneath the snowpack. The ground ice content remained near 75 per cent of the available pore space except at the base of the active layer where all available pores were filled with reticulate ice and some ice lenses. As ground ice near the surface melted after snowmelt, abundant meltwater filled the pore spaces to produce a perched water table which later disappeared as field capacity increased.

Figure 4.12 (*a-c*) shows the seasonal change in soil moisture for six plots at 2 to 10 cm depths. Each diagram shows a pair of adjacent plots one of which was subjected to simulated rainfall. Liquid water content of frozen soils was assumed to be 5 per cent by volume. As the frost table descended, soil liquid water at the surface increased to a maximum immediately after the completion of snowmelt and water content was approximately 30 per cent by volume. Soil moisture declined gradually throughout the summer, ranging between 15 and 20 per cent by volume for the plots without simulated rainfall. For these plots, increases in soil moisture were principally from meteoric water inputs. Although not easily discernible, the volumetric moisture of the *Road* site was on average less than the control plots due to decreased pore space from compaction.

The plots subjected to increased rainfall had approximately five per cent greater moisture content by volume than their adjacent plots. There was some correspondence
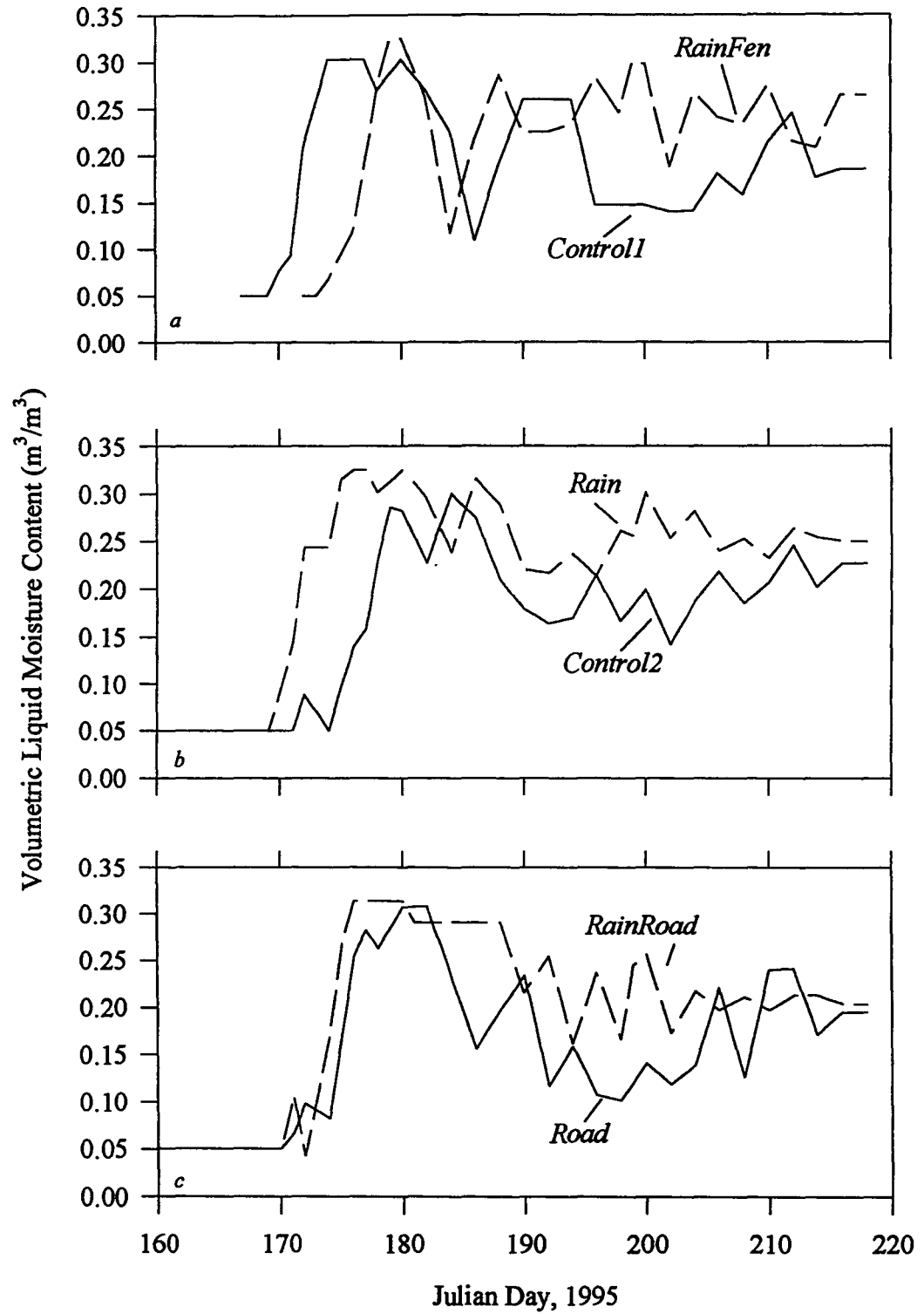
Figure 4.12 (*a-c*). Surface volumetric soil water between adjacent plots; one with simulated rainfall and one without.

between the curves of the rainfall and non-rainfall sites, indicating that plots subject to simulated precipitation also responded to natural rainfall events. After each simulated rainfall event, the surface moisture increased by approximately 4 per cent. At the *RainRoad* site, some ponding occurred after rainfall simulation, but ponding disappeared after approximately 1 hour after the cessation of rainfall. The effect of simulated rainfall on moisture content at depth was not determined.

Soil moisture increased with depth as determined from sampling pits over the course of the study (Figure 4.13). Once the active layer was thawed below 40 cm, soil moisture remained essentially unchanged to a depth of 25 cm, and then increased by several per cent at the 40 cm level.
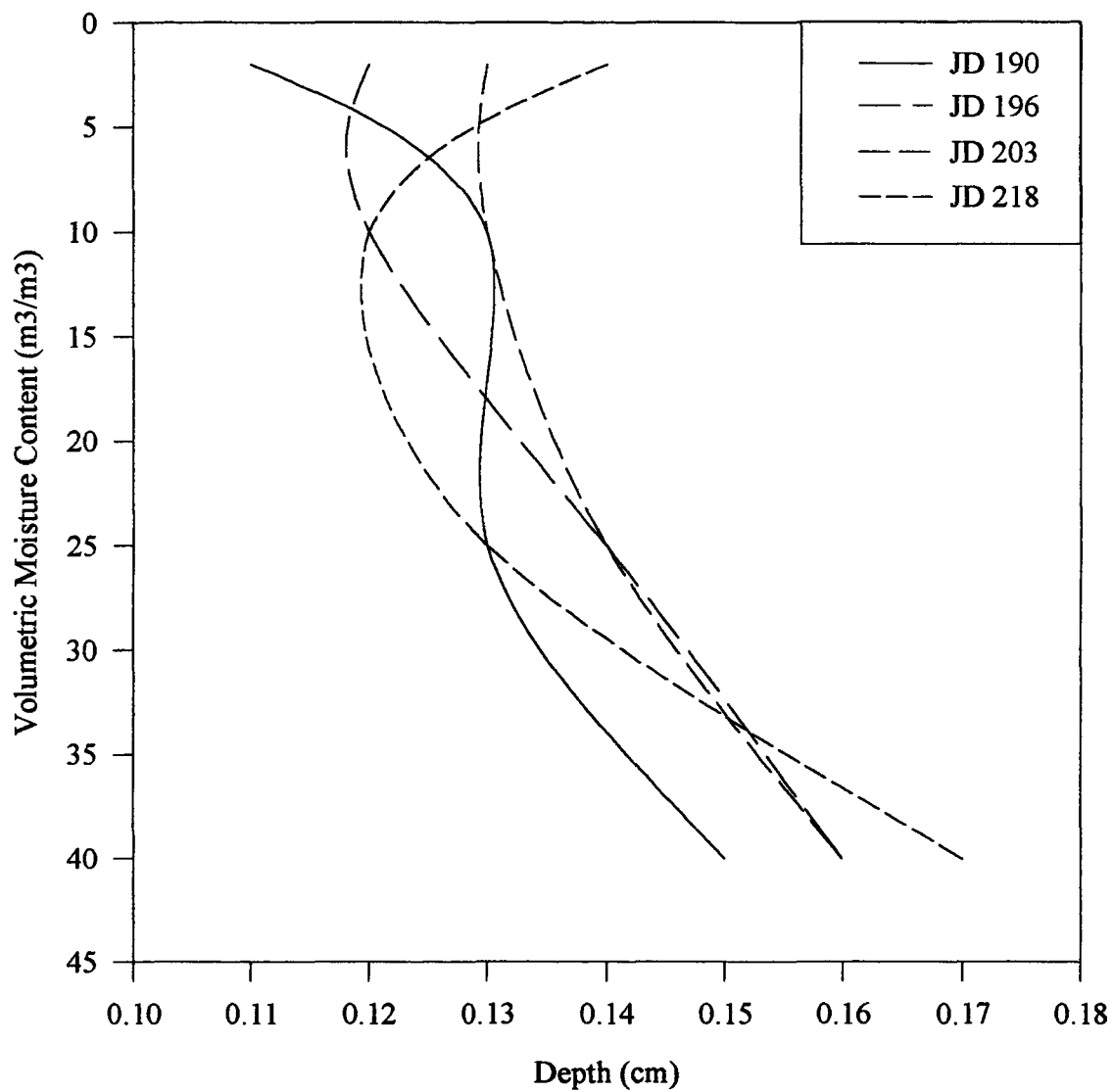
Figure 4.13   Soil moisture variation with depth in the polar desert soils.
Values are representative of a control site.

CHAPTER FIVE

Energy Dynamics

This chapter examines the partitioning of ground heat flux into several components using field data obtained at the experimental sites. As shown by equations 2.2 to 2.13, the soil thermal properties play an important role in the soil energy balance calculations. The determination of thermal conductivity and heat capacity values will be presented.

5.1   Soil Thermal Properties

Soil thermal properties vary with volumetric composition of different constituents; including mineral, organic, air and water in both solid and liquid phase (equations 3.12, 3.14). In permafrost areas, change during the thawed season as ground ice melts causes the replacement of ice by water; and when evaporation or drainage continues, the replacement of water by air.

5.1.1   Organic Soils

Thermal conductivity and heat capacity were determined for both the organic layer and its mineral substrate. The values were updated daily and they showed clear seasonal patterns.

5.1.1.1 Thermal Conductivity

The decline in k at the onset of thaw occurred as ice was replaced by water and air (Figure 5.1). After the frost table descended beneath the organic layer, thermal conductivity stabilized, responding to changes in soil moisture and water table position.

Figure 5.1   Daily variations in thermal conductivity for the surface layer of the organic soils.
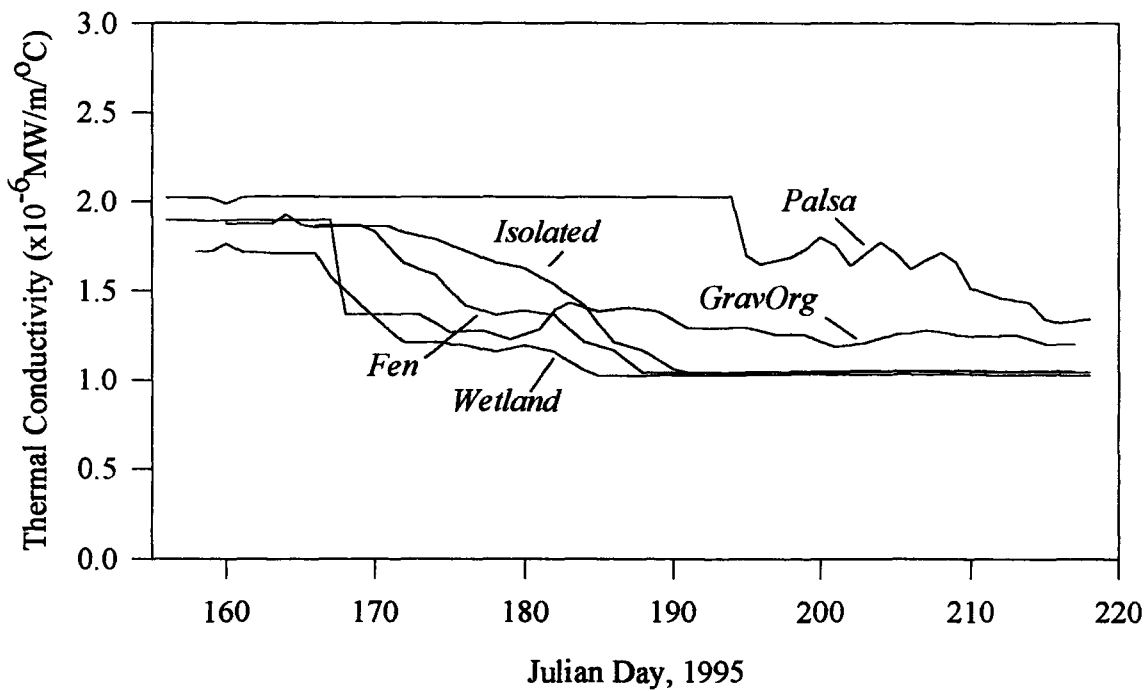
Figure 5.2   Daily variations in thermal conductivity for the mineral layer of the organic soils.

The *Fen* and *Isolated* sites showed little variation in k throughout the summer as the phreatic surface remained at or above the organic surface. Thermal conductivity at the *Wetland* site declined rapidly after melt and remained unchanged until July 14 (JD 195) when the water table began to fluctuate within the organic layer. The *Palsa* and *Desiccated* sites were never saturated and their k values showed some response to changing soil moisture. After the frost table descended beneath the 10 cm gravel pad, the *GravOrg* site exhibited a higher thermal conductivity than the organic layers and remained unchanged due to the insensitivity of gravel to moisture variations as meteoric water rapidly drained through the gravels to the underlying layers.

Thermal conductivity of the mineral soils beneath the organic layer (Figure 5.2), exhibited similar trends as the organic layer, yet absolute values were greater due to the higher k of mineral grains. Significant volumes of ground ice were replaced by water within the void space as this layer thawed, resulting in declining values of k. Thermal conductivity of the *Wetland, Fen* and *Isolated* plots behaved similarly as the mineral layer was saturated throughout the season and when the frost table dropped below 25 cm values stabilized. The *Palsa* site, which was ice rich in the mineral layer, had a high conductivity until the thawing front penetrated beneath the organic layer. Then, the passage of the thawing front moderated k of the mineral layer. The late summer decline in k occurred as water rose into this layer from the melting ground ice. The thermal conductivity of the mineral layer at the *GravOrg* plot showed a similar trend as the *Palsa* site. The

replacement of ice by water, fluctuations in soil moisture and a late season rise in the water table all affected the behaviour of k at the *GravOrg* site.

5.1.1.2 Heat Capacity

Figure 5.3 shows the behaviour of heat capacity, c, within the organic layer. The *Fen*, *Wetland* and *Isolated* plots all showed rapid increases in c as the thawed zone thickened. Heat capacity reached a maximum and remained unchanged at the *Fen* and *Isolated* sites due to presence of the water table at the surface. Heat capacity at the *Wetland* site fluctuated in late summer as water was replaced by air within the organic mat. The *Palsa* and *Desiccated* sites showed different trends in c due to large volumes of air within the pores; the perturbations being more a response to near-surface moisture than to phase change. The heat capacity of the gravel pad was the smallest and remained unchanged as the composition of this layer varied little throughout the study period.

The mineral substrate of the organic plots exhibited similar behaviour in heat capacity (Figure 5.4). For the three plots which had saturated mineral layers (*Fen*, *Wetland* and *Isolated*), c increased as the volume of ice decreased, stabilizing to constant values. The *Palsa* site had a slower decline in the frost table and was not saturated, yielding lower values of heat capacity. The late summer rise and fall in c was a result of the rising water table. At the *GravOrg* plot, fluctuations in heat capacity resulted from changing volumes of ice, water and air within the pore spaces.
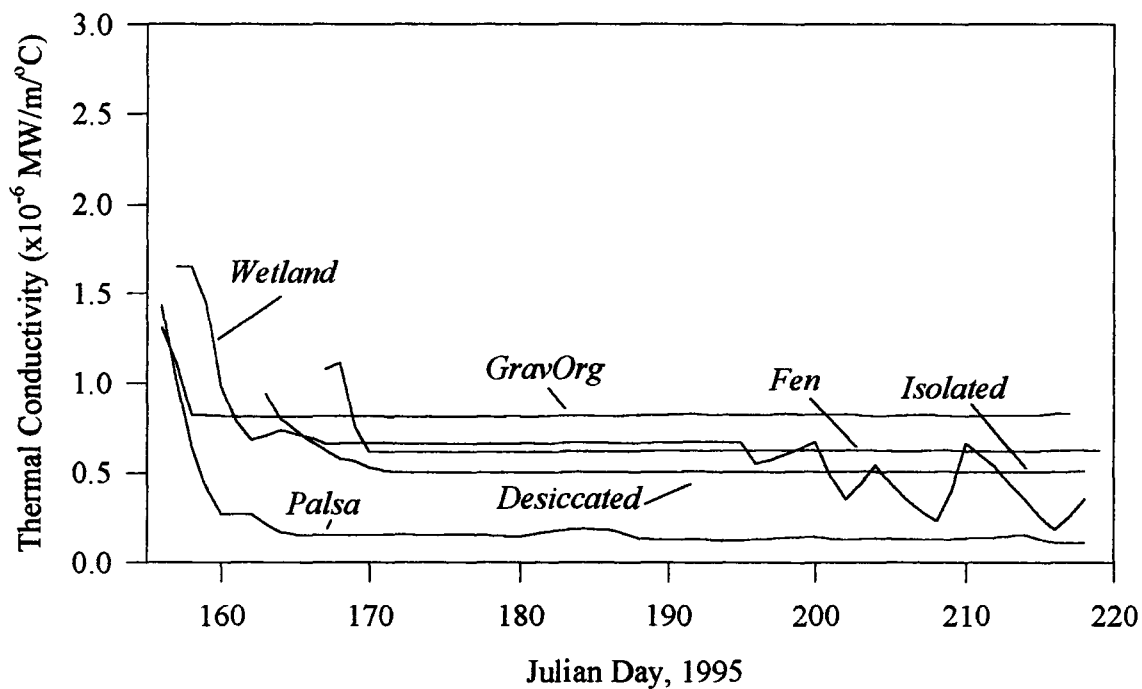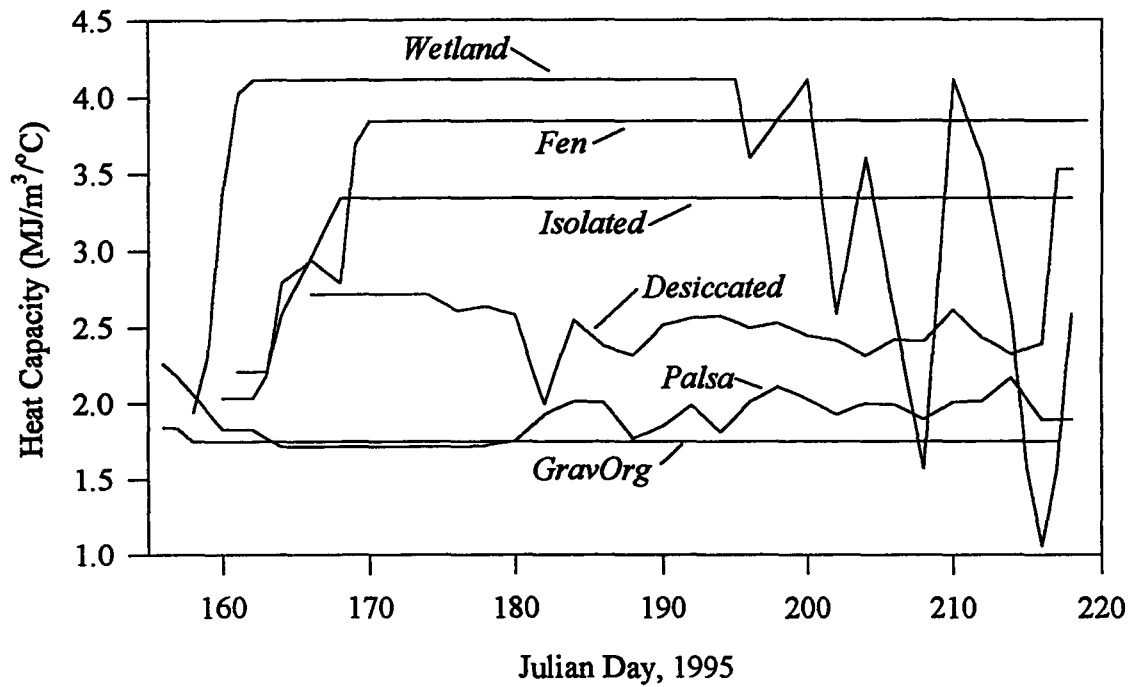
Figure 5.3 Daily variations in heat capacity for the surface layer of the organic soils.
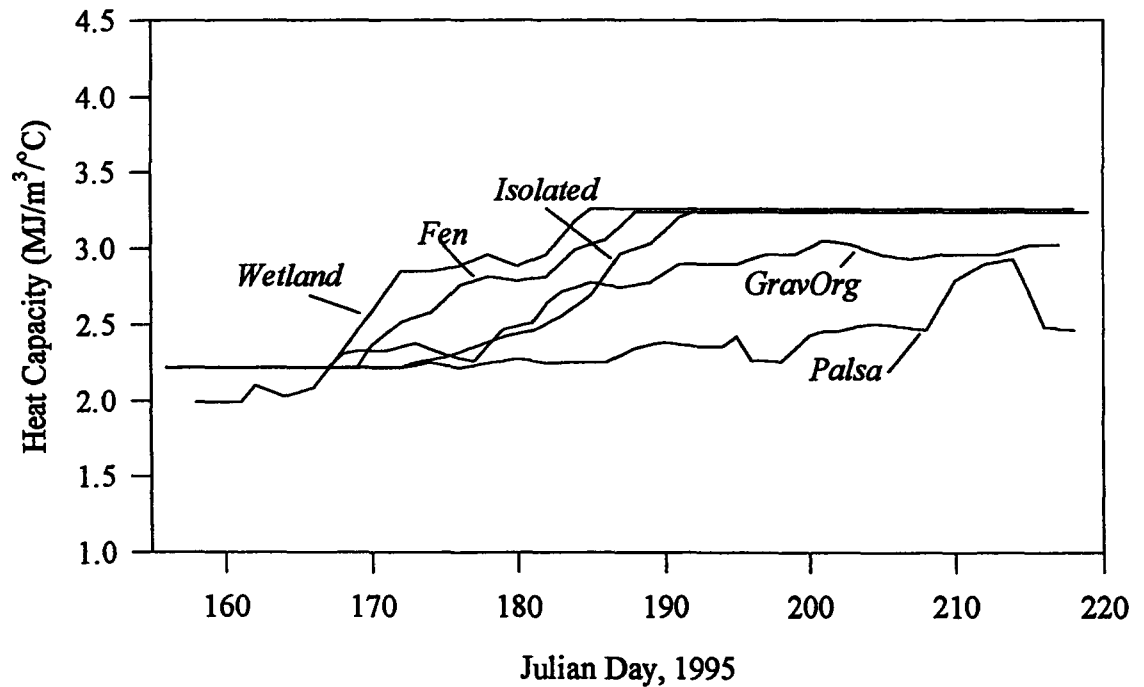
Figure 5.4 Daily variations in heat capacity for the mineral layer of the organic soils.

5.1.2 Polar Desert Soils

The thermal properties of polar desert soil change throughout the season, responding to freeze-thaw and wet-dry events. Unlike organic soils, mineral soil thermal properties are more responsive to mid-summer changes in soil moisture.

5.1.2.1 Thermal Conductivity

Figure 5.5 shows k of the surface (2 to 10 cm) zone of the polar desert soils. After this entire top layer was thawed, the values of k moderated; responding to changes in near surface moisture over periods of several days. The plots with the highest values of k were the *RainRoad* and *Rain* plot, demonstrating the influence of increased soil water on raising the k. The *Road* plot had slightly higher k values than the *Control2* plot; reflecting the effect of compaction on increasing k. The *Gravel* plot had the lowest k values which remained unchanged after the frost table passed below the surface.

There were less pronounced differences in thermal conductivity among the plots at the 25 to 50 cm layer (Figure 5.6). Values of k declined as ice melted through this zone and flattened out as the frost table moved below 50 cm. The point where the thermal conductivity dropped from just above 2.5 W/m/°C was the time when thawing passed through the 25 cm mark. Afterwards, there was no clear distinction among the values of k once the frost table reached approximately 50 cm.
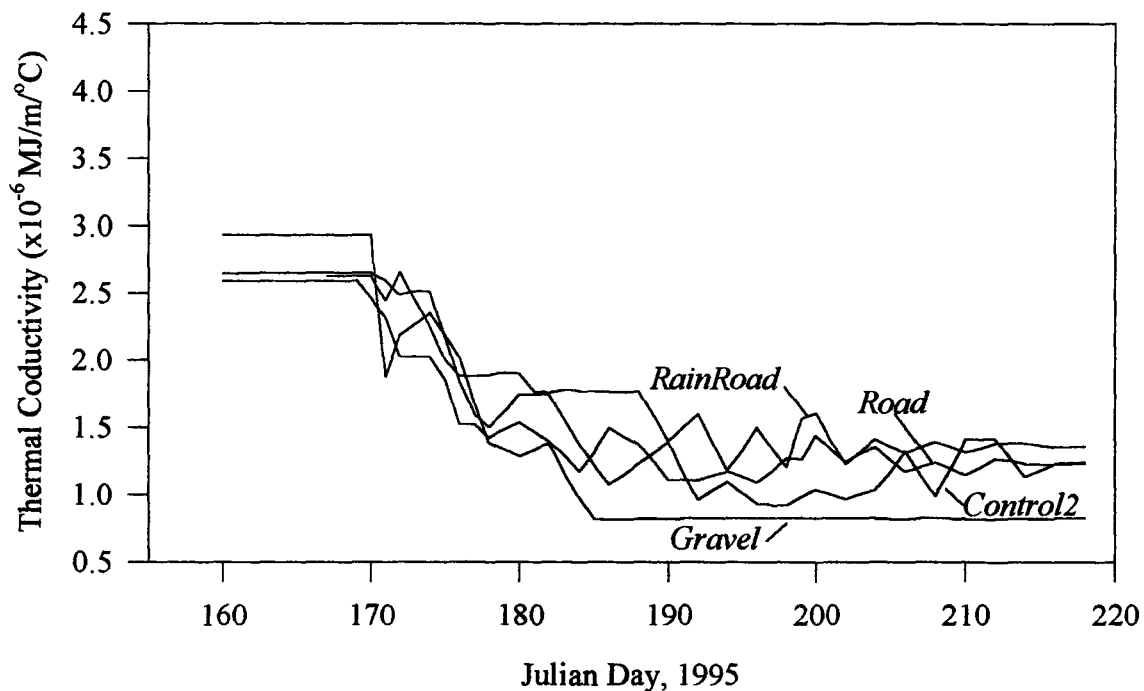
Figure 5.5 Daily variations in thermal conductivity for the 2 to 10 cm zone in selected
polar desert soils.
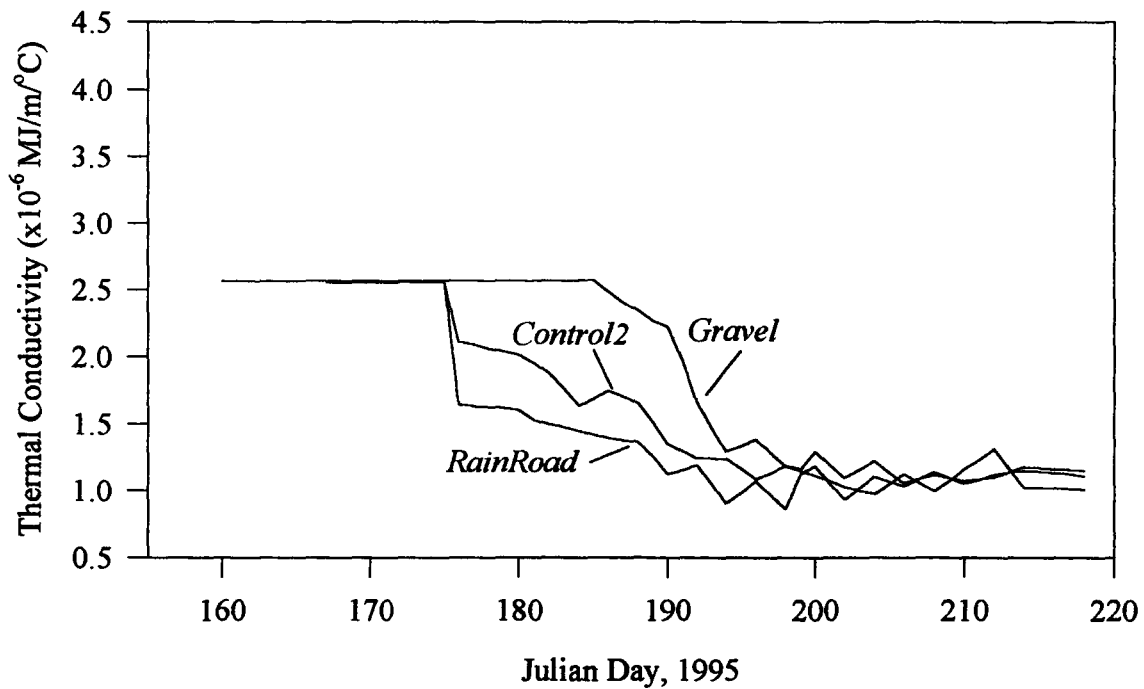
Figure 5.6 Daily variations in thermal conductivity for the 10 to 50 cm zone in selected
polar desert soils.

5.1.2.2 Heat Capacity

Heat capacity increased noticeably as ice was replaced by water within the pore spaces following snowmelt (Figure 5.7). After the initial rise following snowmelt, c declined as the soil began to dry. There was significant variation in heat capacity among the plots, those subjected to increased rainfall had greater values. Compaction of materials at the *Road* site decreased the heat capacity as less pore space was available for water. The *Gravel* site had the lowest heat capacity in the 2 to 10 cm zone as water drained downward rapidly so that the surface layer had a low moisture content. Unlike the saturated organic soils where phase change had the greatest influence on heat capacity, short term wetting and drying influenced the value of c in mineral soils.

5.2   Ground Energy Balance

On a daily basis, heat flux was directed downward into the soil for the entire study period due to positive temperature gradients. Within the active layer, energy was partitioned between melting ground ice, sensibly warming the soil and energy directed downward into the permafrost. These energy values were calculated using equations 2.5, 2.8 to 2.10.

5.2.1   Organic Soils

The cumulative energy balances of the organic sites reveals the partitioning of energy within the active layer (Figure 5.8 *a-f*). Cumulative energy balances are shown because daily variations mask the seasonal signals (Figure 5.9). The total values of the soil
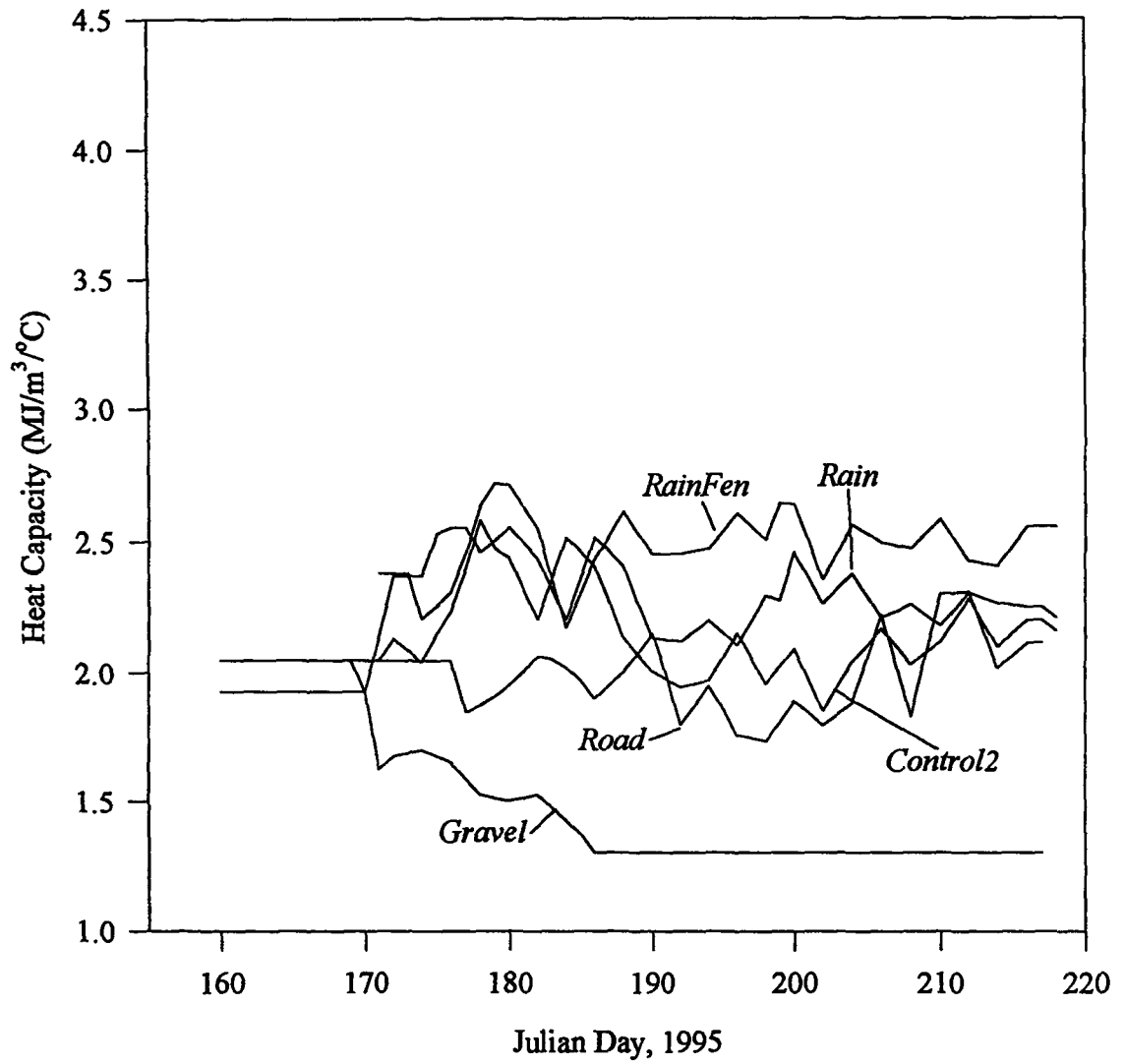
Figure 5.7   Daily variations in heat capacity for the 2 to 10 cm layer of selected polar desert soils.
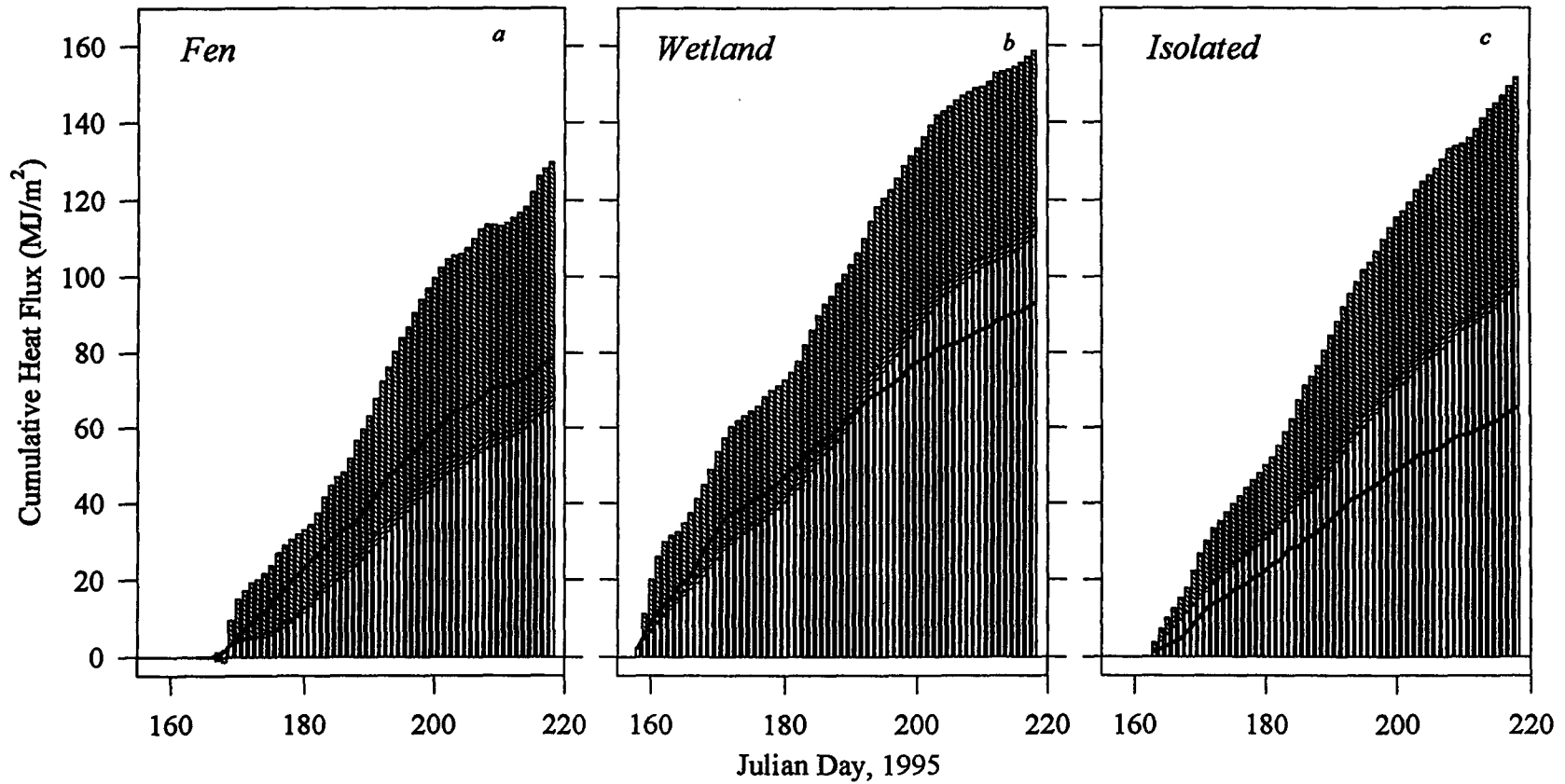
Figure 5.8(a-f)   Cumulative energy balances for the organic soils. The stacked bars from the base up are Q_O, Q_S, and Q_F
The solid line is Q_G.
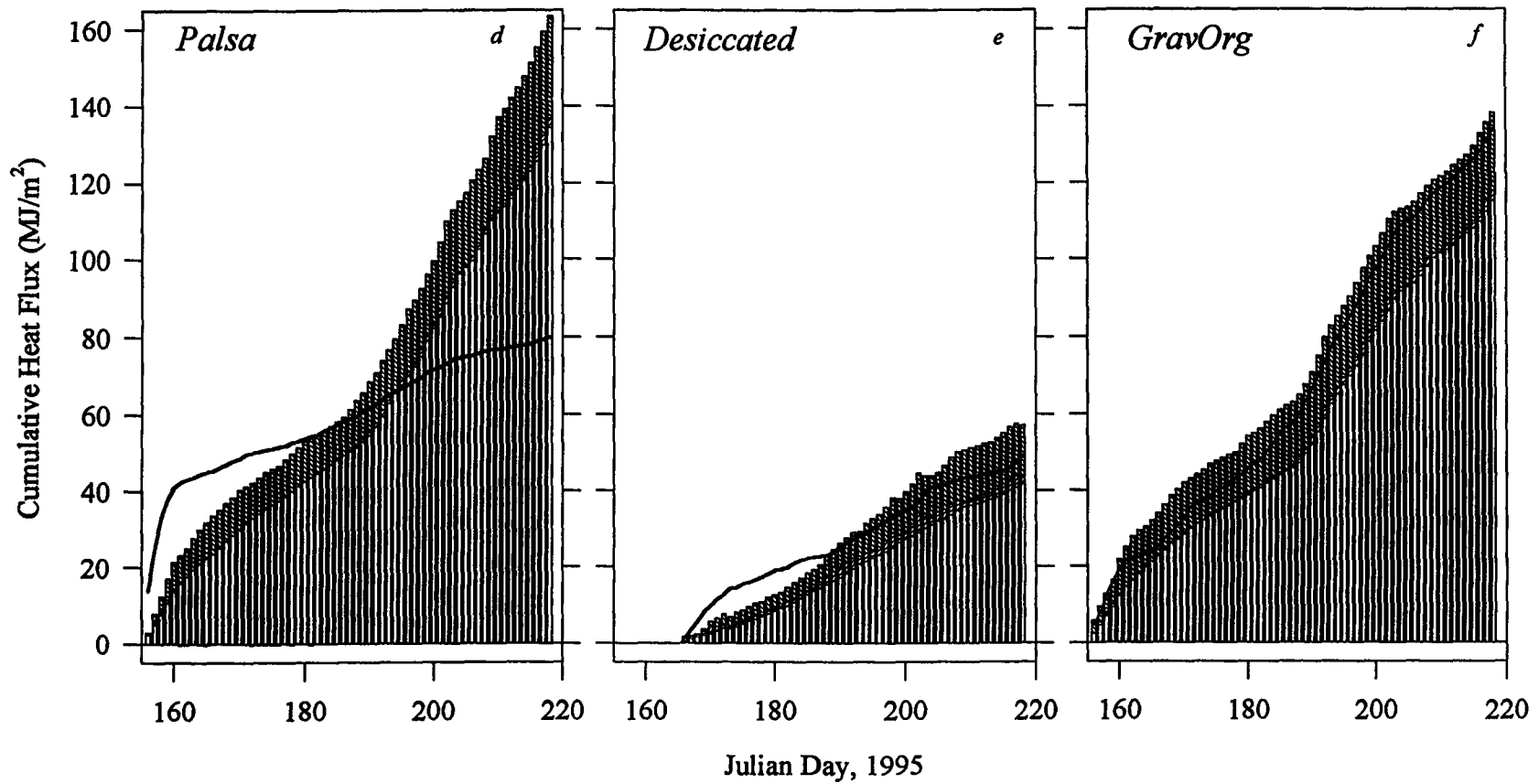
Figure 5.8(a-f) Cumulative energy balances for the organic soils. The stacked bars from the base up are Q_O, Q_S, and Q_F. The solid line is Q_G.
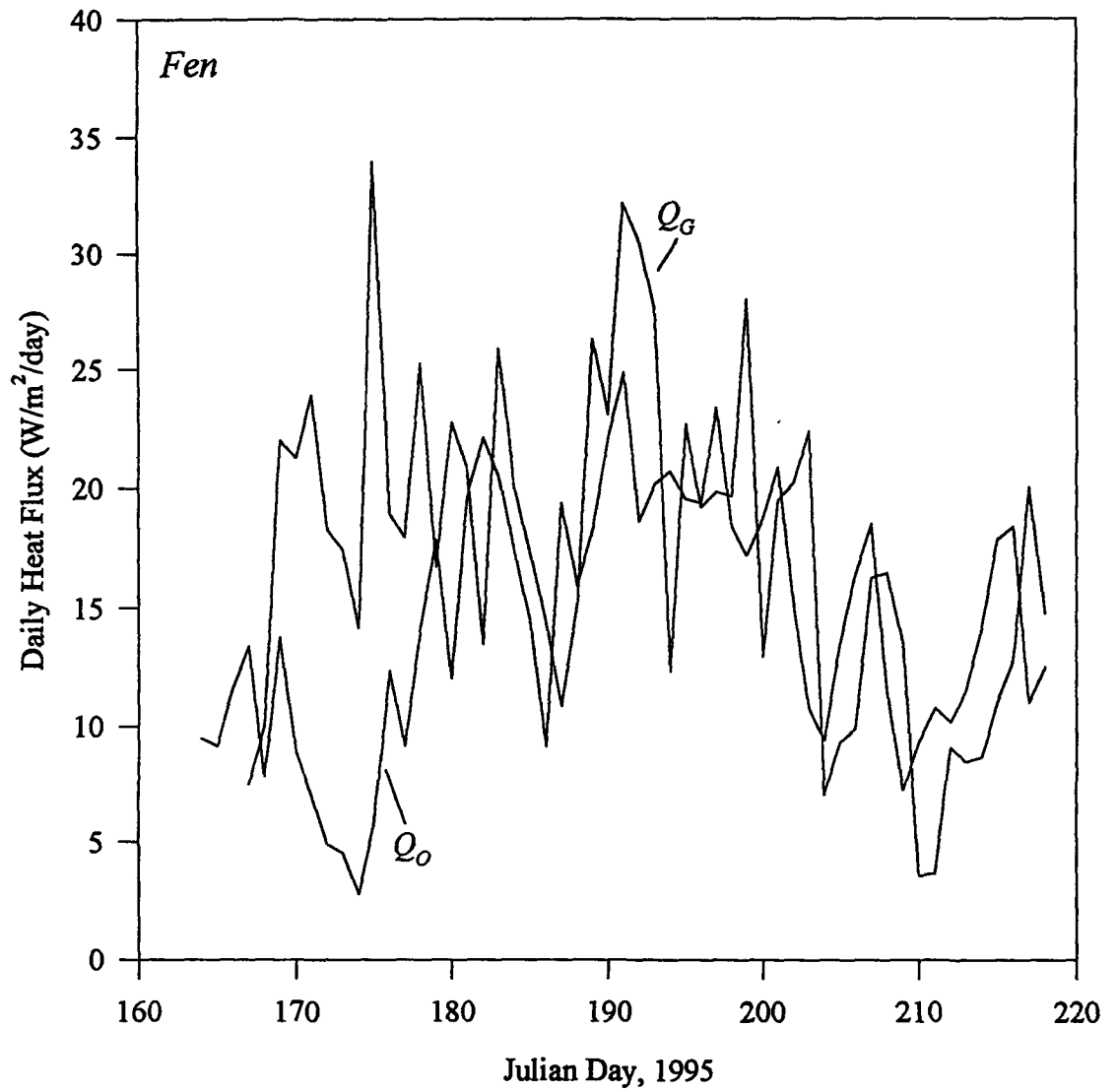
Figure 5.9   Daily variation in heat flux values of Q_G and Q_O for the *Fen* site.

energy balance and their respective percentages are shown in table 5.1. The term Q_{ground} is

obtained as

$$\int_0^\tau Q_{ground} dt = \int_0^\tau (Q_O + Q_S + Q_F) dt \qquad (5.1)$$

where τ is the total duration of the study period. In theory,

$$\int_0^\tau Q_{ground} dt = \int_0^\tau Q_G dt \qquad (5.2)$$

The daily fluxes are measured in W/m^2, a time dependent term. Over the entire study

season, units are converted to MJ/m^2 and the terms redefined as

$$Q_i = \int_0^\tau Q_G dt \qquad (5.3)$$

$$Q_p = \int_0^\tau Q_O dt \qquad (5.4)$$

$$Q_h = \int_0^\tau Q_S dt \qquad (5.5)$$

$$Q_l = \int_0^\tau Q_F dt \qquad (5.6)$$

where Q_i is the total incoming ground heat flux, Q_p is the total heat flux into and from the

permafrost, Q_h is the total energy used in warming and cooling the active layer and Q_l is

the total energy consumed in melting ground ice.

Table 5.1　　**Total Energy Balance for the Organic Soils**

Site	Measurement Period (Julian Day)	Q_i (MJ/m^2)	Q_p (MJ/m^2)	Q_h (MJ/m^2)	Q_l (MJ/m^2)	Q_{ground} (MJ/m^2)
Fen	167-218	79 (61%)	65 (50%)	4.2 (3.2%)	61 (47%)	130 (165%)
Wetland	158-218	93 (59%)	110 (70%)	3.8 (2.4%)	44 (28%)	158 (170%)
Isolated	163-218	65 (43%)	97 (64%)	3.9 (2.6%)	50 (33%)	151 (232%)
Palsa	156-218	80 (49%)	134 (82%)	2.4 (1.5%)	27 (17%)	163 (204%)
Desiccated	166-218	49 (86%)	42 (73%)	2.2 (3.9%)	13 (23%)	57 (117%)
GravOrg	156-218	135 (97%)	115 (83%)	2.9 (2.1%)	20 (15%)	138 (103%)

The bracketed terms in table 5.1 are the values expressed as a percentage of Q_{ground} while the bracketed terms in the Q_{ground} column is the ratio of Q_{ground}/Q_i. From the slopes of the cumulative energy balance, which indicate increases and decreases in the magnitude of energy fluxes, it is clear that the amount of incoming heat flux varied among the organic plots. Q_i for the plots which remained saturated (*Isolated, Fen* and *Wetland*) was significantly less than Q_{ground}. This anomaly will be discussed further in section 6.1.2. Both *Isolated* and *Fen* sites showed constant seasonal trends in Q_G, with some decline during the last ten days at the *Fen* site. The *Wetland* site had large values of Q_G at the beginning of ground thaw when temperature gradients were greatest and declined afterwards, becoming very small at the end of the study as the phreatic surface dropped within the organic layer. Q_G for the *Desiccated* and *GravOrg* site follow more closely the soil energy balance. Values at the *Desiccated* site were highest as measurement began and then declined with some mid-season fluctuation. This site had the lowest total value of Q_i for the entire season. The *GravOrg* site had cumulative Q_G closely following Q_{ground} throughout the summer. Q_G was large when measurements began and gradually declined until approximately July 9 (JD 190) at which point Q_G increased significantly as the frost

table reached the mineral soil, and declined slightly at the end of the summer. The *Palsa* site had extremely large temperature gradients during the first several days of the study period (Figure 4.3 *c*), yielding large values of Q_G, the magnitude of which rapidly declined. By the end of the study period, Q_G underestimated Q_{ground} by more than 50%; the possible reasons for which will be discussed in section 6.1.2.

The out-going heat flux from the base of the active layer to the permafrost below, Q_P, consumed the largest proportion of incoming ground heat flux, ranging between 50 and 83 per cent of Q_{ground}. The *Fen* and *Isolated* plots showed little daily fluctuation in Q_O. As a proportion of the ground energy balance, the *Fen* site had the least amount of energy (50 per cent) directed downward into the permafrost. The *Wetland* site showed a decline in Q_O at the end of the study period. The non-saturated sites, or sites without water tables at or near the surface, had greater percentages of the soil energy spent as Q_P. The *Desiccated* site had consistently small absolute values with little variation throughout the summer. Q_P of the *Palsa* and *GravOrg* sites accounted for over 80 per cent of the ground energy balance. At the *Palsa* site, Q_O was large at the beginning of the study and then gradually declined. When the frost table reached the mineral soil, the rate of downward heat flux increased sharply until the end of the study period. Q_O at the *GravOrg* site behaved similarly showing a sharp increase when the frost table reached the mineral soil around July 9 (JD 190) which was followed by a late season decline.

The smallest proportion of the subsurface energy, between 1.5 and 3.9 per cent, was consumed in warming the active layer. Despite low absolute magnitudes, daily

variations in the sensible heat were large as the active layer responded rapidly to temperature changes. The *Desiccated* site used 2.2 MJ (3.9%) for heating the active layer over the study period. This represented the lowest in absolute value and the largest in proportion among the organic plots (as organic material has a high heat capacity and the *Desiccated* site had a high water content). The *Fen, Isolated* and *Wetland* sites had the three largest values of Q_h at 4.2, 3.9 and 3.8 MJ respectively, caused by the high heat capacity of liquid water. The *GravOrg* and *Palsa* sites had lower values and percentages of total subsurface energy due to large volumes of air within the pore space.

The latent heat used to thaw the ground was the second largest component of the ground energy balance, a notable feature of permafrost soils (Rouse 1984, Roulet & Woo 1986). In general, latent heat was the largest in early summer when ground thaw was rapid. For the *Palsa* and *GravOrg* sites, Q_F was significantly reduced after the frost table reached the mineral soil and ground thaw slackened. The *Wetland* site showed a steady decline in Q_F throughout the season while the *Isolated* and *Fen* sites exhibited steadier values of Q_F. The total amount of latent heat can be related to the depth of thaw and the ice content of the soils. Furthermore, the wet soils had the three highest percentages of Q_l. Despite the presence of an ice-rich cores at the *Palsa* and *GravOrg* plots, their thaw depths were shallow and consequently their Q_F was low.

5.2.2 Polar Desert Soils

Cumulative ground energy balances in the polar desert soils showed much less variation than the organic soils (Figure 5.10 a-i). The partitioning of energy expenditure is presented in table 5.2.

Table 5.2   Total Energy Balance for Polar Desert Soils

Site	Measurement Period (Julian Day)	Q_i (MJ/m²)	Q_p (MJ/m²)	Q_h (MJ/m²)	Q_l (MJ/m²)	Q_{ground} (MJ/m²)
Control1	166-218	83 (93%)	47 (53%)	7.3 (8.2%)	35 (39%)	89 (108%)
Control2	166-218	93 (75%)	80 (65%)	7.2 (5.8%)	36 (29%)	123 (132%)
CarbonBlack	166-218	120 (100%)	74 (61%)	7.5 (6.2%)	39 (32%)	121 (100%)
Snow	169-218	71 (61%)	78 (67%)	4.2 (3.6%)	35 (30%)	117 (165%)
Rain	166-218	95 (80%)	79 (67%)	6.4 (5.4%)	33 (28%)	118 (125%)
RainFen	168-218	92 (75%)	78 (63%)	6.4 (5.2%)	39 (32%)	123 (132%)
RainRoad	166-218	99 (87%)	72 (64%)	7.3 (6.4%)	34 (30%)	113 (114%)
Road	166-218	71 (58%)	82 (67%)	6.9 (5.7%)	33 (27%)	122 (172%)
Gravel	166-218	130 (120%)	69 (63%)	5.7 (5.2%)	34 (30%)	109 (84%)

Q_i varied among the plots with absolute values ranging between 71 MJ and 130 MJ and with percentages ranging from 61 to 120 of Q_{ground}. Daily variations in Q_G were high in polar desert soils (Figure 5.11). The seasonal behaviour of Q_G was not as distinct, the exception being the *Snow* and *Control1* sites which were higher at the beginning of the study. The *Gravel* site showed the greatest magnitude and percentage of Q_i, followed by the *Carbon Black* site which had the highest Q_i for the polar desert soils. Over the entire study period, there was no consistent relationship in Q_i among the sites with simulated rainfall and those without. The *Road* plot was anomalous in that Q_i was very low compared to the total ground energy balance. In all cases except the *Gravel* and *Carbon Black* sites, Q_i underestimated Q_{ground} between 12 and 42 per cent.
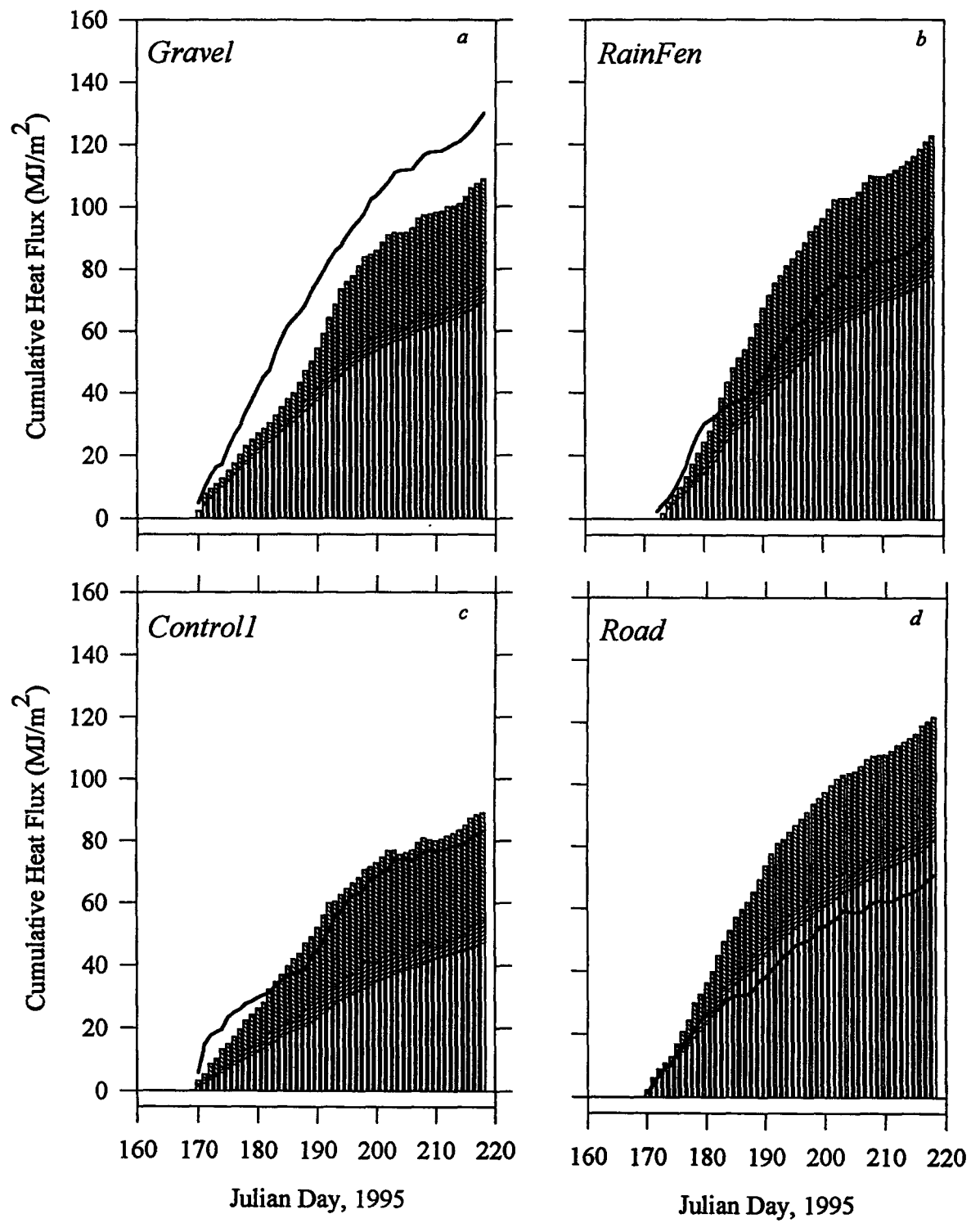
Figure 5.10 (*a-i*)   Cumulative energy balances for the polar desert soils. The stacked bars from the base up are Q_O, Q_S and Q_F. The solid line is Q_G.
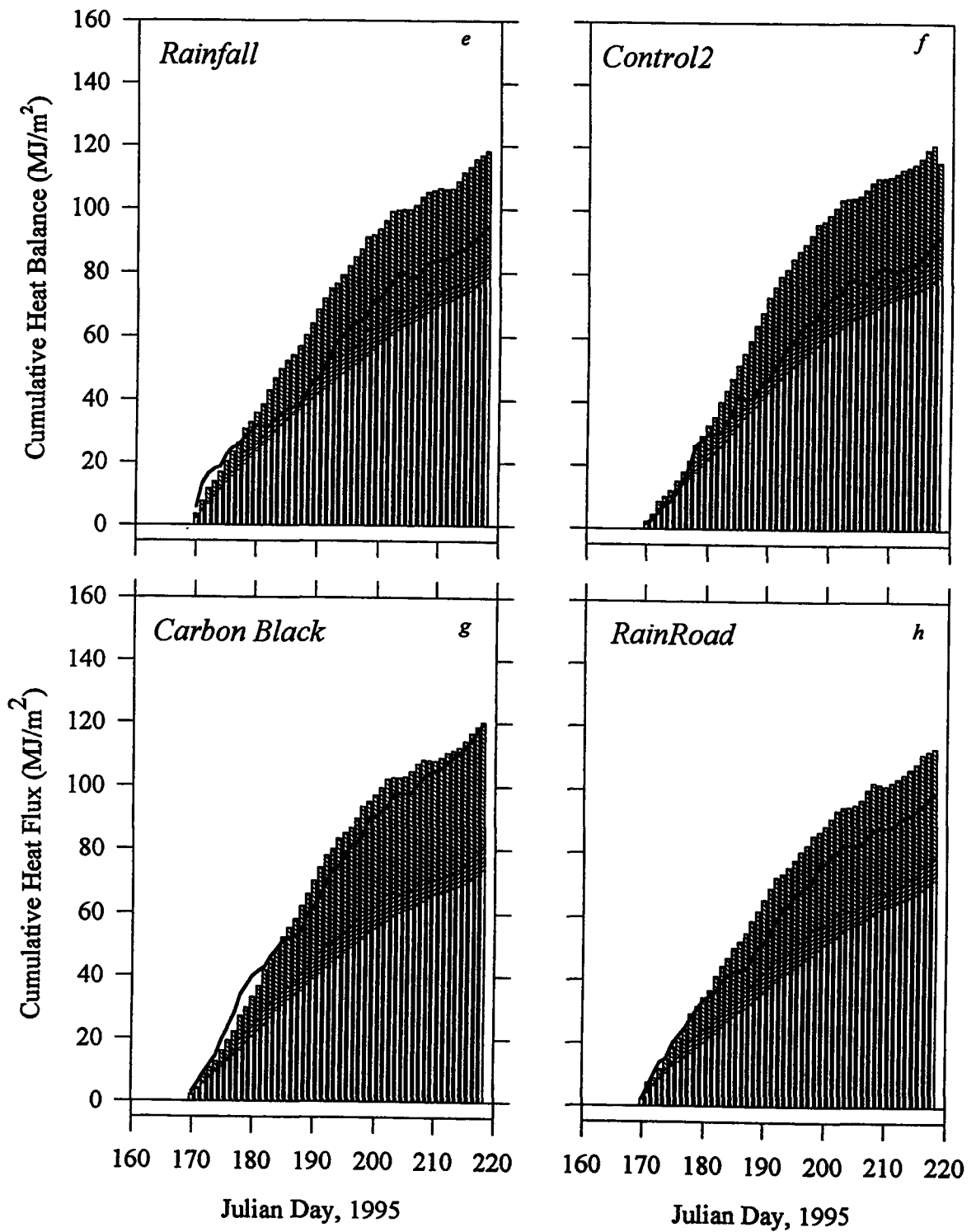
Figure 5.10 (a-i)   Cumulative energy balances for the polar desert soils. The stacked bars from the base up are Q_O, Q_S and Q_F. The solid line is Q_G.
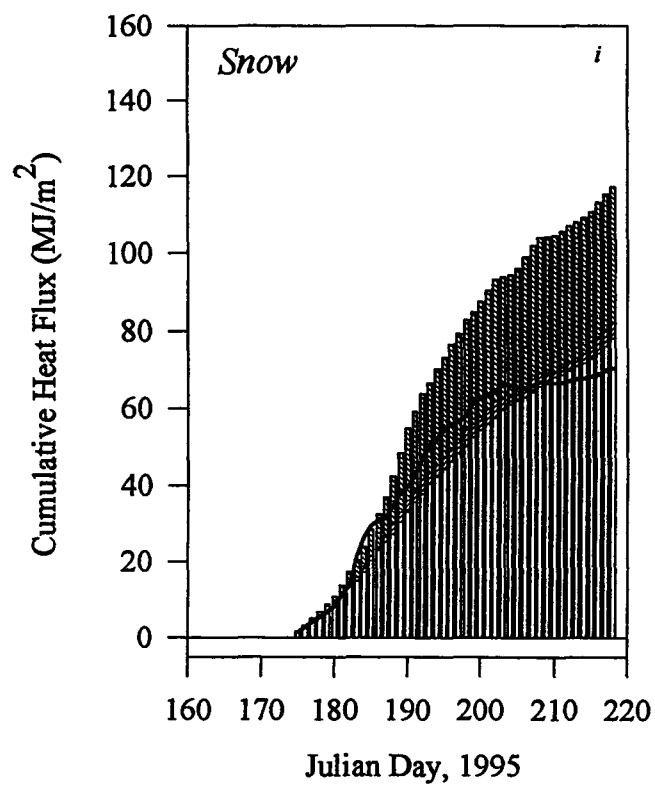
Figure 5.10 (*a-i*) Cumulative energy balances for the polar desert soils. The stacked bars from the base up are Q_O, Q_S and Q_F. The solid line is Q_G.
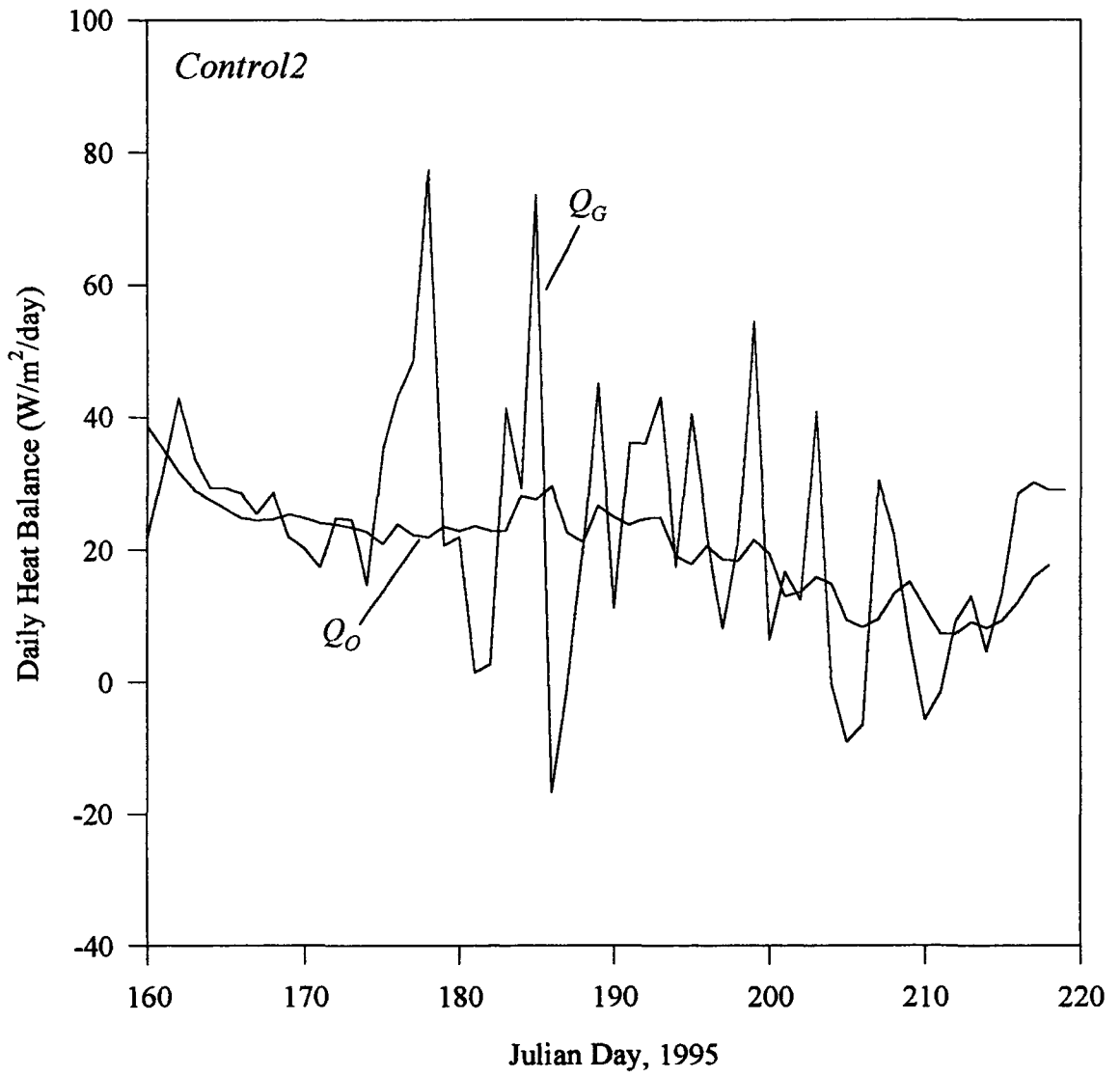
Figure 5.11   Daily variations in heat flux values of Q_G and Q_O for the *Control2* site.

Heat flux directed into the permafrost was greatest just after snowmelt and gradually declined throughout the summer as inferred from the slope of the Q_O curve. Outgoing heat flux was the largest portion of the ground energy balance at all plots. As a percentage of Q_{ground}, Q_p ranged from 53 to 67 per cent; 53 per cent at the *Controll* plot being 10 per cent lower than the next smallest value. Again, there was no clear distinction between plots except the *Gravel* site which showed a reduction in Q_O around July 11 (JD 192) when ground thaw slowed down dramatically (Figure 4.7 *e*). The *Controll* site had a Q_O much less than the rest of the plots and was perhaps influenced by its proximity to the fen which cooled soil temperatures reducing the downward heat flux.

Energy used in heating the polar desert soils was greater than values obtained for the organic soils, yet represented the smallest fraction of the ground energy balance. Day to day fluctuations in sensible heating were noticeable and maximum values of Q_F were achieved by the middle of the study period as the active layer was warmest before July 24 (JD 205). Of the total ground energy balance, between 3.6 (*Snow*) and 8.2 (*Controll*) per cent were used in warming the active layer. The *Snow* plot had the smallest value of Q_h as it had the latest ground thaw. The largest value of Q_h was the *Carbon Black* site.

Latent heat used to thaw the soil was the second greatest element of the ground energy balance, with relative proportions similar to those found in organic soils. Q_l was greatest after thaw began at all sites except the gravel pad where the frost table descended slowly until the mineral soil was reached. As thaw slackened, so did the rise in Q_F. Values of Q_l for all sites were similar.

CHAPTER SIX

Discussion

In chapters 4 and 5, field observations and ground energy balances were used to asses the effects of organic soil development and environmental disturbances on active layer thaw. This chapter discusses the relationships with regards to previous studies and the processes involved.

6.1   Organic Soils

Organic soil development in continuous permafrost environments is controlled by external sources of water through the short growing period. Humification is principally dependent upon the long-term water table position. If the water table drops below the organic layer, aerobic condition occurs and decomposition will follow (Gorham 1991).

In this study, six organic soils in different stages of growth and decay were used to assess active layer development under different micro-environments. By using space as an analogue for time, it is possible to speculate how changes to hydrologic and organic soil conditions will affect active layer thaw.

Water table position exerts direct and indirect controls on active layer thermodynamics. The increased heat capacity of saturated soils cooled the surface temperatures and moderated temperatures throughout the profile. Thermal transfer was

greater in saturated soils than those with air in the pore spaces, providing for warmer temperatures deeper in the profile. Furthermore, thermal diffusivity (k/c) of saturated organics was greater than the dry organic layers, providing for deeper active layer development. Previous research has shown that thermal diffusivity is the primary control of active layer depths (Rouse *et al.* 1992, Nakano & Brown 1971).

Active layer depth declined as organic decomposition increased. The *Palsa* site, similar to the *Wetland* site in composition yet without a water table near the surface, had shallower thaw depths due to the insulative ability of the dry organic mat, a phenomenon often cited in permafrost studies (e.g. Brown 1977, Nelson *et al.* 1985). Beneath this organic mat, soil moisture was high and not linked closely to moisture changes in the dry organic layer (Figure 4.5). In effect, the soil beneath the organic layer was 'uncoupled' from the surface organics with little moisture uptake from the mineral soils (Riseborough & Burn 1988). This observation is in contrast to those of Rouse *et al.* (1992), who showed only the top organic layer dried while the underlying peat remained moist, providing water for high evaporation rates. In this study, the uncoupling of moisture from the mineral substrate is important as it implies that water table drawdown beneath the organic layer will result in steep declines in thermal conductivity and diffusivity of the surface layer; reducing active layer development.

The rate of active layer thaw at the *Desiccated* site was slow as the organic rich soil had low thermal diffusivities, with only the *Palsa* site being less. Soil moisture remained high throughout the summer (Figure 4.5), with only the top few centimeters becoming dry late in the season. Beneath the surface the organic soil remained wet,

suggesting that evaporation was limited. Reduced evaporation rates in highly humified organics can be caused by the lack of sufficient pore structure to draw water under tension to the surface (Ingrham 1984) and because of a shallow rooting zone which limits transpiration.

6.1.1 Energy Balances

The heat balance approach has been previously applied to ground heat flux studies in permafrost environments (Rouse 1984, Woo & Xia 1996). The most distinctive feature of permafrost soils is the large latent heat term, dissipating up to one half of the annual energy balance (Riseborough & Burn 1988). In organic soils, it is the second dominant term in the summer active layer energy balance (table 5.1). Q_l is the greatest at sites with water tables near the surface and extensive thawed zones. Shallower active layers have less energy consumed in phase change and more energy is directed into warming the permafrost.

The total volume of ground ice is critical in determining the maximum thaw depth, as more energy is required to melt ice and liberate latent heat in permafrost soils than to raise soil temperatures. Both the *Palsa* and *GravOrg* sites were underlain by a massive body of ice (Figure 3.5). The amount of energy received at the soil/ice interface was insufficient to melt it, limiting active layer depth to the soil/ice boundary. There is also subjective evidence that the *Wetland* site, located near both the *Palsa* and *GravOrg* sites, is underlain by ground ice because even though Q_l was proportionately small, there was a sudden retardation of frost table descent during the final 20 days of the study (Figure 4.4).

A possible explanation for this abrupt decline, which was not observed at the other saturated sites, is the lack of energy to melt massive ground ice at depth.

Heat flowing downwards into the permafrost was the dominant energy sink at all sites. The greatest values of Q_p as a percentage of Q_{ground} were in the three sites no longer accumulating organics (*Palsa, GravOrg* and *Desiccated*). Large values of Q_p, (also found at the *Wetland* site) may be partially explained by the presence of massive ground ice.

Rouse (1984) in continuous permafrost near Churchill, Manitoba, found latent heat comprising 87 and 90 per cent of the total ground heat flux during the summer warming phase in tundra and forest soils respectively. Although these values are higher than the ones obtained in this study, thaw depths were between 1.5 and 2 m. Woo and Xia (1996) in a fen near the *Wetland* site calculated 60 per cent of the ground heat consumed as latent heat, 44 per cent passing downward into the permafrost and 2.4 per cent used in heating the active layer. Conversely, this study shows Q_p, not Q_l dominating over the course of the summer thaw. Discrepancies may occur from different methods of calculating the ground heat balance and the potential for measurement and parameter error.

6.1.2   Heat Transfer

Nixon (1975), stated that conduction is the principal mechanism of heat transfer within frozen soil. Woo and Xia (1996) supported this statement when applying the energy balance to a High Arctic fen. In this study, Q_G significantly underestimated Q_{ground} at the three saturated sites (*Fen, Wetland* and *Isolated*) and the *Palsa* site, raising the possibility of other heat transfer mechanisms. Convection of water, and therefore heat, within the soil column will cause Q_G, a term based purely on conduction, to fall short of

Q_{ground}. If warmer surface waters are transported downward in the soil column; either though temperature induced convection or forced convection, temperature gradients are reduced and conduction declines. In the porous organic layer, convection is not restricted by low soil permeability. High winds may promote mixing at sites when water tables are above the surface and at the *Wetland* site, water is already flowing laterally through the active layer from the late-lying snowbank.

At the *Palsa* site, evaporation is low and the vapour pressure gradient is dominated by the soil temperature gradient, forcing vapour towards the frost table. The flux of vapour may account for a significant transfer of heat. Halliwell and Rouse (1987) calculated that vapour can account for up to 40 per cent of the total downward heat flux at certain times in dry peat. At the *Palsa* site, which was dry over the entire summer, this may account for inability of Q_G to predict Q_{ground}.

At the *Desiccated* and *GravOrg* sites, Q_G closely follows Q_{ground} over the study period, showing that the energy balance method adequately describes heat transfer in soils dominated by conduction. In summary, although conduction is important in all organic soils, convective methods of heat transport within the saturated organic layer and dry, aerated organic mats may be significant.

6.1.3 Environmental Implications

Organic soil development in the High Arctic can be traced through a series of processes from the initial stages of organic development with phreatic surfaces at the surface and deep active layers (*Fen*), through maturation and thickening of the organic layer (*Wetland*), and for the possible removal of constant summer water sources through

drainage dislocation (*Isolated*). Several mechanisms exist which deprive organic materials of their water sources, halting growth and causing humification. Humification decreases heat transfer in the thawed zone, shallowing up active layer depths. At the *Palsa* site, an ice-cored mound has isolated the organic soil from its primary source of water, the late-lying snowbank. This has initiated the decomposition of the organic layer, reducing heat transfer and curtailing thaw depths. At the *Desiccated* site, decomposition has probably been occurring for a long time. A shallow active layer exists beneath this soil as the thick organic mat is now unable to effectively transfer heat due to it's highly humified state. Comparisons among the plots show that water table position plays an important role in controlling organic soil development and active layer dynamics. The change in water table position through time must be considered the principal factor in understanding changes in active layer hydrology and thaw beneath organic soils.

By placing a gravel pad over humified organic soils, thaw depths increased as gravels have better heat transfer properties than dry organics. The increased flux in downward directed energy thickened the active layer and initiated melt of the ice-rich substrate. The *GravOrg* site is important as it shows the ground energy balance is an effective and accurate method of accounting for fluxes of heat in soils dominated by conduction.

Current theories on the impacts of climate change call for the widespread disappearance of wetlands in permafrost environments as increased temperatures thicken the active layer, increasing storativity and dropping water tables (Woo *et al.* 1992). Neglecting thermokarst and water from melting ground ice, dropping water tables will

deprive surface organics of water, causing them to decompose and/or be replaced by different plant communities. Water table position has an important influence on both the active layer energy balance and organic soil development. If the water table drops in response to a thickening active layer, surface organics will dry, reducing heat transfer as thermal conductivity and diffusivity decline. Thus, further deepening of the active layer will be retarded. A feedback mechanism may exist where permafrost wetlands maintain themselves by keeping the active layer shallow from a reduction in heat transfer when dry. Another consequence of drying organics is that they become more friable and can be eroded by running water (*Desiccated*). Desiccated organics develop cracks which allow water penetration and hence convection of heat. More research on moisture and heat interactions in organic soils is necessary to adequately predict the response of permafrost wetlands and organic soils to a warming climate.

Numerical models of active layer development do not consider the response of surface organics, predicting that in all cases warming temperatures will increase active layer thickness (Kane *et al.* 1991, Hinzman & Kane 1992). Furthermore, modeling the presence of massive ground ice is ignored as the substrate beneath the active layer is assumed similar to the near-surface material. Massive ground ice beneath the present active layer will require large volumes of latent heat to melt which cannot be achieved by slight temperature increases over decades or centuries. Models of active layer development must provide for the inclusion of ground ice and the unique behaviour of organic soils when forecasting the effects of climate change.

6.2 Polar Desert Soils

In polar desert soils, there is a lack of consistent relationships among the plots, the exception being the *Gravel* plot. While changes in soil structure and surface moisture content had discernible influences on thermal properties (Figure 5.5), the energy balance did not always follow the expected trends.

Throughout the summer, the frost table was the location of the major heat sink. Mean summer temperatures were affected by the timing of snowmelt as temperatures were kept below 0°C until the snow overlying the plot melted. Frost table descent was similar at all sites except the *Gravel* plot. The proximity to wetland appeared to have an influence on active layer heat transfer as thaw depths at the *Control1* and *RainFen* sites were shallower than the other plots. Unlike large water bodies, which have a high thermal inertia and thick thawed zones, thaw depths in the adjacent wetland were shallow exhibiting the same general active layer development as the *Fen* site. The shallower and cooler active layer in the wetland may have acted as a heat sink for the adjacent polar desert sites (*Gravel, RainFen* and *Control1*), explaining their less extensive thaw depths.

The *Gravel* plot had the coolest temperatures throughout the profile. Thaw depth was also shallowest and by placing a 10 cm pad over the polar desert soil, the depth of thaw in the polar desert substrate was reduced significantly from the previous year. Conversely, Woo & Marsh (1990) showed increased active layer depth in gravel soils, suggesting improved heat transfer. This apparent disparity may be explained by the fact

that the gravel pad was not a true gravel soil as it was disturbed when moved. The proportion of sand and silt in the gravel pad was reduced, with poorer contacts between gravel particles. These factors reduce heat transfer in the gravel pad, resulting in shallower thaw depths.

The practicality of using seasonal temperature means to compare plots is unclear due to their insensitivity to processes operating over shorter time scales. Aside from the *Gravel* plot, there are no clear temperature relations among plots. Furthermore, short term temperature trends did not give conclusive results. There were only minimal effect from rainfall on hourly temperatures when comparing the adjacent *Control2* and *Rain* plots (Figure 4.8), differences in c being the probable mechanism. Increased surface moisture had no effect on temperatures at the 10 cm level, confirming the observations of Tedrow (1966) that low intensity summer rainfall affects moisture content only in the top few centimeters of polar desert soils. Surface cooling from increased evaporation was not observable in the wetter soils.

The *Carbon Black* site had warmer hourly temperatures between Julian Days 200 and 205 than the adjacent *Control2* plot (Figure 4.9). Increased surface temperatures can be attributed to lower albedo which increased ground heat flux though equation 2.2. Higher values of Q_i corresponded with warmer soil temperatures and deeper thaw depths, the notable exceptions are the *Gravel* plot with high Q_i and limited thaw depth and the *Road* plot with the opposite tendencies. Calculated thermal diffusivities did not adequately predict differences in thaw depth because there were few soil moisture samples at depth to permit a detailed representation of the entire soil profile.

6.2.1 Energy Balances

There are few clear trends among the energy balances of the polar desert soils. Thermal parameters compare well with published studies (Farouki 1981, Hinzman *et al.* 1991), eliminating spurious calculations as a source of error. The *Snow* plot was anomalous in that after Julian Day 200, Q_G became small on a daily basis, for which the reason is unclear.

Conduction is established as the dominant heat transfer mechanism in mineral permafrost soils (Nixon 1975, Farouki 1981, Woo & Xia 1996). There is little contradictory evidence from this study, yet Q_i consistently underpredicted Q_{ground} at all sites except *Carbon Black* and *Gravel*, raising the possibility of other heat transfer mechanisms or systematic errors in the determination of Q_G. Hinkel *et al.* (1993) showed the importance of non-conductive processes in permafrost soils, such as internal distillation, transferring heat over short time scales. These processes, however, are driven by large temperature gradients which are not found in this study and can be eliminated as significant heat transfer mechanism. Errors are incurred when calculating Q_G from daily averages of temperature and soil parameters, along with the empirical methods of determining soil parameters (equations 2.11 to 2.13).

Sensible heating of the active layer was the smallest component of the heat balance. There were few clear trends among plots with regard to absolute values or percentages. The results of this study agree well with those of Woo and Xia (1996), who measured 5 MJ of energy consumed in warming the active layer over the thaw season, accounting for 5 per cent of the active layer heat balance.

Latent heat was the second dominant term in the active layer heat balance. The sites with the deepest thaw had higher absolute values of Q_l. The high percentage of Q_l at the *Control1* site was an artifact of the low value of Q_p. Ground ice is abundant at the base of the active layer in polar desert soils (Woo and Xia 1996), the mechanisms of formation is well known (Cheng 1983, Mackay 1983). The presence of this ground ice which can vary over short distances, may play an important role in the heterogeneity of thaw depths among the sites. Several centimeters of thaw represents significant quantities of energy. Without accurate determination of ice content at all depths, values of Q_l are subject to error. The values of Q_l found in this study were low compared with the results of Woo and Xia (1996) who show that Q_l accounts for 49 per cent of ground heat in polar desert soils. Differences may arise in that they calculated Q_l as a residual term, insuring balance between Q_i and Q_{ground}.

In polar desert soils, heat flow downward into the permafrost is the major component of the active layer energy balance. At all sites except *Control1*, Q_p was between 61 and 67 per cent of the active layer heat balance. This indicates that most heat incident at the surface passed through the active layer into the permafrost. Q_p was large compared to values found in other permafrost environments where Q_l is the dominant term (Rouse 1984, Woo & Xia 1996). In the polar desert soils, no systematic trends were evident in Q_p among plots.

6.2.2 Environmental Implications

There have been several attempts to model active layer thaw under present day and climate change scenarios (Smith & Riseborough 1983, Kane *et al.* 1991, Hinzman & Kane

1992). Kane *et al.* (1991) and Hinzman & Kane (1992) calculated the effects of several warming and moisture change scenarios over different times scales, showing dramatic increases in active layer depths over 50 years. Evaporation also increased with rising temperatures, competing with runoff as the major source of water loss. Although providing insight into active layer responses, these models do not consider the full spectrum of responses, neglecting the heterogeneity of subsurface material, ground ice and proper consideration of soil moisture. Smith & Riseborough (1983) in a boundary layer model state that soil moisture and snow cover have the greatest influence, and surface albedo the least, on active layer thaw. This contradicts the short term results of this study which show more discernible effects from lowering the albedo than from increases in surface soil moisture. Increased snowfall delays the onset of ground thaw. Increases in summer precipitation, as indicated for the high arctic by GCMs, may be insufficient to dramatically alter soil moisture conditions in polar desert soils.

By placing a gravel pad over mineral soils as a thaw stable aggregate, active layer depth declines. This is important as it implies gravel pads provide insulation in mineral soils and may prevent the melting of massive ground ice often found at the base of the pre-disturbance active layer. Compaction of soils from human activity increases thaw depth as thermal conductivity is increased. Even limited compaction can cause ground subsidence and ponding water (Figure 3.9).

6.3   Sources of Error

Imprecision in the calculations, parameter determination and boundary layer effects are all sources of error. Boundary layer effects are present due to the limited plot size.

Lateral advection of water and heat, such as from the adjacent fen in the polar desert study area, will affect energy balances. The magnitude of boundary layer effects on the calculations at each plot is impossible to determine and thus remains a source of unknown error.

The validity of using cumulative totals in energy balance calculations remains unclear. While cumulative values preserve short term relations without obscuring long term trends, the theory of ground thaw is essentially a Stefan problem, with time as a variable. It is possible that time overwhelms all other variables on a seasonal basis, insuring close agreement in energy balances when in fact large differences occur among the plots. On a daily basis, it is impossible to insure a balance between Q_G and Q_{ground} due to lag effects.

Parameter estimation remains a significant source of error. Surface moisture was obtained every second day, yet moisture content at depth was sampled less frequently and away from the plots. Furthermore, the presence of ground ice at the base of the active layer was often inferred and not measured.

When calculating parameters at depth, the 0°C isotherm was considered to be located precisely at the freezing front as determined from probing, a fact which has been shown to be inaccurate (Nelson & Outcalt 1982). Both the diameter of the probe and soil type affect the depth where frozen ground is encountered. This imprecision will create errors in Q_O, Q_F and Q_S.

CHAPTER SEVEN

Summary

This study evaluated the effects of organic terrain in various stages of development and surface modification on active layer development. By examining energy fluxes in conjunction with hydrologic conditions, it was possible to assess the possible effects of environmental change on active layer dynamics.

In organic soils, heat transfer was related to both the level of humification and position of the water table, two variables which by their nature cannot be separated. In all soils, Q_p was the greatest component of the subsurface energy balance, followed closely by Q_l with Q_s being the smallest. Organic soils with water tables near the surface (*Fen, Wetland* and *Isolated*) had deeper thawed zones, warmer soil profiles and more energy consumed in melting ground ice and heating the active layer. In dry humified organics, heat transfer was reduced, thermal conductivity declined and temperatures could not penetrate to depth. In these soils (*Palsa, Desiccated*) active layers remained shallow and greater amounts of energy were directed into the permafrost. A feedback mechanism may exist where wetland organics act to maintain themselves by keeping the active layer shallow from a reduction in heat transfer when dry. The presence of massive ground ice in limiting active layer thaw was evident. Large amounts of energy necessary to melt ground

ice may buffer the active layer from slight increases in temperature, yet eventual melt will have both geomorphic and hydrologic consequences.

Although conduction dominated heat transfer in organics, convection of heat from both water and vapour may account for the inability of Q_G to predict Q_{ground}. If environmental change has a significant impact on the extent and composition of organic soils in permafrost regions, an improved understanding of heat transfer processes in these soils is necessary to predict and model future changes.

The short term response of mineral soils to changing boundary conditions was inconclusive. Although there were some trends among the plots, energy balances and soil temperatures did not display clear results. Simulated rainfall had a discernible effect on soil parameters, yet did not noticeably alter soil temperatures or ground energy balances. Of the treatments, increased snowcover and decreased albedo showed the greatest influence on active layer thaw. The effect of compaction on thaw depths was also evident.

Stratigraphic change of the soil profile affects heat transfer by changing the surface boundary condition, modifying all components of the ground energy balance. In both organic (GravOrg) and mineral (Gravel) soils, thaw depths were modified significantly, reflecting the change in heat transfer associated with changing soil composition. The effectiveness of gravel as a building material was seen at the Gravel site, which had thaw depths reduced from the previous year.

Present models of active layer development fail to consider soil heterogeneity, surface organics, non-conductive heat transfer and the presence of massive ground ice.

The results of this study demonstrate the importance of these variables in active layer thermodynamics. Quantification of heat and moisture fluxes while considering the composition of the soil column is an advance necessary to properly model the response of permafrost soils to changing environments.

REFERENCES CITED

Boelter, D.H. (1969) Physical properties of peats as related to degree of decomposition. *Proceedings of the Soil Science Society of America*, **83**, 606-609.

Bostock, H.S. (1970) Physiographic subdivisions of Canada. In: *Geology and Economic Minerals of Canada*, Douglas, R..J.W. (ed), Geologic Survey of Canada Economic Report 1, Information Canada, Ottawa, 10-30

Brown, R.J.E. (1973) Influence of climatic and terrain factors on ground temperatures at three locations in the permafrost region of Canada. *Proceedings of the Second International Conference on Permafrost, Yakutsk, USSR, North American Contribution*, pp 27-34. Washington D.C.

Brown, R.J.E. (1977) Muskeg and permafrost. In: *Muskeg and the Northern Environment*, N.W. Radforth & C.O. Brawner (eds). University of Toronto Press, pp 148-163.

Cheng. G. (1983) The mechanism of repeated-segregation for the formation of thick layered ground ice. *Cold Regions Science and Technology*, 8, 57-66.

Cruickshank, J. (1971) Soil and terrain units around Resolue, Cornwallis Island. *Arcitc*, **24**, 195-209.

Farouki, O.T. (1981) *Thermal properties of soils*. U.S. Army Cold Regions Research and Engineering Laboratory, Hanover. Report 82-08, 90 pp.

French, H.M. (1975) Man-induced thermokarst, Sachs Harbour airstrip, Banks Island, N.W.T. *Canadian Journal of Earth Science*, **12**, 132-144.

French, H.M. (1980) Terrain, land use and waste drilling fluid disposal problems, Arctic Canada. *Arctic*, **33**(4), 794-806.

Goodrich, L.E. (1982) The influence of snow cover on ground thermal regime. *Canadian Geotechnical Journal*, **19**, 421-432.

Gorham, E. (1991) Northern peatlands: role in the carbon cycle and probably responses to climatic warming. *Ecological Applications*, **1**(2), 182-195.

Hallet, B. & Rasmussen, L.A. (1993) Calculation of the thermal conductivity of unsaturated frozen soil near the melting point. In: *Proceedings of the Sixth International Conference on Permafrost*. South China Univeristy of Technology Press, Beijing, pp. 226-231.

Halliwell, D.H. & Rouse, W.R. (1987) Soil heat flux in permafrost: characteristics and accuracy of measurement. *Journal of Climatology*, 7, 571-584.

Harris, S.A (1986) *The Permafrost Environment*. Croom Helm Ltd. London. 276 pp.

Hayhoe, H. & Tarnocai, C. (1993) Effect of site disturbance on the soil thermal regime near Fort Simpson, Northwest Territories, Canada. *Arctic and Alpine Research*, 25(1), 37-44.

Heginbottom, J.A. (1973) Some effects of surface disturbance on the permafrost active layer at Inuvik, N.W.T., Canada. In: *North American Contribution, Second International Permafrost Conference*. Washington. pp 649-657.

Hinkel, K.M. & Outcalt, S.I. (1993) Detection of nonconductive heat transport in soils using spectral analysis. *Water Resources Research*, 29 (4), 1017-1023.

Hinzman, L.D. & Kane, D.L. (1992) Potential response of an arctic watershed during a period of global warming. *Journal of Geophysical Research*, 97, (D3), 2811-2820.

Hinzman, L.D., Kane, D.L., Gieck, R.E. & Everett, K.R. (1991) Hydrologic and thermal properties of the active layer in the Alaskan Arctic. *Cold Regions Science and Technology*, 19, 95-110.

Ingram, H.A.P. (1984) Hydrology. In; *Ecosystems of the World 4A: Mire - Swamp, Bog, Fen and Moor*, A.J.P. Gore (ed). Elsevier, Amsterdam, pp67-158.

Kane, D.L., Hinzman, L.D. & Zarling, J.P. (1991) Thermal response of the active layer to climatic warming in a permafrost environment. *Cold Regions Science and Technology*, 19, 111-122.

Kane, D.L., Hinzman, L.D., Woo, M-k, & Everett, K.R. (1992) Arctic hydrology and climate change. In; F.S. Chapman *et al.* Eds., *Arctic Ecosystems in a Changing Climate:Ecophysiological Perspective*. Academic Press, San Diego. pp35-57.

Lawson, D.E. (1986) Response of permafrost terrain to disturbance: a synthesis of observations from Northern Alaska, U.S.A. *Arctic and Alpine Research*, 18(1), 1-17.

Lunardini, V.J. (1981) *Heat Transfer in Cold Climates.* Van Nostrand Reinhold, New York, 731 pp.

Mackay, J.R. (1970) Disturbances to the tundra and forest tundra environment of the western Arctic. *Canadian Geotechnical Journal,* 7, 420-432.

Mackay, J.R. (1983) Downward water movement into frozen ground, western Arctic coast, Canada. *Canadian Journal of Earth Science,* 20, 120-134.

Marsh, P & Woo, M-k. (1993) Infiltration of meltwater into frozen soils in a continuous permafrost environment. In: *Proceedings of the Sixth International Conference on Permafrost.* South China Univeristy of Technology Press, Beijing, pp. 226-231.

Maxwell, J.B. (1980) *The climate of the Canadian Arctic Islands and adjacent water,* vol. 1, Environment Canada, Atmospheric Environment Serivice, 532pp.

Maxwell, J.B. (1992) Arctic climate: potential for change under global warming. In *Arctic Ecosystems in a Changing Climate: an Ecophysiological perspective,* F.S. Chapin *et al.,* eds. Academic Press, San Diego, pp. 11-34.

Meisner, A.D. (1955) Heat flow and depth of permafrost at Resolute Bay, Cornwallis Island, N.W.T., Canada. *Transactions of the American Geophysical Union,* 36, 1055-1066.

Moore, T.R. (1987) Thermal regime of peatlands in subarctic eastern Canada. *Canadian Journal of Earth Science,* 24, 1352-1359.

Nakano, Y. & Brown, J. (1971) Effects of a freezing zone of finite width on the thermal regime of soils. *Water Resources Research,* 7, 1226-1233.

Nelson, F.E. & Outcalt, S.I (1982) Anthropogenic geomorphology in northern Alaska. *Physical Geography,* 3(1), 17-48.

Nelson, F.E., Outcalt, S.I., Goodwin, C.W. & Hinkel, K.M. (1985) Diurnal thermal regime in a peat-covered palsa, Toolik Lake, Alaska. *Arctic,* 38(4), 310-315.

Nicholson, F.H. (1976) Permafrost thermal amelioration tests near Schefferville, Quebec. *Canadian Journal of Earth Science,* 13, 1694-1705.

Nixon, J.F. (1975) The role of convective heat transport in the thawing of frozen soil. *Canadian Geotechnical Journal,* 12, 425-429.

Racine, C.H. & Ahlstrand, G.M. (1991) The response of tussock-shrub tundra to experimental all-terrain vehicle disturbances in South-Central Alaska. *Arctic*, **44**(1), 31-37.

Ramanathan, V. (1988) The greenhouse theory of climate change: a test by an inadvertent global expermiment. *Science*, **240**, 293-299.

Riseborough, D.W. & Burn,C.R. (1988) Influence of an organic mat on the active layer. In: *Proceedings, Fifth Inernational Conference on Permafrost, Trondenheim, Norway*. vol 1. Tapir Publishers, Trondheim, pp 633-638.

Roots, E.F. (1989) Climate change: high-latitude regions. *Climatic Change*, **15**, 223-253.

Rouse, W.R. (1984) Microclimate of Arctic tree line. 2: Soil microclimate of tundra and forest. *Water Resources Research*, **20** (1), 67-73.

Rouse, W.R., Carlson, D.W., & Weick, E.J. (1992) Impacts of summer warming on the energy and water balance of wetland tundra. *Climatic Change*, **22**, 305-326.

Schlesinger, M.E., & Mitchell, J.F.B. (1987) Climate model simulations of the equilibrium climatic response to increased carbon dioxide. *Reviews of Geophysics*, **25**, 760-798.

Smith, M.W. (1990) Potential response of permafrost to climatic change. *Journal of Cold Regions Engineering*, **4**(1), 29-37.

Smith, M.W. & Riseborough, D.W. (1983) Permafrost sensitivity to climate change. In: *Proceedings, Fourth International Conference on Permafrost,Fairbanks, Alaska*, pp 1178-1183.

Steer, P. (1983) *Hydrology of a slope in the high Arctic*. Unpublished MSc. Thesis. Department of Geography, McMaster University, Hamilton, 111pp

Tarnocai, C. (1980) Summer temperatures of cryosolic soils in the north-central Keewatin, N.W.T. *Canadian Journal of Soil Science*, **60**, 311-327.

Tedrow, J.C.F. (1966) Polar Desert Soils. Soil Science Society of America Proceedings, 30 (3), 381-387.

Thorsteinsson, R (1958) Cornwallis and Little Cornwallis Islands, District of Franklin, N.W.T. *Geological Survey of Canada Memoir*, No. 294.

van Everdingen, R.O. (1987) The importance of permafrost in the hydrological regime. In: *Canadian Bulletin of Aquatic Resources*, No. 215. Healey, M.C. & Wallace, R.R. (eds). Department of Fisheries and Oceans, Ottawa, Ont, pp. 243-267.

Washburn, A.L. (1979) *Geocryology - A Survey of Periglacial Processes and Environments*. Edward Arnold, London. 406pp.

Williams, P.J. (1982) *The Surface of the Earth: An Introduction to Geotechnical Science*. Longman, London. 212pp.

Williams, P.J. and Smith, M.W. (1989) *The Frozen Earth: Fundamentals of Geocryology*. Cambridge University Press, Cambridge. 306pp.

Woo, M-k (1976) Hydrology of a small Canadian High Arctic basin during the snowmelt period. *Catena*, 4(2), 155-168.

Woo, M-k. (1990) Consequences of climatic change for hydrology in permafrost zones. *Journal of Cold Regions Engineering*, 4(1), 15-20.

Woo, M-k. (1986) Permafrost hydrology in North America. *Atmosphere-Ocean*, 24(3), 201-234.

Woo, M-k. & Marsh, P (1990) Response of soil moisture change to hydrologic processes in a continuous permafrost environment. *Nordic Hydrology*, 21, 235-252.

Woo, M-k. & Xia, Z. (1995) Suprapermafrost groundwater seepage in gravelly terrain, Resolute, NWT, Canada. *Permafrost and Periglacial Processes*, 6, 57-72.

Woo, M-k. & Xia, Z. (1996) Effects of hydrology on the thermal conditions of the active layer. *Nordic Hydrology*, 27, 129-142.

Woo, M-k & Young, K.L. (1990) Thermal and hydrological effects of slope disturbances in a continuous permafrost environment. *Proceedings, Fifth Canadian Permafrost Conference, Quebec*. National Research Council of Canada, 175-180.

Woo, M-k., Lewkowicz, A.G. & Rouse, W.R. (1992) Response of the Canadian permafrost environment to climatic change. *Physical Geography*, 13(4), 287-313.

Woo, M-k., Marsh, P. & Steer, P. (1983) Basin water balance in a continuous permafrost environment. In: *Proceedings, Fourth International Conference on Permafrost, Fairbanks, Alaska*, pp 1407-1411.